1985

Polarization-labelling Spectroscopy Of Iodine-monochloride: The D-prime (2) And A-prime (2) States

Denis Bussieres

Follow this and additional works at: https://ir.lib.uwo.ca/digitizedtheses

CANADIAN THESES ON MICROFICHE

THÈSES CANADIENNES SUR MICROFICHE

NOTICE

The quality of this microfiche is heavily dependent upon the quality of the original thesis submitted for microfilming Every effort has been made to ensure the highest quality of reproduction possible.

If pages are missing, contact the university which granted the degree.

Some pages may have indistinct print especially if the original pages were typed with a poor typewriter ribbon or if the university sent us an inferior photocopy.

Previously copyrighted materials (journal articles, published tests, etc.) are not filmed.

Reproduction in full or in part of this film is governed by the Canadian Copyright Act, R.S.C. 1970, c. C-30. Please read the authorization forms which accompany this thesis.

AVIS

La qualité de cette microfiche dépend grandement de la qualité de la thèse soumise au microfilmage Nous avons tout fait pour assurer une qualité supérieure de reproduction

S'il manque des pages, veuillez communiquer avec l'université qui a conféré le grade

La qualité d'impression de certaines pages peut laisser à désirer, surtout si les pages originales ont été dactylographiées à l'aide d'un ruban usé ou si l'université nous a fait parvenir une photocopie de qualité inférieure.

Les documents qui font déjà l'objet d'un droit d'auteur (articles de revue, examens publiés, etc.) ne sont pas microfilmés

La reproduction, même partielle, de ce microfilm est soumise à la Loi canadienne sur le droit d'auteur, SRC 1970, c C-30 Veuillez prendre connaissance des formules d'autorisation qui accompagnent cette thèse.

THIS DISSERTATION HAS BEEN MICROFILMED EXACTLY AS RECEIVED

LA THÈSE A ÉTÉ MICROFILMÉE TELLE QUE NOUS L'AVONS REÇUE

Canadä

POLARIZATION-LABELLING SPECTROSCOPY OF ICl :

THE D' (2) AND A' (2) STATES.

by

Denis Bussières

Department of Chemistry

Submitted in partial fulfilment
of the requirements for the degree of
Doctor of Philosophy

Faculty of Graduate Studies
The University of Western Ontario
London, Ontario
May, 1985.

ABSTRACT

Iodine stands as the best known diatomic halogen molecule. It is now followed by iodine monochloride. One of the three lowest ion-pair states, namely D' (ω=2), is characterized by using the Optical-Optical-Double-Resonance, ↑↑, state-selective polarization-labelling technique. Data were cumulated for vibrational levels v=0-2 and 15-28, including extensive coverage of two avoided crossings between D' and E states, at v=0 and 1. The main spectroscopic constants for D'state of $I^{35}Cl$ are T_e = 39061.830(80), ω_e= 173.63(35), $\omega_e x_e$= 0.5372(27), $10^2 B_e$ = 5.4782(41), $10^4 \alpha_e$ = 2.019(10) cm^{-1} and $10 r_e$= 3.350 nm. The Rydberg-Klein-Rees (RKR) potential is given for the $D'(2)$ ion-pair state of $I^{35}Cl$ up to v=28. The D' state is perturbed by the neighboring β state, their electronic interaction term is evaluated at 1.860(77), 93% of the Van Vleck pure precession value. The three lowest ion-pair states in ICl, D', β and E, have very similar electronic energy, vibrational energy and equilibrium bond distance as it can be expected.

By extending the technique to three steps (OOTR), ↑↑↓,

we characterized the first excited state A' (Ω=2) above the ground state of ICl. Data from v=2 to 28 were fitted to a Dunham expansion, and v=23 to 38 were fitted to a near-dissociation expansion. The main spectroscopic constants for A'(2) state of $I^{35}Cl$ are T_e = 12682.05(27), ω_e = 224.57(15), $\omega_e x_e$ = 1.882(29), $10^2 B_e$ = 8.648(48), $10^4 \alpha_e$ = 6.48(23), $10^8 D_e$ = 5.27(20) cm^{-1} and $10 r_e$ = 2.665nm. The A'(2) state shows some similarity with the other $(^3\pi)_0$ case (a) signature states, namely A(1) and B(0^+), their vibrational energy and equilibrium bond distance being very close. No sign of perturbation has been observed in A' state even if data of partial coverage go up to $\sim 70 cm^{-1}$ from the dissociation limit, 17557.57cm^{-1}, $I(^2 P_{3/2})$ + Cl $(^2 P_{3/2})$ to which converge ten electronic states. The Rydberg-Klein-Rees (RKR) potential curve is given for A'(2) state of $I^{35}Cl$ up to v=38.

ACKNOWLEDGEMENTS

A Hélène

et à Christine

On ne peut marcher en regardant les étoiles
quand on a une pierre dans son soulier.

<div align="right">sagesse chinoise</div>

TABLE OF CONTENTS

LIST OF TABLES

x

LIST OF FIGURES

LIST OF PLATES

xiii

LIST OF SYMBOL

Symbol	Description
c	Speed of light
cm	Centimeter
e	Charge of an electron
h	Planck's constant
i	Imaginary unit (not used as a subscript)
k	Wavenumber in radian per centimeter
l	Azimuthal quantum number
m	Mass of a particle
m_ℓ	Magnetic quantum number
n	Principal quantum number
nm	Nanometer (10^{-9}m)
ns	Nanosecond (10^{-9}s)
p_x	Angular momentum in the x direction
r	Distance of an electron from the nucleus or Distance between the two atoms of a molecule
r_e	Internuclear distance at equilibrium
s	Spin quantum number or Second
t	Time
v	Vibrational quantum number or Vibrational level or Speed of a particle

Symbol	Description
A	Amplitude
A_i	Amplitude in the i direction
$A(z)$	Amplitude in function of the z axis
B_e	Rotational constant at equilibrium
B_v	Effective rotational constant at vibrational level v
$\hat{B}_{ij}$	Off-diagonal rotational constant
D_e	Centrifugal distortion constant at equilibrium or Dissociation energy related to the potential minimum
D_o	Dissociation energy related to the vibrational level 0
E	Energy level or Electric field
E_i	Electric field in the i direction
F	Force
$G(v)$ or E_v	Vibrational energy or Term value
I	Moment of inertia or Intensity Imaginary part of the following complex quantity
J	Rotational quantum number
J	Total electronic angular momentum
K	Constant
kW	Kilowatt (10^3watt)
L	Electronic orbital angular momentum
M	Projection of total angular momentum along some laboratory fixed axis

Symbol	Description
M_1, M_2	Function modulating amplitude of signal and probe waves due to non-zero third order susceptibility
M_e	Electric moment
MW	Megawatt (10^6 watt)
OODR	Optical-Optical-Double-Resonance
OOTR	Optical-Optical-Triple-Resonance
P transition	Transition from rotational level J to another rotational level J-1
Q transition	Transition from rotational level J to another rotational level J
R	Nuclear rotational quantum number
R transition	Transition from rotational level J to another rotational level J+1
R'	Constant
R_e	Electric transition moment
	Real part of the following complex quantity
RKR	Rydberg-Klein-Rees potential curve
S	Electronic spin angular momentum
SEEPOL	Stimulated Enhanced Emission Polarization-Labelling
T_e	Electronic energy of a state or its minimum energy
$W_{i,j}$	Electronic interaction term between two states
$Y_{i,j}$	General term of Dunham expansion
Z	Atomic number

Symbol	Description
α_e	Variation of rotational constant with v
$\frac{\partial}{\partial x}$	Partial derivative in function of x
η	Refractive index
λ	Wavelength
μ	Reduced mass of a molecule
μ_{ij}	Dipole moment coupling the i'th to the j'th state
μm	Micrometer (10^{-6}m)
μs	Microsecond (10^{-6}s)
π	Pi (3.14159265....)
ω	Vibrational frequency
ω_e	Vibrational frequency at equilibrium
$\omega_e x_e$	Variation of vibrational frequency in function of v
Σ	Electronic spin quantum number or Mathematical summation
Ψ	Total wavefunction
ψ	Partial wavefunction
Λ	Electronic orbital quantum number
Ω	Total electronic quantum number
χ_{ij}	1st order susceptibility (dimensionless)
χ_{ijk}	2nd order susceptibility ($g^{-1/2}cm^{1/2}s$)
χ_{ijkl}	3rd order susceptibility ($g^{-1}cm\ s$)

FOREWORD

For thousands of years, man has sought to master his environment. His efforts began by controlling fire. Then came the wheel, the land, the sea, the sky, the atoms. From, this power came all sorts of knowledge called sciences.

Today, there is a diversity of sciences which are divided into many branches and specific fields. Humanity is now probing the infinitely small, the infinitely far and the infinitely deep. The universe reveals itself as a whole well structured and able to support an organized system of numerous components. The pursuit of knowledge leads us to the elaboration of more and more complex models.

Even with the power of today's computers, one model is barely sufficient to correctly describe a diatomic molecule which stands as fairly simple compared to many organic compounds. There is still much information to be acquired from relatively simple diatomic molecules before developing a model satisfactory to describe them all.

CHAPTER 1

INTRODUCTION

A lot of spectroscopic work has been done on dihalogen and interhalogen molecules. Iodine is the most thoroughly studied molecule in that group so far; it has revealed more than half of its ion-pair states and almost half of its valence states [1]. The next best known molecule is iodine monochloride, ICl.

The interaction of two neutral halogen atoms gives rise to a manifold of 23 molecular states [2]. These are called valence states and can be identified by their Hund's case c quantum number Ω. Only few of them are believed to be strongly bound. Similarly, two halogen ions give rise to 20 ion-pair states which are believed to all be strongly bound.

Before this study, only three valence states of ICl were well known, $X(0^+)$ [3], $A(1)$ [4] and $B(0^+)$ [5] (see Table 1.1). The B state predissociates due to a crossing by

Table 1.1 Summary of previously known electronic states of ICl with their notation according to Hund's coupling case (c).

State	Label	T_e (cm^{-1})	Dissociation limit (cm^{-1})
X	0^+	0	$I\ (^2P_{3/2}) + Cl\ (^2P_{3/2})$ (17557.57)
A	1	13742.9	
B	0^+	17375.578	
B'	0^+	18155	$I\ (^2P_{3/2}) + Cl\ (^2P_{1/2})$ (18439.9)
E	0^+	39059.485	$I^+\ (^3P_2) + Cl^-\ (^1S_0)$ ($\approx$72554)
β	1	39103.666	
f	0^+	44923.79	$I^+\ (^3P_1) + Cl^-\ (^1S_0)$
	1	45552.805	$I^+\ (^3P_0) + Cl^-\ (^1S_0)$

another 0^+ state, mainly repulsive, and has been the subject of studies which identified a $B'(0^+)$ adiabatic state resulting from that intersection. From the six lowest ion-pair states, four have been characterized to some extent. Otherwise, parts of spectra were left unexplained and sometimes very puzzling.

This thesis began as a study of one of the three low-lying ion-pair states not yet characterized, namely, the $D'(\omega=2)$ state. By analogy with I_2, it was believed to lie quite close to the other two ion-pair states which converge to $I^+(^3P_2) + Cl^-(^1S_0)$ [6]. Even though selection rules for optical-optical-double-resonance (OODR) permit a sequence of two upward $\Delta\omega=1$ transitions, ↑↑, these had not yet been observed in our OODR experiments involving an ion-pair state as the terminus.

Because of the proximity of the three ion-pair states, β, E and D', some perturbations arise between them [7]. Making use of these perturbations, we were able to get $D' \leftarrow A$ signals as a complement of stronger $\beta \leftarrow A$ transitions. In so doing, the access to D' state was restricted to where the perturbations with β were sufficiently strong. Nevertheless, we have cumulated enough data to characterize the lower part (about 12%) of the potential well of D' state. At the same time, we have an extensive coverage of two avoided crossings between $D'(2)$ and $E(0^+)$ states at vibrational level 0 and 1. A simultaneous non-linear least-

squares fit of the three ion-pair states allows us to obtain values for the interaction matrix elements [8]. The Rydberg-Klein-Rees (RKR) potential is given up to the 28th vibrational level together with the Dunham parameters for D' ($\Omega = 2$) ion-pair state of $I^{35}Cl$ (see chapter 5).

Being the first $\omega = 2$ electronic state of ICl to be characterized, D' opens the door to access other $\omega = 2$ states, either lower or higher in energy than D'. Only one of the valence states not yet observed in ICl , A' ($\omega = 2$), is expected to be a relatively deeply-bound state*. The other ones are considered essentially repulsive with possibly a shallow minimum. By analogy with I_2, the A'(2) state was expected to be the first excited state above the ground state X, therefore lower than the A(1) state. The A'(2) state, a natural-complement to the study of D' state, makes the second part of our work.

At that point, the challenge of extending the polarization-labelling technique to three steps was even more stimulating. In a triple sequence of optical resonance, ↑↑↓, data on A'(2) valence state were cumulated to cover almost its entire potential, from v=2 to 38 [8]. Practical and theoretical limitations, like Franck-Condon factors, frustated our efforts to obtain data for the two lowest vibrational levels of A', namely v=0 and 1. However, the

* While this work was in progress, Spivey and others [1] published a partial fit of D' and A' states.

large range covered in this rather anharmonic state enables us to determine its spectroscopic constants including its centrifugal distortion constants as a function of v for most of its potential depth. The RKR potential of A' (2) state of $I^{35}Cl$ is given (see chapter 6) with the other known valence states in the same region.

Subsequently, the above experiments helped to initiate studies of other valence states of ICl leading to the characterization of three new states [9] together with new data relative to high vibrational levels of the ground state X [10]. We now know eight of the fifteen valence states correlating with the first two dissociation limits and five out of the six lowest ion-pair states of ICl. This work has lead to a significant addition to the knowledge of the electronic states of ICl.

CHAPTER TWO

MOLECULAR SPECTROSCOPY

This chapter presents a brief outline of the nomenclature related to the spectroscopic study of the electronic states of ICl [12,13] followed by a description of the potential for electronic states. The selection rules for transition by optical resonance and a short presentation of perturbation phenomena occuring in ICl conclude the subject.

2.1 Nomenclature

As Bohr first suggested, an atom can exist only in certain discrete energy states; for example, in an atom with one electron, like H, the electron can take only certain values of energy. If the energy of the atom without its electron is set at zero, equation 2.1 is respected

$$E_v = - R' \; z^2/n^2 \qquad 2.1$$

where n is the principal quantum number, Z is the atomic number and R' a constant.

DeBroglie believed that the motion of any particle of matter is associated to a wave motion of wavelength λ

$$\lambda = h/mv \qquad\qquad 2.2$$

where h is the Plank's constant, m the mass of the particle and v its velocity. This idea is now widely accepted. Let Ψ be the wave function which must vary periodically with time in space

$$\Psi = \psi \sin 2\pi\nu't$$
$$\text{or} \quad \Psi = \psi \cos 2\pi\nu't \qquad\qquad 2.3$$

where ψ is the amplitude of the wave motion and ν' the frequency of the vibration. These two expressions can be combined to get

$$\Psi = \psi \exp(-2\pi\nu't) \qquad\qquad 2.4$$

If the motion of a single electron is considered in the field of a nucleus, then

$$\frac{1}{m}\left[\frac{\partial^2\psi}{\partial x^2} + \frac{\partial^2\psi}{\partial y^2} + \frac{\partial^2\psi}{\partial z^2}\right] + \frac{8\pi^2}{h^2}(E-V)\psi = 0 \qquad 2.5$$

Here, m is the mass of the electron and V is the potential energy equal to $-Ze^2/r$. The solution of this Schrödinger or wave equation is possible only for certain values of E, so-

called eigenvalues. The resultant energies correspond to those of equation 2.1. The solution of equation 2.5 for several electrons in an atom gives values in very good agreement with experimental results on such atoms. At the same time, the Schrödinger equation predicts that the energy can have any value bigger than zero, which agrees with spectroscopic observations.

From the principal quantum number, n, one defines the azimuthal quantum number λ with the integral values

$$0 \leqslant \lambda \leqslant n \qquad 2.6$$

The equivalent of the classical angular momentum, mv, is given in wave mechanics for an electron by

$$\sqrt{\lambda(\lambda+1)}/(h/2\pi) \qquad 2.7$$

It can take only discrete values as can the energy. From the fact that the angular momentum of an electron has definite values, it follows that its orbit around the nucleus is not definite at all. This effect is reflected by Heisenberg's uncertainty principle which can be expressed as follows

$$\Delta x \, \Delta p_x \geqslant h/2\pi$$
$$\text{or} \quad \Delta E \, \Delta t \geqslant h/2\pi \qquad 2.8$$

From the first equation in 2.8, if the momentum of an electron in one direction, p_x, is well known, then its

position is indefinite, in order to respect the uncertainty principle.

In quantum theory, the component of the orbital angular momentum of an electron in a field direction is constant and can only take discrete values, m_ℓ $(h/2\pi)$, where

$$m_\ell = \ell, \ell-1, \ell-2, \ldots, -\ell \qquad 2.9$$

The number m_ℓ is called the magnetic quantum number of the electron. From figure 2.1 , it can be seen that the angular momentum cannot point in the direction of the field.

The electron also has an angular momentum of its own called the electron spin, referring to its rotation about its own axis. The spin quantum number, $s=1/2$, gives rise to the angular momentum with magnitude equal to

$$\sqrt{s(s+1)}/(h/2\pi) \qquad 2.10$$

For one unpaired electron, the component of the spin angular momentum in a magnetic field, m_s , can take only the values of $+1/2$ and $-1/2$. Whenever there is no orbital angular momentum, that is $\ell=0$, a two-fold degeneracy arises from these two values of m_s. When $\ell\neq0$, there is a $(2\ell+1)-$ fold degeneracy.

In a diatomic molecule, a precession of the electronic orbital angular momentum, L, takes place about the inter-nuclear axis with a constant component $\Lambda(h/2\pi)$ along it (see Figure 2.2), where
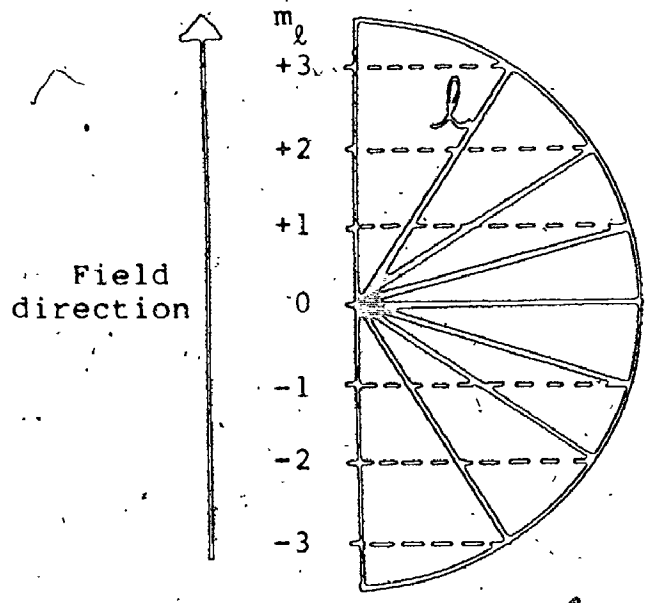
Figure 2.1 The orbital angular momentum, $\ell(h/2\pi)$, of an electron and its components, m_ℓ (in units of $h/2\pi$), along the field direction.
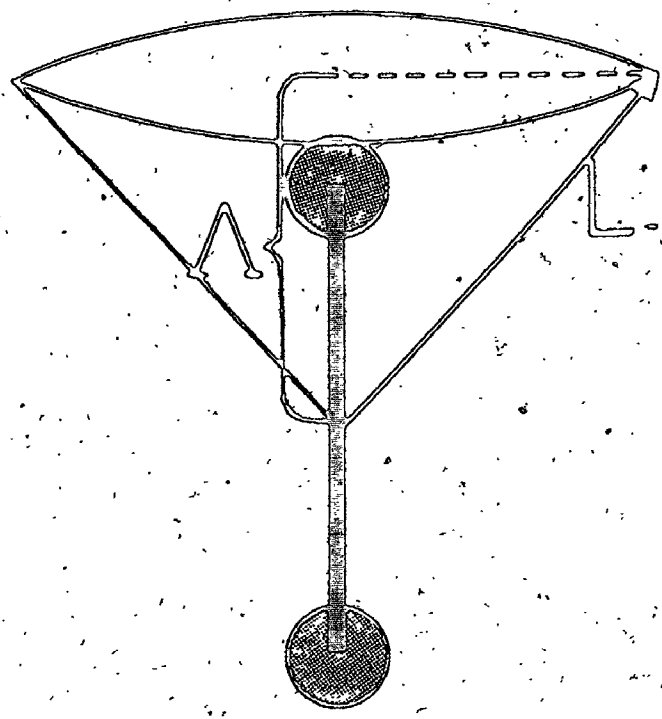
Figure 2.2 The electronic orbital angular momentum, $L(h/2\pi)$ in a diatomic molecule with its component (in $h/2\pi$ units) along the internuclear axis.

$$\Lambda = L, \ L-1, \ L-2, \ \ldots, \ -L \qquad \qquad 2.11$$

The spins of the individual electrons combine to form a total spin from which we get the corresponding quantum number S which can be integral or half-integral. Whenever $\Lambda \neq 0$, the internal magnetic field produced by the electron motion causes a precession of the total electronic spin about the field direction (in this case, the internuclear axis) with a constant component $\Sigma \ (h/2\pi)$, where

$$\Sigma = S, \ S-1, \ S-2, \ \ldots, \ -S \qquad \qquad 2:12$$

The total electronic angular momentum about the internuclear axis $\Omega \ (h/2\pi)$, is defined by

$$\Omega = \Lambda + \Sigma \qquad \qquad 2.13$$

In the case of ICl, the interaction between the orbital and the spin angular momenta is stronger than their individual interaction with the internal field. As a consequence, one cannot consider Λ and Σ as they are no longer defined. These two momenta couple together (see Figure 2.3) to define directly $\Omega(h/2\pi)$ as the component of the total electronic angular momentum along the internuclear axis. This situation refers to Hund's coupling case (c). In ICl, the absolute value of the total electronic quantum number, Ω, is then used to label the electronic states which are simply called 0, 1, 2, ... From now on, we will consider Ω
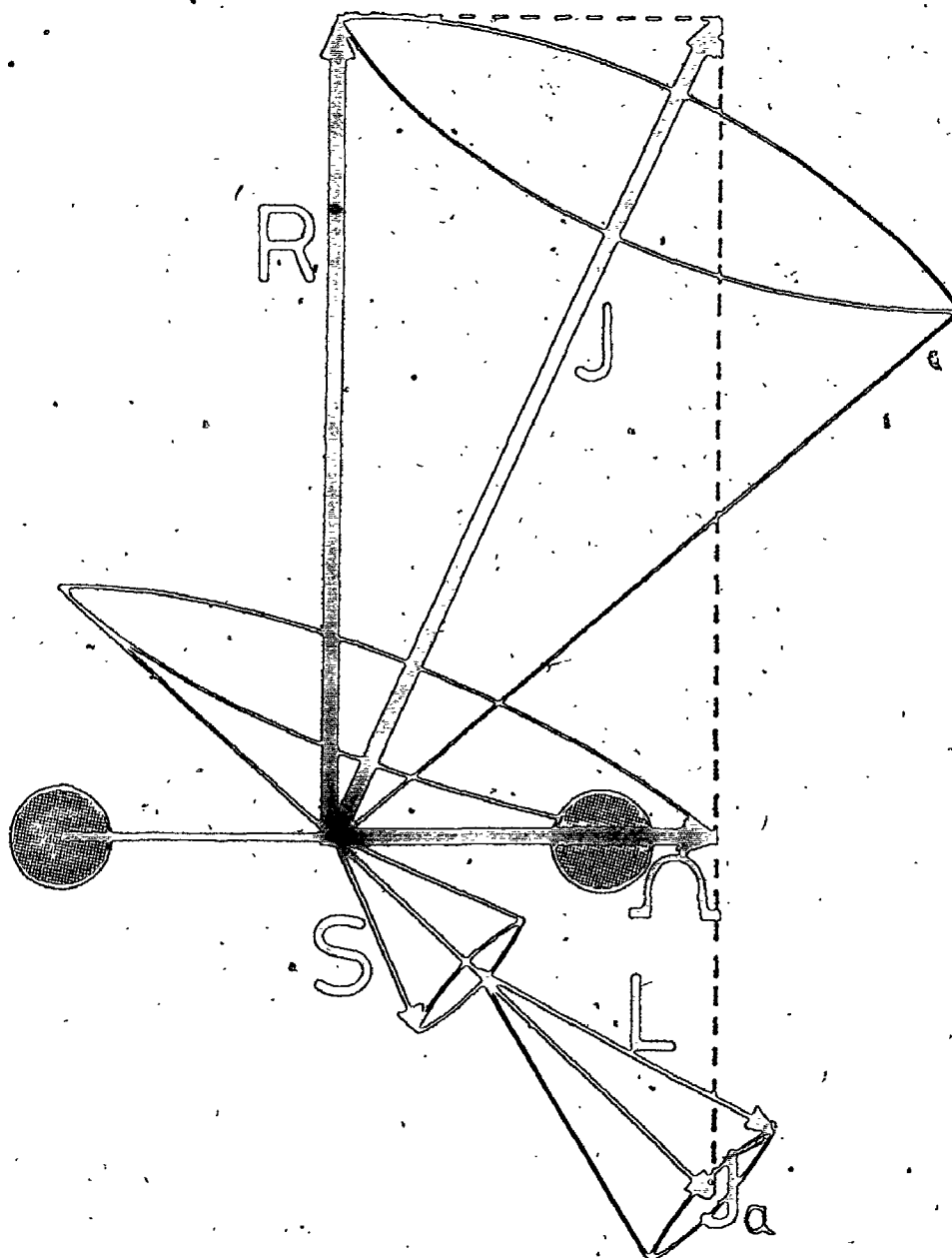
Figure 2.3 Coupling of the different angular momenta (in h/2π units) in ICl, referring to Hund's case c.

as a positive value used to label the electronic states of ICl. A state with $\Omega=0$ is singly degenerate and $\Omega \neq 0$ states are doubly degenerate.

The rotational quantum number J is then defined by the addition of the nuclear rotational quantum number, R, with Ω (see Figure 2.3). It naturally follows that J cannot be smaller than Ω; for ICl, Ω and J are integral due to an even number of electrons in the molecule

$$J = \Omega, \Omega+1, \Omega+2, \ldots \qquad 2.14$$

A molecule is never at rest. Its movement encompasses three different kinds of motion : vibration, rotation and translation. With polarization-labelling spectroscopy the internal molecular motions are studied, that is the motions related to the molecular set of coordinates' : vibrations and rotations.

2.2 Potential for electronic states

In nature, molecules are usually in their ground state or stable state, but they are vibrating and rotating all the time. One particular molecule can have only certain values of vibrational and rotational energy. A quantum of vibrational energy is typically much larger than one of rotational energy.

The simplest assumption about the form of vibration is that each atom of a diatomic molecule moves away from the

other and back towards it in a simple harmonic motion. In classical mechanics, a harmonic oscillator refers to a force F proportional to the distance x from an equilibrium position acting on a mass point m

$$F = -kx = m \, d^2x/dt^2 \qquad\qquad 2.15$$

The resulting vibrational frequency is given by

$$\nu_{osc} = \sqrt{k/m} \, /2\pi \qquad\qquad 2.16$$

Using the expression of force in equation 2.15 to get the potential energy of the oscillator by integration, wave mechanics gets the following expression for the energy of harmonic vibrations in a molecule

$$E_v = \frac{h}{2\pi}\sqrt{\frac{k}{\mu}}\,(v+1/2) = h\nu_{osc}\,(v+1/2) \qquad 2.17$$

Here, μ is the reduced mass of the molecule and v is the vibrational quantum number which can take integral values bigger than or equal to 0.

The representation of the potential energy of a molecule with harmonic oscillations as a function of the internuclear distance gives a parabola (dotted curve on Figure 2.4). However, it is clear that when the atoms move far apart they will eventually become dissociated. Therefore, the potential curve of the molecule has the form of an anharmonic oscillator potential(solid curve on Figure 2.4). The eigenvalues of an anharmonic oscillator can be expres-
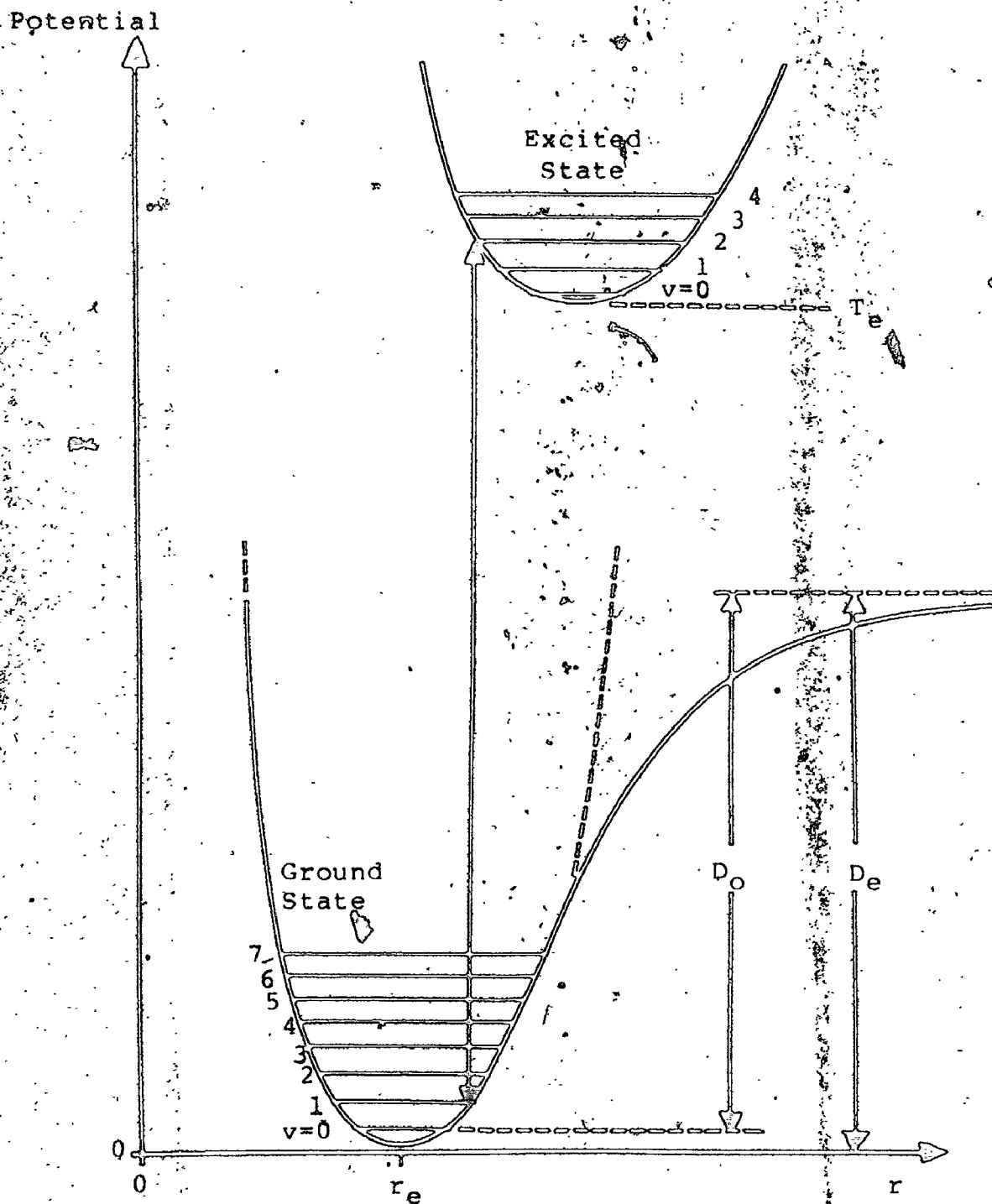
Figure 2.4 Potential energy in function of the internuclear distance: the dotted curve is for a harmonic oscillator and the solid curve for an anharmonic one. An example of a transition to an excited state is shown. D_e and D_o are the dissociation energy relative to the bottom of the state and to the vibrational level 0, respectively. T_e is the minimum energy of a state.

sed in the form of a series expansion

$$E_v = h\nu [\omega_e(v+1/2) - \omega_e x_e(v+1/2)^2 + \ldots] \qquad 2.18$$

In spectroscopy, the Dunham expansion is widely used

$$G(v) = \omega_e(v+1/2) - \omega_e x_e(v+1/2)^2 + \ldots \qquad 2.19$$

where $\omega_e > \omega_e x_e$ are expressed in wavenumber units (cm^{-1}). A potential curve for a molecule in a specific electronic state is composed of many vibrational levels (see Figure 2.4). The symbol T_e is associated with the bottom of the potential; when the potential curve in question is the ground state of a molecule, $T_e = 0$. Therefore, in a molecule, the energy scale is positive and starts at the bottom of the ground state (usually called X state). The symbol D_e is associated with a dissociation limit and has a positive value (in cm^{-1} or in eV) calculated from the bottom of the state. The symbol D_0 refers the dissociation energy to the level $v=0$. The first dissociation of a diatomic molecule normally gives the two separate atoms in their ground state.

Concurrently to its vibrational levels, the rotation of the same molecule also stores some energy in a quantum manner. The energy of a rigid rotator (in units of cm^{-1}) is then expressed by

$$F_v(J) = \frac{E_{rot}}{hc} = \frac{h\ J(J+1)}{8\pi^2\ cI} = B_v J(J+1) \qquad 2.20$$

where I is the moment of inertia of the molecule (μr^2) and B_V is the rotational constant. The dependence on the vibrational level for the rotational constant is expressed by a series expansion in v

$$B_V = B_e - \alpha_e(v+1/2) + \ldots \qquad 2.21$$

Here B_e is called the rotational constant at equilibrium from which the internuclear distance at equilibrium r_e is easily extracted. It is as easy to compute that the rotational constant decreases slowly as v increases, α_e being positive and small compared to B_e.

As a direct consequence of the molecular rotation, a centrifugal force comes into play and affects the internuclear distance which affects the moment of inertia and the rotational constant B. Therefore, with a massive molecule such as ICl, one or several centrifugal corrections to the rotational constant must often be applied

$$F_V(J) = B_V J(J+1) - D_V J^2(J+1)^2$$
$$+ H_V J^3(J+1)^3 + L_V J^4(J+1)^4 + \ldots \qquad 2.22$$

Here, D_V, H_V, L_V are all considered as centrifugal distortion constants used to correct the rotational energy. As the rotational quantum number increases, the effect of these correction constants becomes more and more important. Again, D_V, H_V and L_V can be expressed by a series expansion in v as B_V is in equation 2.21.

Two isotopes of Cl occur in a relative abundance of 1:3. $I^{37}Cl$ shows different values of vibrational and rotational energy than those of $I^{35}Cl$. From this difference, new mass-reduced quantum numbers can be defined [14]

$$\eta = (v+1/2)/\sqrt{\mu}$$
$$\xi = J(J+1)/\mu \qquad\qquad 2.23$$

In order to work with integer quantum numbers, the isotopic ratio for ICl is defined by

$$\rho = \frac{\nu_{osc}37}{\nu_{osc}35} = \sqrt{\frac{\mu_{35}}{\mu_{37}}} = 0.978595 \qquad 2.24$$

This ratio is used to express the vibrational and rotational energy of the less abundant isotopic molecule, $I^{37}Cl$, with the same terms as for the main isotopic molecule, $I^{35}Cl$

$$G(v) = \omega_e \rho(v+1/2) + \omega_e x_e \rho^2 (v+1/2)^2 + \ldots \qquad 2.25$$
$$F_v(J) = B_v \rho^2 J(J+1) - D_v \rho^4 J^2 (J+1)^2 + \ldots \qquad 2.26$$

When dealing with $I^{35}Cl$ data, ρ equals unity and for $I^{37}Cl$, ρ has the value 0.978595. The fact that the rovibrational separations are different between the two isotopes is used to validate the vibrational and rotational levels assigned to signals in an early stage of analysis. Then, data from both isotopes can be used in the model to determine only one set of parameters.

For convenience, a Dunham expansion is widely used to express the energy of an electronic state

$$Y_{00} + Y_{10}\rho(v+1/2) + Y_{20}\rho^2(v+1/2)^2 + \ldots$$
$$+ Y_{01}\rho^2 J(J+1) + Y_{11}\rho(v+1/2)\rho^2 J(J+1) + \ldots$$
$$+ Y_{02}\rho^4 J^2(J+1)^2 + \ldots \qquad \qquad 2.27$$

where $Y_{00} \simeq T_e$

$Y_{10} \simeq \omega_e$

$Y_{20} \simeq -\omega_e x_e$

$Y_{01} \simeq B_e$

$Y_{11} \simeq -\alpha_e$

$Y_{02} \simeq -D_e$ (not dissociation energy)

The Dunham terms Y_{ab} do not give precisely the terms T_e, ω_e and others, but are so close as to be practically equivalent.) Once the first few terms in the Dunham expansion are determined for an electronic state, some other ones can be estimated [12,15]

$$\alpha_e = [6\sqrt{\omega_e x_e B_e^3} - 6B_e^2]/\omega_e \qquad 2.28$$
$$\text{for a Morse potential}$$

$$D_e = 4\,B_e^3/\omega_e^2 \qquad 2.29$$

$$H_e = 2D_e(12B_e^2 - \alpha_e\omega_e)/3\omega_e^2 \qquad 2.30$$

$$L_e = \frac{1}{B_e^2 D_e}\left[3B_e H_e D_e^2 - 5D_e^4 + B_e^2 H_e^2 - \frac{8D_e^3 B_e^2 \omega_e x_e}{3\,\omega_e^2}\right] \qquad 2.31$$

Quite frequently, the above equations do not represent the observed values accurately but should be used only as an

estimated value for these terms. Dunham also gives a correction to be added to the bottom of the potential [12]

$$Y'_{00} = \frac{B_e}{4} + \frac{\alpha_e \omega_e}{12 B_e} + \frac{\alpha_e^2 \omega_e^2}{144 B_e^3} - \frac{\omega_e x_e}{4} \qquad 2.32$$

which is usually a small fraction of a wavenumber.

2.3 Selection rules.

The spectra of diatomic molecules are affected by the quantum numbers and their properties through the selection rules. Here, the ones relevant to ICl molecule with Hund's case c signature will be outlined for optical resonance transitions.

The selection rule on the rotational quantum number is

$$\Delta J = 0, \pm 1 \qquad 2.33$$

with the restriction that $J=0 \not\leftrightarrow J=0$. Underlying this one, there is a symmetry rule which holds quite generally for electric dipole transitions

$$+ \leftrightarrow - \quad \text{but} \quad + \not\leftrightarrow + \quad - \not\leftrightarrow - \qquad 2.34$$

This positive and negative symmetry, or parity, of the wavefunctions is associated alternatively with the successive rotational levels in a given electronic state

for $\omega = 0$ $J = 0(+), 1(-), 2(+), 3(-), \quad \rightarrow 0^+$

or $\omega = 0$ $J = 0(-), 1(+), 2(-), 3(+), \quad \rightarrow 0^-$

for $\Omega = 1, 2, 3$ the state comprises two substates

first, (e) $\quad J = 1(-), \ 2(+), \ 3(-), \ 4(+), \ \ldots$

second, (f) $\quad J = 1(+), \ 2(-), \ 3(+), \ 4(-), \ \ldots$

It must be remembered that $J \geqslant \Omega$. Another selection rule applies to the total electronic angular momentum

$$\Delta\Omega = 0, \pm 1 \qquad\qquad 2.35$$

and $\quad 0^+ \leftrightarrow 0^+, \quad 0^- \leftrightarrow 0^-, \quad 0^+ \not\leftrightarrow 0^-$.

From these, it can be deduced for a specific transition from the ground state in ICl, $\Omega = 0^+$ to another $\Omega = 0^+$ state, that there is no Q branch ($\Delta J = 0$). From the ground state to a state with $\Omega = 1$, Q signals access the f substate and P,R signals ($\Delta J = \mp 1$) access the e substate. Using the above selection rules, the observed signals characterize different electronic states and substates. In designating a given electronic transition, the upper state is always written first; a B-X transition refers to a transition between the ground state X and an upper state B.

Some other restrictions arise from the fact that the light interacts during a very short period of time with the molecule. This time scale is of the order of magnitude of the reciprocal of the transition frequency; for ultra-violet and visible light, it is of the order of the femto-second (10^{-15}s). This means that after the interaction the molecule has the same internuclear distance as before the

interaction, the inverse of the vibrational frequency being of the order of one to ten picosecond ($10^{-12}-10^{-11}$s). From our point of view, a transition can occur vertically between two potential energy curves which represent two electronic states (see Figure 2.4). This intuitive idea is referred to as the Franck-Condon principle.

Quantum mechanics considered that the total wavefunction Ψ describing each of the two levels between which a transition is considered, can be separated into two parts

$$\Psi = \psi_e \psi_v \qquad \qquad 2.36$$

where ψ_e are the electronic and ψ_v the vibrational wavefunctions respectively. The electronic transition moment is defined

$$R_e = \int M_e \psi_e'^* \psi_e'' dr \qquad \qquad 2.37$$

by use of the electric moment M_e. The integral over the product of the ψ_v's of the two states involved is called the overlap integral

$$\int \psi_v' \psi_v'' dr \qquad \qquad 2.38$$

This equation translates the Franck-Condon idea into a mathematical form. Then, assuming that the variation of R_e with r is slow

$$R = \overline{R_e} \int \psi_v' \psi_v'' dr \qquad \qquad 2.39$$

where $\overline{R_e}$ is an average value of R_e. The intensity of a transition is proprotional to R^2 as long as the other selection rules are respected. Here again, quantum mechanics allows for some uncertainty or variation in the internuclear distance during a transition, according to the Heisenberg's uncertainty principle(2.8).

2.4 Perturbation phenomena

a) Ω doubling

The ICl molecule corresponds to Hund's coupling case (c) which refers to an idealized situation. Small and large deviations from these cases are often observed. In ICl, an interaction or perturbation between two neighboring states, $\Omega=0$ and 1 of the same parity gives rise to a splitting of the two rotational sublevels, e and f, of the $\Omega=1$ state. Effectively the sub-level e of $\Omega=1$ state is perturbed by the neighboring $\Omega=0^+$state (non-degenerate), and its resultant energies differ slightly from the f sub-level. This effect is called Ω splitting or Ω doubling and is frequently of the order of a fraction of a wavenumber. This heterogeneous perturbation, $\Delta\Omega=\pm1$, is possible only in the rotating molecule; some refer to this as electronic-Coriolis interaction in the rotating molecule. An homogeneous perturbation operates between two states with the same Ω and is possible in the non-rotating molecule [16]. In both types, the upper level in question is shifted up as the

lower level is shifted down by the same amount. This perturbation is always expressed as a repulsion of two states.

The rotational part of the Hamiltonian can be expressed this way

$$H_{rot} = B_v[(\hat{J}_x - \hat{L}_x - \hat{S}_x)^2 + (\hat{J}_y - \hat{L}_y - \hat{S}_y)^2]. \qquad 2.40$$

which can then be rearranged to give

$$H_{rot} = B_v[\; \hat{J}^2$$
$$-\hat{J}_z^2 + \hat{L}^2 - \hat{L}_z^2 + \hat{S}^2 - \hat{S}_z^2 - \hat{L}_+\hat{S}_- - \hat{L}_-\hat{S}_+$$
$$-\hat{J}_+\hat{L}_- -\hat{J}_-\hat{L}_+ -\hat{J}_+\hat{S}_- -\hat{J}_-\hat{S}_+] \qquad 2.41$$

where $\hat{J}_\pm = \hat{J}_x \pm i\hat{J}_y$, $\hat{L}_\pm = \hat{L}_x \pm i\hat{L}_y$ and $\hat{S}_\pm = \hat{S}_x \pm i\hat{S}_y$ and where these angular momentum operators are in $h/2\pi$ units. The term in J on the first line of 2.41 gives the usual expression for the rotational term.

$$F_v(J) = B_v J(J+1) \qquad 2.42$$

The terms produced by the operators from the second line in 2.41 are independent of J and are therefore included in the electronic term value. The third line of 2.41 shows the terms responsible for the J dependence coupling between states of different ω

$$\langle J,M,\omega\pm 1| -B_v(\hat{J}_+(\hat{L}_- + \hat{S}_-) + (\hat{J}_-(\hat{L}_+ + \hat{S}_+)))|\omega,M,J\rangle$$
$$= \langle \omega\pm 1|\hat{L}_+ + \hat{S}_+|\omega\rangle\langle\omega\pm 1|B_v|\omega\rangle$$
$$\times [J(J+1) - \omega(\omega\pm 1)]^{1/2}$$
$$= W_{\omega,\omega\pm 1}\; B_{\omega,\omega\pm 1}\; [J(J+1) - \omega(\omega\pm 1)]^{1/2} \qquad 2.43$$

The above equation generates the off-diagonal elements for a 'rotational' Hamiltonian matrix. The off-diagonal rotational constant $B_{\Omega,\Omega\pm1}$ is readily evaluated from numerical wavefunctions if the potential curve of the electronic states are known. The term $W_{\Omega,\Omega\pm1}$ is usually not calculable and is treated as an adjustable parameter in the fit of the experimental data.

The first family of ion-pair states in ICl consists of three electronic states, $\beta(\Omega=1)$, $E(0^+)$ and $D'(2)$, with their T_e lying in a 50 cm^{-1} range. This gives rise to an Ω doubling in both β and D' states. This splitting in D' is due to the interaction of the E state through the perturbed β state which is partly assuming the E properties. Therefore, the fit for these three states should be considered simultaneously to obtain a reasonable accuracy. The original 5x5 matrix factorizes into a 3x3 (e sublevels of $\Omega=0,1$ and 2 states) and a 2x2 matrix (f sublevels of $\Omega=1$ and 2 states) by symmetry; there are off-diagonal elements of the form of equation 2.43 for interaction between $\Omega=1$ and $\Omega=0$ states, and interaction between $\Omega=1$ and $\Omega=2$ states.

In a first approximation, the interaction by a vibrational level with a different v is considered negligible. If necessary, it can be included by transforming the above 3x3 matrix into a 6x6 when considering only one neighboring vibrational level, and the 2x2 would become a 4x4 matrix. The magnitude of these new off-diagonal elements are

usually much smaller than the ones considered before for the same v number and can be evaluated by perturbation theory. This is because the interaction in play is inversely proportional to the energy difference between the two levels considered.

The only term in equation 2.43 which can have some dependence on v is $B_{\Omega,\Omega\pm1}$. Being a difficult factor to calculate a priori, it is usually evaluated numerically from the wavefunctions describing vibrations in the Rydberg-Klein-Rees (RKR) potential curve, but first, the Dunham parameters are needed to make the RKR curve. An iterative process takes place by starting with an "approximate" set of Dunham parameters which then make an RKR curve, and we calculate these $B_{\Omega,\Omega\pm1}$ for same and different v's using the Numerov-Cooley method [17]. These factors can then be used in the fit of the data to get a new set of Dunham parameters. The procedure is repeated until there is convergence, usually after few cycles.

The first term in equation 2.43 can be compared to the interaction term in the case referred to as pure precession, developped by Van Vleck [18], where L+S = J_a is a defined quantity

$$\langle J_a,\Omega\pm1|\hat{L}_\pm+\hat{S}_\pm|J_a,\Omega\rangle = [J_a(J_a+1)-\Omega(\Omega\pm1)]^{1/2} \qquad 2.44$$

The family of ion-pair states considered gives upon dissociation $Cl^-(^1S_0)$ and $I^+(^3P_2)$, then $J_a = 2$ and $\Omega = 0,1,2$

$$W_{1,0} = [2(2+1) - 1(0)]^{1/2} = \sqrt{6} = 2.45 \qquad 2.45$$

$$W_{1,2} = [2(2+1) - 1(2)]^{1/2} = \sqrt{4} = 2. \qquad 2.46$$

The overall magnitude of the shift due to the perturbation is function of the overlap of the two vibrational or rovibrational wavefunctions (equation 2.38) of the two states. Unless some "selection rules" are respected, the overlap vanishes. The selection rules relevant to ICl so that a perturbation can happen are

- same total angular momentum $(\Delta J = 0)$
- $\Delta \Omega = 0, \pm 1.$
- same parity, $+ \leftrightarrow +$ or $- \leftrightarrow -$

As well, there is a classical equivalent of the Franck-Condon factor [19] : "Two vibrational states belonging to two different electronic states and lying at approximately the same height will influence each other strongly only if classically the system could go over from the one state to the other without a large alteration of position and momentum".

In the case of ICl, heterogeneous perturbation($\Delta \Omega = \pm 1$) is present and arises on account of finer interactions of rotational and electronic motion. The magnitude of the perturbation between the two states is then proportional to $J(J+1)$ according to the basic theory. The wavefunctions of perturbed states are considered hybrid or mixed wavefunctions. Both states now assume each others properties. Then,

when one allowed transition is in resonance with the energy
of the beam, extra lines can appear from the neighboring
perturbed state. One may say that the extra lines "borrow"
intensity from the regular lines.

This can explain the appearance of some extra lines in
spectra. By considering levels from an $\omega=1$ state as not
pure but hybrid levels, one can consider an $\omega=2$ state being
perturbed by the $\Omega=1$ state as well as by the $\omega=0$ state but
to a lesser extent. This is how an $\omega=2$ state shows an ω
doubling effect. By the same process, this is how an $\omega=2$
state can experience a local perturbation by an $\omega=0^+$ state
in the form of an avoided crossing between the two levels.

b) Avoided crossing

When two electronic states are very close, they may
show an apparent crossing of their potential curves which
is formally forbidden for two electronic states with the
same parity (see selection rules for perturbations). This
is shown schematically on Figure 2.5. The two electronic
states in such a situation have the same rotational quantum
number J, and at the point of closest approach would have
the same total energy. Both states are then pushed apart as
in other perturbation phenomena in a way proportional to
the r^{-2} matrix element and inversely proportional to their
energy difference. The magnitude of the perturbation is
greatest at the point of closest approach and decreases on
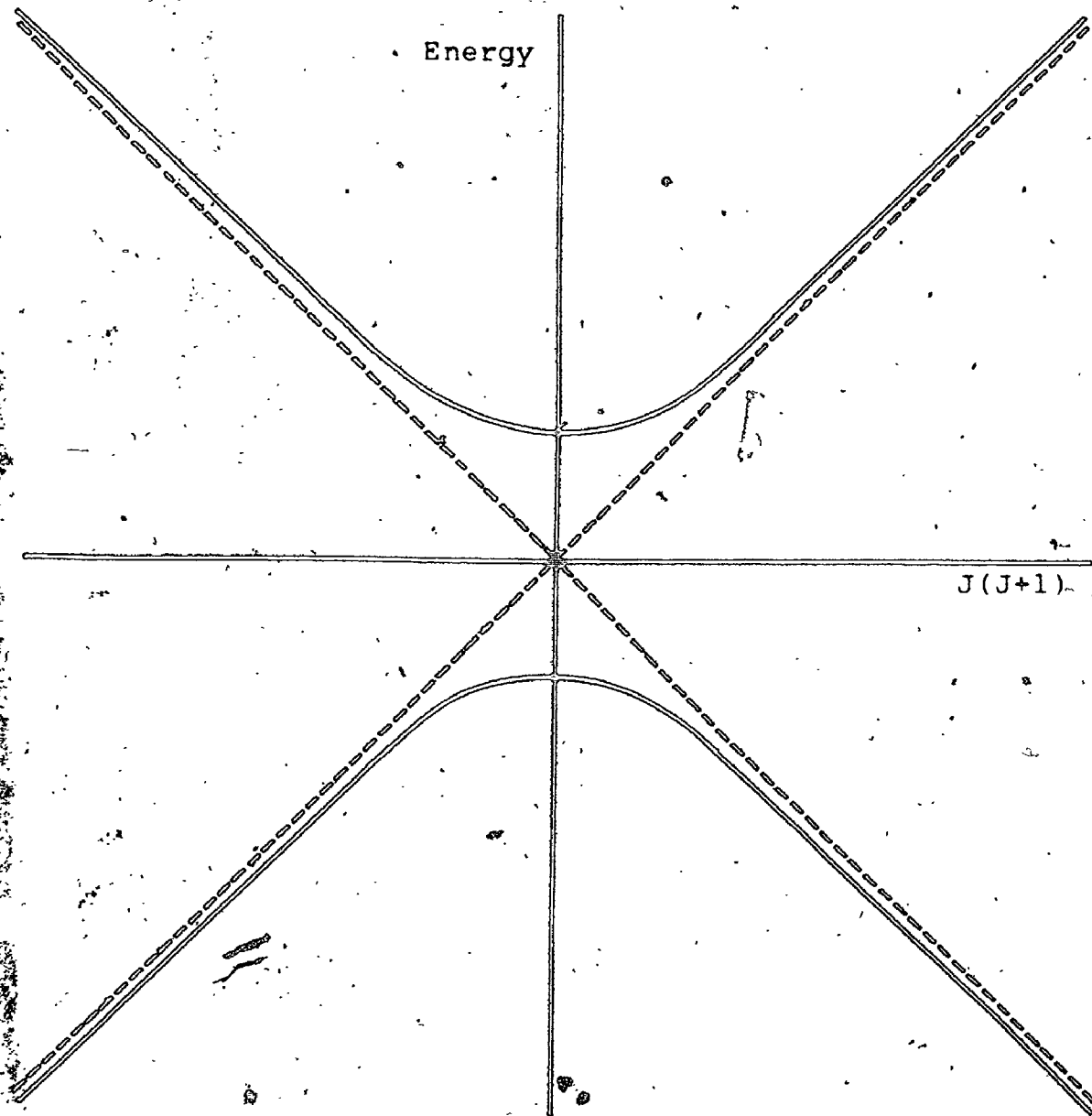
Figure 2.5 Perturbation of two energy levels as a function of J(J+1); the dotted lines represent the unperturbed levels and the solid lines the perturbed (actual) ones.

both sides (seen as the distance betwen the dotted and the solid line on Figure 2.5). Because such a phenomenon appears only at some J values in a vibrational level, it is sometimes called a rotational perturbation. The wavefunctions are assumed to be a 50-50 mixing of both states at the point of closest approach, therefore a label cannot be assigned to one state or the other.

It can happen frequently that two electronic states have the same energy but it is not common for this to occur while the selection rules for perturbation are respected. The sum of the rotational intensity distribution for the two states shows a usual dependence on $J(J+1)$. However, on an individual basis, one state can steal more or less intensity than the other for different J values [20]. At the point of closest approach, it can be expected that both signals ($\Delta\Omega=\pm 1$) have the same intensity, assuming a 50-50 mixing of the wavefunctions, but in practice, the distribution of intensity between the two signals has a unique behavior in each situation.

In summary, the electronic states of ICl are characterized by the value of their case (c) quantum number Ω. As states of different Ω approach one another, perturbations arise from this proximity producing Ω doubling for states with $\Omega \neq 0$. Contamination of the wavefunctions allows transitions to occur between states whose radiative combination is forbidden in the absence of perturbations.

CHAPTER THREE

POLARIZATION-LABELLING SPECTROSCOPY

This chapter gives a resume of the theory for the polarization-labelling spectroscopy which was developed in more detail by Teets [21] and Cross [22]. The experimental conditions are given later for both two- and three-beam configurations along with a typical signal.

The relatively new technique of polarization-labelling greatly simplifies crowded molecular spectra. It relies on the creation of a population of specific angular momentum asymmetric in M, by means of a narrow-band laser called the pump beam (see Figure 3.1). At the same time the pump leaves an asymmetric M population in the ground state. These populations cause an asymmetric absorption or transmission of a linearly polarized probe beam at frequencies corresponding to transitions to or from these labelled levels (see Figure 3.1). To find at which frequencies such transitions occur in the molecule, the
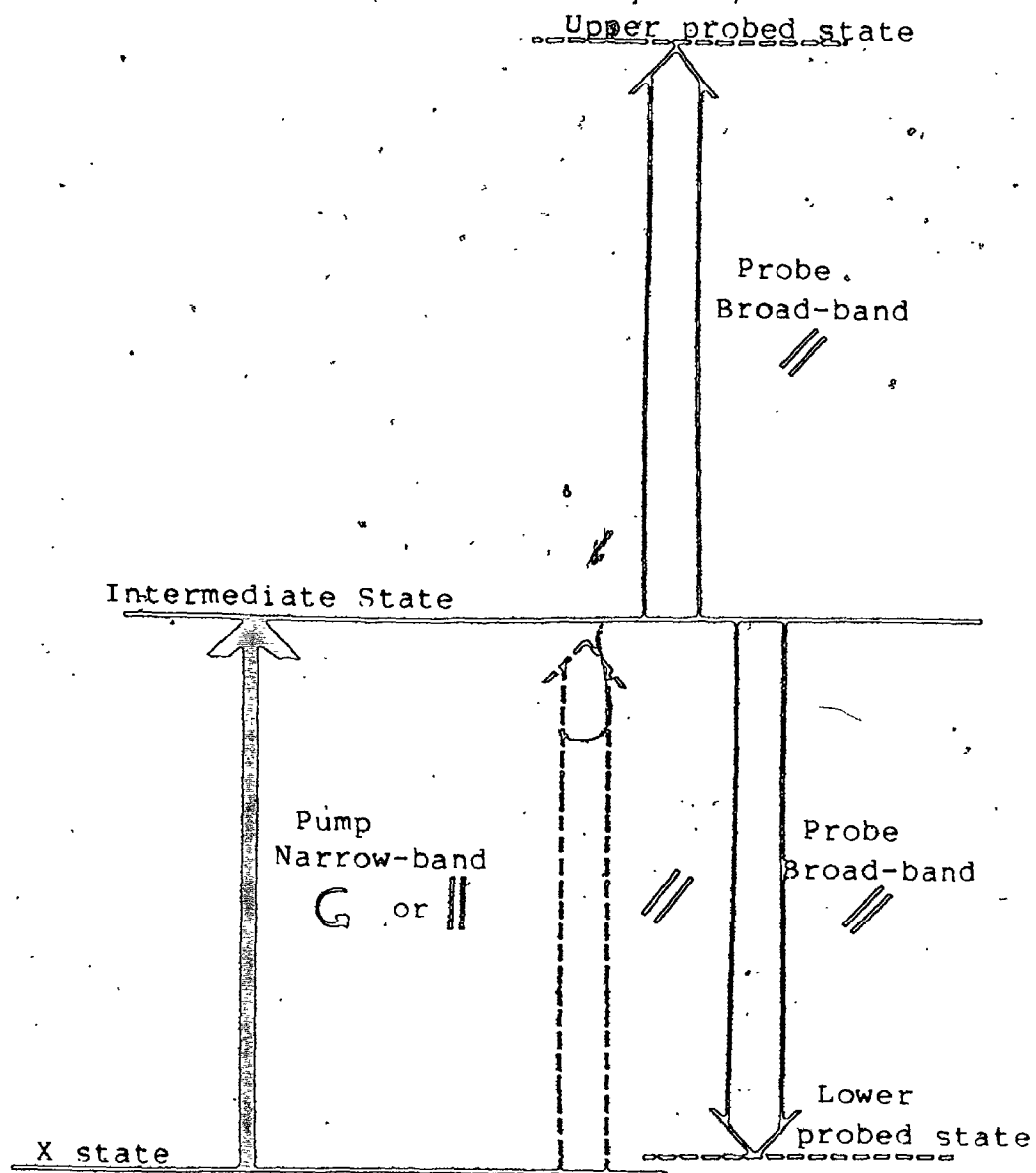
Figure 3.1 Typical optical-optical-double-resonance experiment with the polarization-labelling technique.

sample is placed between two crossed polarizers (one oriented at 90 degrees from the other in the probe beam axis). Then, the rotation of the plane of polarization of the probe allows only some frequencies to pass through the second polarizer (analyser) and to be received at the spectrograph. The assignment of these signals to specific transitions is much facilitated when the frequency of the pump is known.

3.1 Theory

a) Two-beam

Whenever electromagnetic radiation propagates through a dielectric medium, it induces a polarization of the medium. The electric field of the radiation is described by this wave equation (in cgs units)

$$\nabla \times (\nabla \times E) + \frac{1}{c^2}\frac{\partial^2}{\partial t^2}\{E + 4\pi P\} = 0 \qquad 3.1$$

where E is the electric field, P is the polarization of the medium and c the speed of light. P is expanded as a power series in the electric field, where the indices i,j,k,l refers to the x,y and z axes

$$P_i = \chi_{ij}E_j + \frac{\sum\sum\chi_{ijk}E_jE_k}{2} + \frac{\sum\sum\sum\chi_{ijkl}E_jE_kE_l}{6} \qquad 3.2$$

For plane waves propagating along the z axis, a solution to equation 3.1, considering P=0, has the form

$$E = A(z)\ \exp\ i(kz - \omega t) \qquad\qquad 3.3$$

where $A(z)$ is the amplitude of the wave and k is the wavenumber in radians per centimeter.

The first term of equation 3.1 becomes

$$\nabla \times (\nabla \times E) = -\left[\frac{\delta^2 A}{\delta z^2} + 2ik\frac{\delta A}{\delta z} - k^2 A \right]$$

$$\times\ \exp\ i(kz - \omega t) \qquad 3.4$$

and the differentiation of 3.3 with respect to time gives

$$\frac{1}{c^2}\frac{\delta^2 E}{\delta t^2} = A\left(\frac{\omega}{c}\right)^2 \exp\ i(kz - \omega t) \qquad\qquad 3.5$$

Then, equation 3.1 becomes

$$\left[\frac{\delta^2 A}{\delta z^2} + 2ik\frac{\delta A}{\delta z} - k^2 A + \left(\frac{\omega}{c}\right)^2 A \right]$$

$$\times\ \exp\ i(kz - \omega t) = \frac{1}{c^2}\frac{\delta^2}{\delta t^2}4\pi P \qquad 3.6$$

The two last terms in the upper brackets are eliminated, as $k = \omega/c$ by definition. The general form of the amplitude equation is [22]

$$\frac{\delta A_i}{\delta z} = 2\pi i \left(\frac{\omega_i}{c\eta_i}\right)\left[\chi_{ij}A_j + \frac{1}{6}\sum_{jkl}\chi_{ijkl}A_jA_kA_l\exp(iz\Delta k) \right.$$

$$\left. + \frac{1}{6}\sum_{j=1}^{3}\chi_{iijj}A_iA_jA_j^* + \dots \right] \qquad 3.7$$

where $\Delta k = k_j + k_k + k_l - k_i$ and i,j,k,l refer to the labels 1 for the signal, 2 for the probe and 3 for the pump beam.

By conservation of energy, $\omega_j + \omega_k + \omega_l - \omega_i$ is zero. The "phase matching" requirement given by $\Delta k = 0$ is needed to keep the exponential term close to unity. By doing so, the third-order susceptibility term is kept non-negligible. The polarization of the medium induces a change in its refractive index and absorption coefficient which can be expressed in term of the real and imaginary parts of the first order susceptibility

$$\eta_i = 1 + \frac{2\pi}{\eta_i} Re \, \chi_{ii} \cong 1 + 2\pi \, Re \, \chi_{ii} \qquad 3.8$$

$$\alpha_i = \frac{-4\pi\omega_i}{c} Im \, \chi_{ii} \qquad 3.9$$

where ω is the angular frequency in radians per second. Assuming solutions to equation 3.7 for the signal and the probe amplitude of the form

$$A_1(z) = M_1(z) A_2(0) \exp\left(2\pi i \frac{\omega_1}{c\eta_1} \chi_{11} z\right) \qquad 3.10$$

$$A_2(z) = M_2(z) A_2(0) \exp\left(2\pi i \frac{\omega_2}{c\eta_2} \chi_{22} z\right) \qquad 3.11$$

we get

$$M_1(\ell) = \sin\left[\frac{2\pi\omega_1}{c\eta_1} \frac{2}{3} \chi_{1233} |A_3|^2 \ell\right] \qquad 3.12$$

Therefore, after assuming the argument of the sine function is small, the leading term in the expression for the signal intensity depends on the square of the interaction length of the two lasers, the square of the pump intensity

and the first power of the probe beam intensity

$$I \quad \alpha \quad A_1^2(\ell) \quad \alpha \quad \left(\frac{2\pi\omega_1}{c\eta_1}\right)^2 \frac{4\chi_{1233}^2}{9} A_2^2(0) |A_3|^4 \ell^2$$

$$\times \exp\left[\frac{4\pi i\omega_1}{c\eta_1} \chi_{11} \ell\right] \qquad 3.13$$

The above equation describes qualitatively the signal amplitude in the case of a small signal with a circularly polarized pump and a plane polarized probe beam. The approximations used to derive equation 3.13, namely steady-state solutions with short-pulse durations, a beam frequency resonant to the transition and a small intensity signal, may not be reasonable in some cases. In practice, we may not have the same pulse profile as used in the calculations and a beam frequency well in resonance with the transition.

An equation for χ_{1233} is derived by Cross [22] who shows that χ_{1233} is proportional to the square of the dipole moment coupling the ground state and the interme-diate level pumped, and to the difference of the square of the dipole moments for the right and left circular compo-nent of the probe, at a signal frequency

$$\chi_{1233} \quad \alpha \quad |\mu_{ba}|^2 \left\{ |\mu_{ca}|^2 - |\mu_{da}|^2 \right\} \qquad 3.14$$

where the pump is tuned to the transition $b \leftarrow a$ and the probed transitions are $c \leftarrow a$ and $d \leftarrow a$; μ_{ij} is the dipole moment coupling the j level to the i level.

It is an appropriate time to examine the M-dependence (not shown here in 3.14) of the absorption cross-section. The allowed transition with a right circularly polarized pump beam is (M+1) ← M. The absorption cross-section for R and Q branch transitions is plotted in Figure 3.2. An R branch transition shows a strong M-dependence for right circularly polarized light, giving preference to large positive M; the same is true for the P branch at large negative M. A Q branch transition is favored by a linear polarization, which can be thought of as a beam of a right(+) circularly polarized component in phase with a left(-) circularly polarized one. A pump beam in resonance with a transition creates a population asymmetric in M in both lower and upper level of that transition:

Two different values of the absorption coefficient can be measured by using a right and a left circularly polarized beam. The same phenomenon is observed for the refractive index. The components (+) and (-) of a linearly polarized probe each see a different absorption cross-section (see Figure 3.2) when interacting with an M-asymmetric population. This circular dichroism, $\alpha_+ - \alpha_-$, introduces some ellipticity in the probe polarisation. The birefringence of the medium due to different refractive indices, η_+ and η_-, seen by each component of the probe (right and left circularly polarized) rotates the plane of polarization of the probe. This is how the polarization-

$$J \longrightarrow J + 1$$
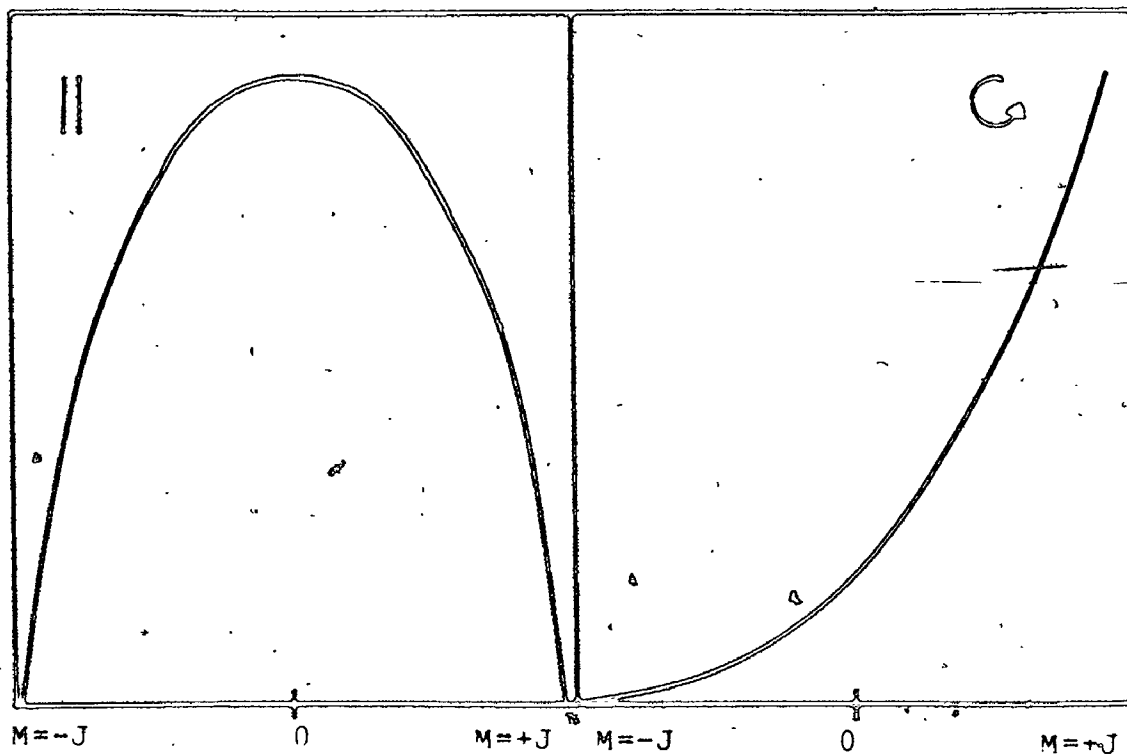
$$J \longrightarrow J$$
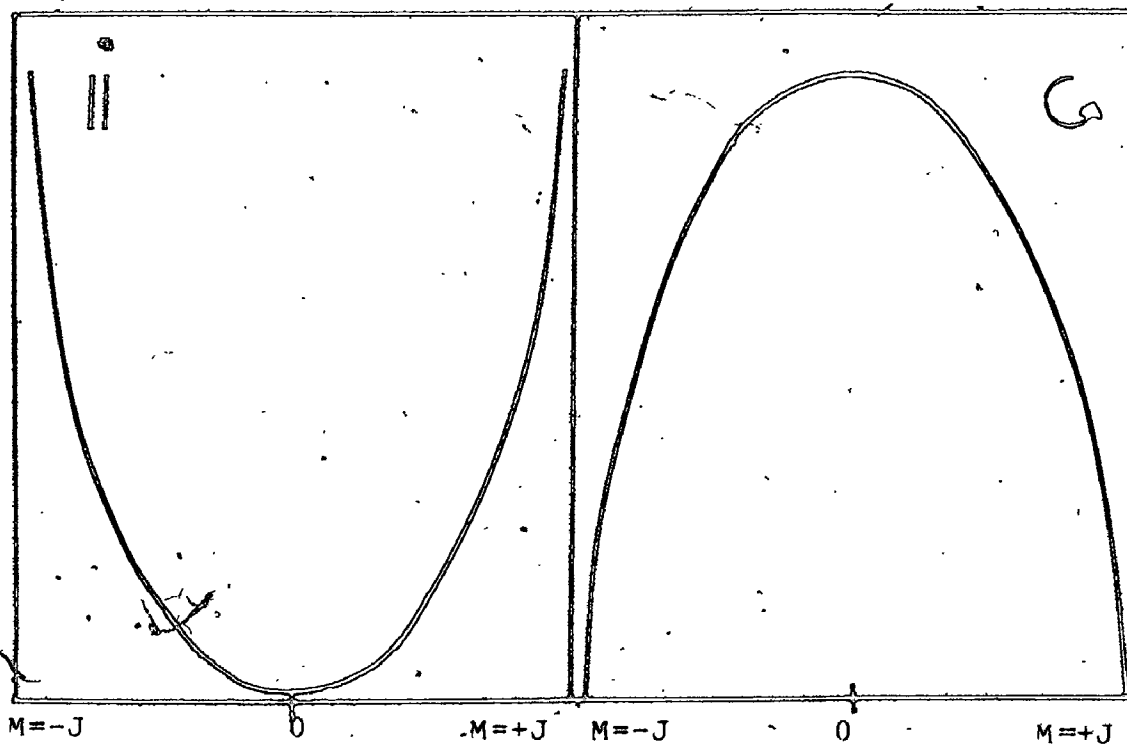
Figure 3.2   Absorption cross-section in function of M,
part A is for R transition and part B for Q transition,
the left and right are for plane and right circularly pola-
rized light.

labelling technique works with a circularly polarized pump creating an asymmetric upper and lower population.

When we work with a linearly polarized pump, this one creates symmetric populations in M (or very close to symmetric) in both upper and lower states. The probe polarization is set at 45 degrees to the pump plane and is best seen as composed by two linearly polarized component at 90 degrees one to the other. One component is interacting primarily with one of the two populated states resulting in a slight rotation of the overall plane of polarization of the probe which then gives a signal.

It is worth mentioning that Yamashita [24] developed an equation based on first order result of Maxwell's equation (3.1) relating the signal intensity to the square of the circular dichroism, to the square of the interaction length in the sample and to the probe intensity. Unfortunately, in his development, he neglected the non-linear effects so important in polarization-labelling.

b) Three-beam

An experiment with three overlapping laser pulses of short duration is a non-subtle affair. The use of two narrow-band lasers as pumps is strongly recommended to sufficiently populate the upper level sought. Figure 3.3A shows the two kinds of three-photon signal produced by a first configuration of laser beam polarization. The two
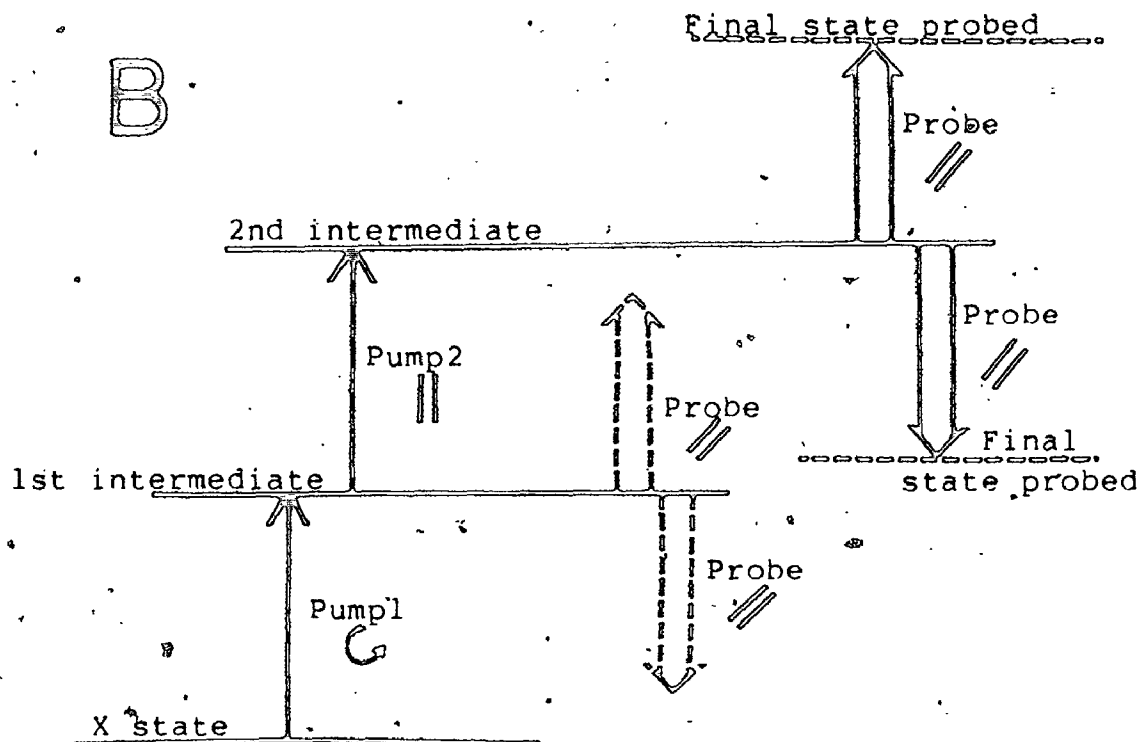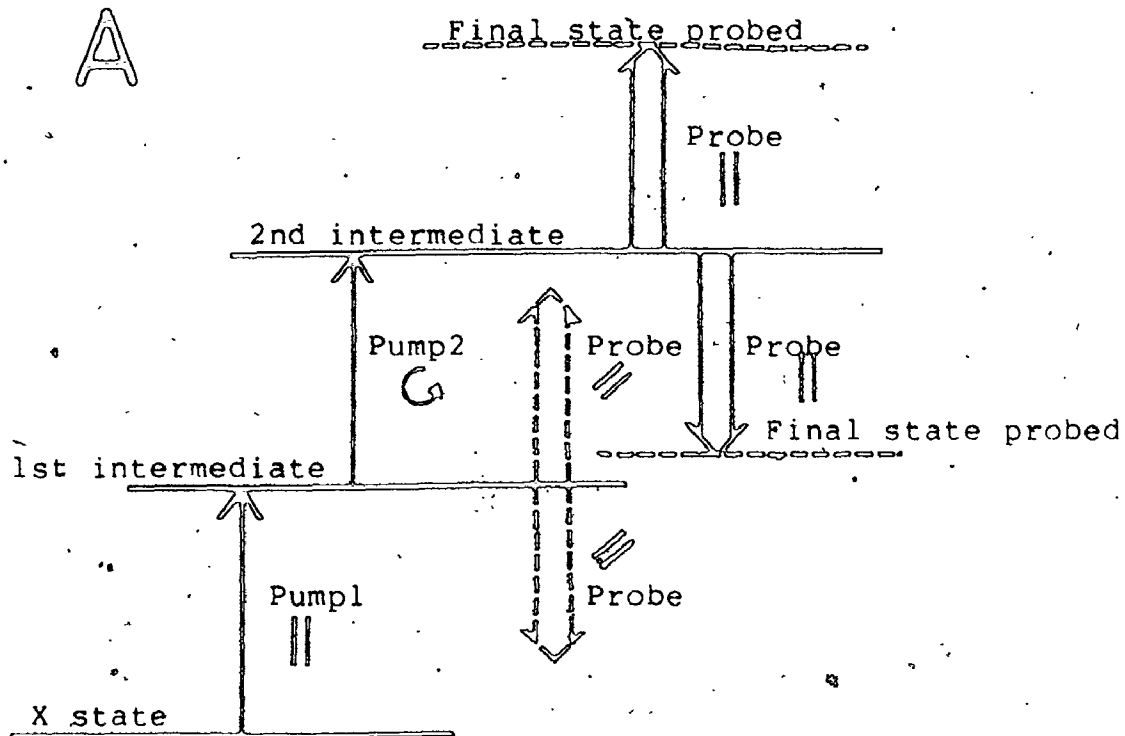
Figure 3.3 Two schematic representations for a three-beam polarization-labelling experiment; A: pump1 and pump2 are respectively plane and circularly polarized, B: the polarization of the two pumps are reversed.

last steps, pump 2 and probe, correspond to the same two steps sequence as above with the difference that, in the three-beam experiment, these two steps do not start from a Boltzmann population in the ground state. With this scheme, the f substates are probed preferentially, the selection being accomplished by the first pump. Figure 3.3B illustrates another configuration which accesses the e substates of the intermediate and final levels using circular polarization in the first stage. In the two configurations, both two- as well as three-photon signals can be recorded by the spectrograph.

The scheme of interest in this study is the one where the probe induces downward transitions from the second intermediate level. This technique is called stimulated enhanced emission polarization-labelling, SEEPOL [25], where the probe may, in fact, experience intensity gain at the frequency of interaction with the sample to give a signal. It is beyond this study to develop an expression for the signal intensity generated by the interaction of three different beams of light on the same molecule. Equation 3.13 gives a qualitative description for a two-photon signal of small intensity.

3.2 Experimental

The experimental arrangements are represented schematically on Figure 3.4. A Lumonics laser model TE-
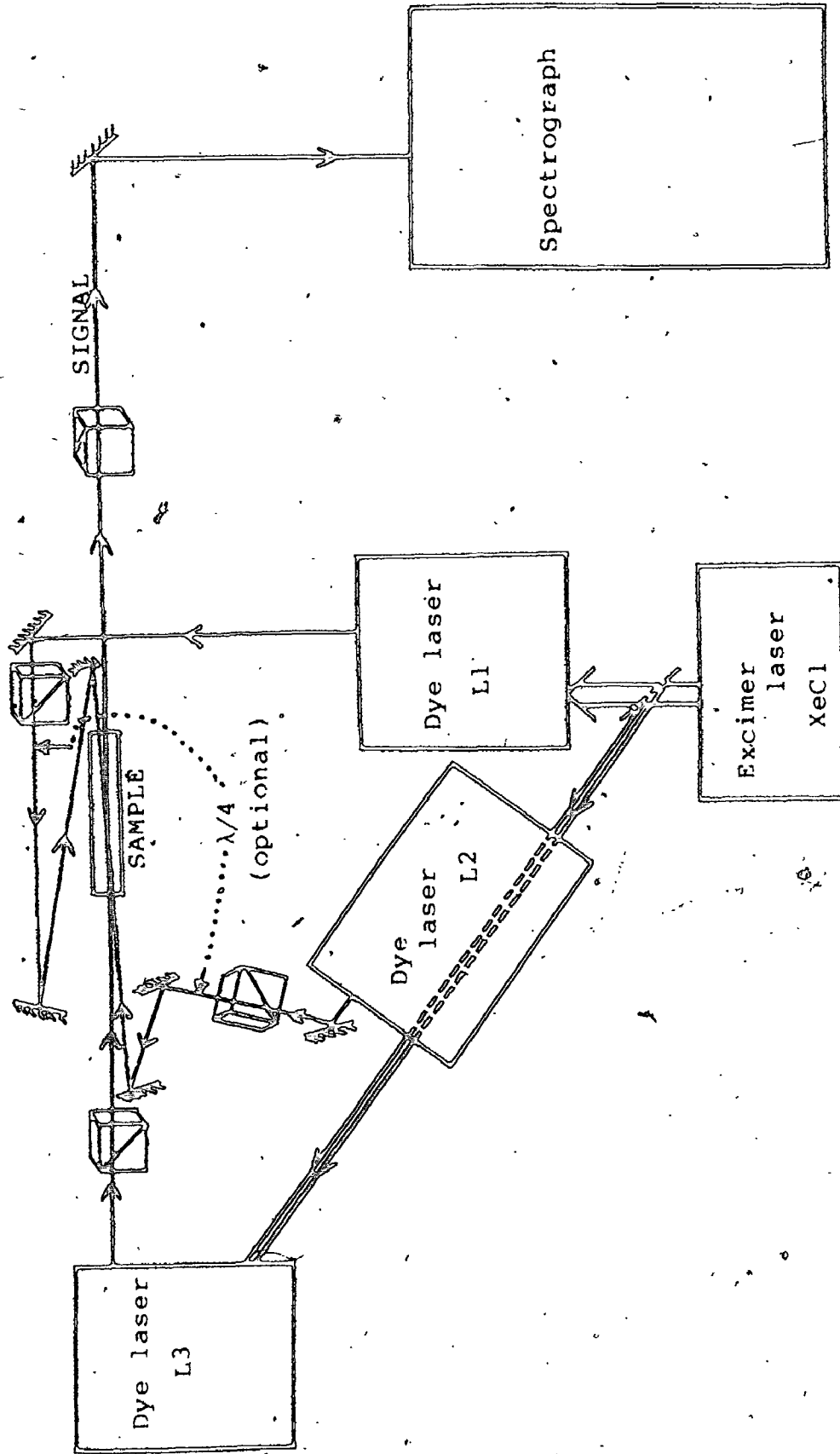
Figure 3.4 Experimental arrangements to carry two- and three-photon polarization labelling experiments. The dye lasers L1 and L2 produced the beams for Pump1 and Pump2 which can either be plane or circularly polarized. The probe beam (L3) is plane polarized.

861T** was operated as a XeCl laser at 6 to 8 pps. The peak power at 308 nm was 4 to 9 MW per pulse of approximately 10 ns. This beam was split a few times to pump the two or three dye lasers necessary to the experiment.

The dye laser L1 (see Figure 3.4) was a Lumonics model EDP-330 equipped with an intra-cavity beam expander and a dye circulator. Its output beam, plane or circularly polarized, and having a linewidth smaller than 0.3 cm^{-1} , was used as the first pump. The dye laser L2 was a Molectron model DLII-14P giving a typical linewidth of about 0.4 cm^{-1} without etalon. This laser was only used for three-photon experiments and, depending upon need, was either linearly or circularly polarized. It was aligned in such a way that its beam was coincident with the L1 beam, but travelling in the opposite direction. The quarter-wave plates used were stressed quartz blocks whose pressure was adjusted at the operating wavelength. The third laser was operated in broad-band mode, with a frequency bandwidth ranging up to several hundred cm^{-1} depending upon the dye used (see Table 3.1); this probe beam was always plane polarized. This laser consisted of an oscillator stage with output coupler and a plane end-mirror, and an in-line amplifier stage, both pumped tranversely.

The sample of ICl (natural isotopic mixture) from Eastman was distilled in the sidearm of either a 20cm or a 6cm cell equipped with flat silica windows and was kept

Table 3.1 List of dyes used during this work with the lasing range and maximum lasing wavelength as stated by the manufacturer (Exciton Inc. or Lambda-Physics for QUI only).

Dye	Solvent	Lasing wavelength(nm)	
		Range	Maximum
p-Terphenyl PTP	p-dioxane	336-355	342
TMQ	p-dioxane	344-366	356
PBD	Toluene:Ethanol (1:1)	358-386	367
BBQ	p-dioxane	368-393	387
QUI	p-dioxane	363-395	386
DPS	p-dioxane	397-417	407
Stilbene 420	Ethanol	405-467	425
Coumarin 440	Ethanol	425-464	440
Coumarin 460	Ethanol	442-482	460
Coumarin 480	Methanol	461-514	480
Rhodamine 590 R6G	Methanol	566-610	583
Rhodamine 610 RhB	Methanol	588-644	600
Rhodamine 640	Ethanol	608-668	618

just below room temperature. The pressure of ICl under these conditions was relatively high, about 36mbar (27mmHg), which favors the development of collisional satellites allowing more data to be gathered on average per experiment. The signal was directed through a cylindrical lens onto the slit, 30 to 70 μm wide, of a 3.4m f/35 Ebert-mounted Jarrell-Ash spectrograph. Real-time exposure ranged between 7 and 50 μs. Spectra were recorded in the 13th to 17th order on a 50cm (20in) camera, using Kodak Tri-X-Pan film. Calibration lines from a Fe/Ne hollow cathode lamp were superimposed just before or after each spectrum and their wavelength values from Crosswhite's table [26] were used.

The dyes used for L1 were Rhodamine 590 (R6G), Rhodamine 610 (RhB) and Rhodamine 640 to cover a spectral range from ~580 to ~645nm, with peak power between 0.1 to 0.7MW per pulse (~8ns). The L2 beam was generated with BBQ, QUI or Coumarin 440 to cover a range from ~380 to ~400nm and ~430 to ~445nm, with peak power of 30 to 150kW per pulse (~8ns nominal). The probe beam L3 had to cover a very broad spectral range, ~340 to ~485nm, thus a series of dyes was used : p-terphenyl (PTP), TMQ, PBD, BBQ, QUI, DPS, Stilbene 420, Coumarin 440, Coumarin 460 and Coumarin 480. All these dyes were from Exciton (see Table 3.1), except for QUI (Lambda-Physics), and had different peak power, 10 to 90kW per pulse (~8ns nominal), related to the

conditions of usage. The powers stated were measured before any polarization device and do not reflect the losses due to that process.

The signal lines and the Fe/Ne lines making the calibration were measured on a comparator with a resulting precision of ~5μm. The final term values for a two-photon experiment were obtained by summing the measured frequency of the signal and the appropriate A state term value taken from the extensive table of Hulthén and others [4]. Each transition assignment was made by comparing the pump frequency to the difference between the term values for the A state [4] and the ground state [3] in conjunction to the frequency difference between P and R branches in the probed transition to the final state. In a three-photon experiment, the two pump frequencies were measured and identified in relation to the P-R splitting in the A' state. The A' term values were given by the difference between the D' state terms (in regions well characterized) and the measured signal frequencies.

In a two-photon experiment, the pump and probe beams counter-propagated and, once L3 was aligned with the axis of the spectrograph, the two beams were crossed through an aperture of ~0.1mm. For a three-photon experiment, the exercise is more elaborate. Once the probe is correctly aligned, the two pumps are in turn crossed with the probe using the same aperture. Fortunately, in most experiments,

fluorescence intensity was monitored visually in optimizing the final crossing of the two pumps.

A typical signal of a two-photon experiment is shown on Plate 3.1 along with its assignment; it is of some interest to notice that the intensity of the D'+A signal is sometimes stronger than some collisional satellites of the very intense β+A pair.

frequency →
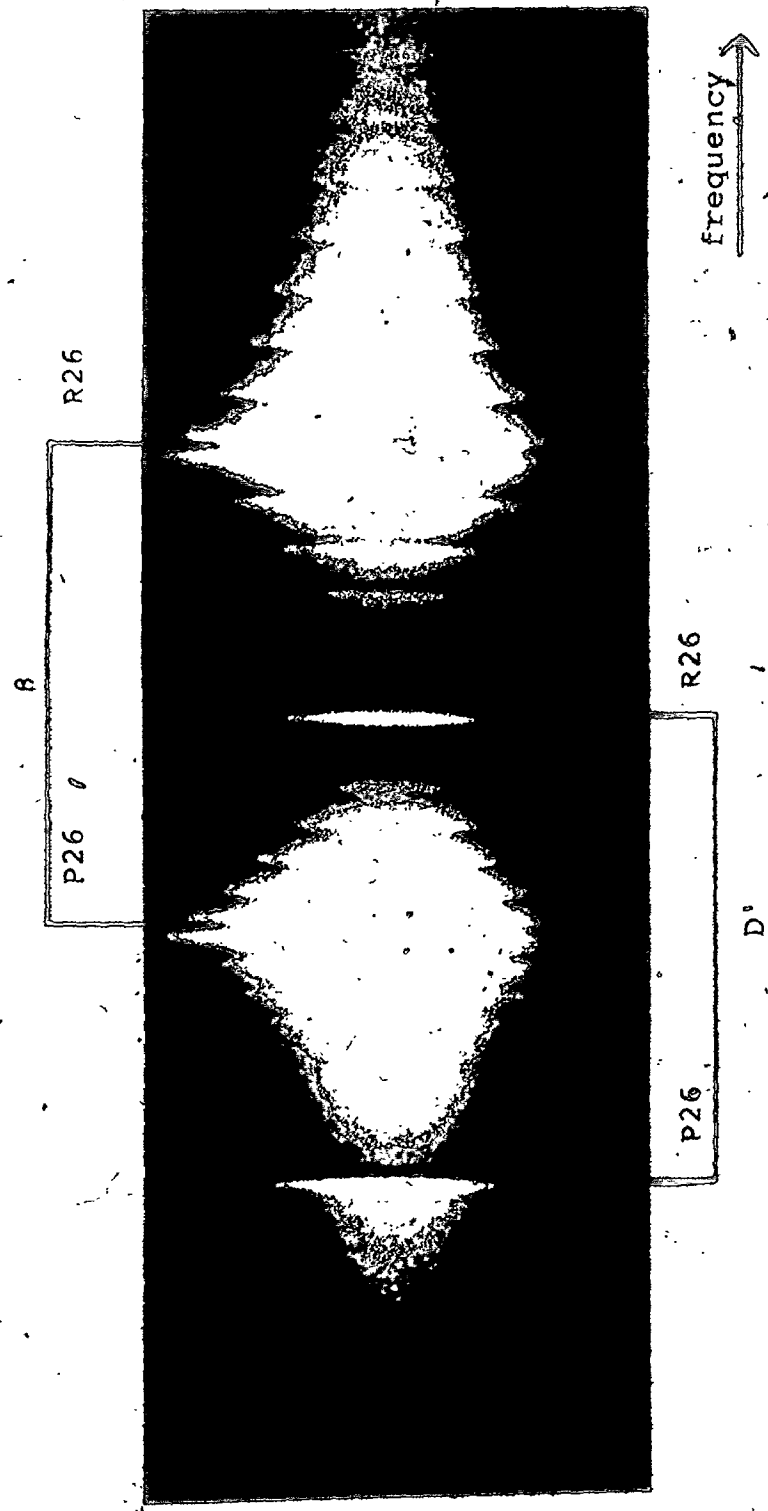
Plate 3.1 . Typical D' A signal beside β A signal; the pump was tuned to a Q26 transition, A(v=27)←X(v=0) at 17116.350cm^{-1} and the probed signals are the P26 and R26 pairs going to v=25 of the D' and β states, respectively weak and strong.

CHAPTER FOUR

ELECTRONIC STATES OF ICl

The valence states of ICl show some similitude to those of iodine, I_2. Therefore, the label given to the ICl states are related to the ones for iodine [2]. The manifold of electronic states leading to a specific dissociation can be obtained with the build-up principles given by Herzberg [12]. The procedure will be outlined in this chapter for the four dissociation limits leading to neutral I and Cl and the three first ionic dissociation limits which give I^+ and Cl^-. A brief summary of the known electronic states of ICl is given for valence as well as for the ion-pair states.

4.1 Build-up principles

In the case of iodine monochloride, Hund's coupling case (c) considers a strong coupling between L and S

$$J_a = L + S \qquad\qquad 4.1$$

Thus far, we have worked everywhere with case c signatures for ICl; for comparison with I_2, Cl_2, and the literature at large, Table 4.1 gives the corresponding case a signature for valence states of ICl. By combination of all possible M_{J_a} for each atom, all molecular state labels leading to such atoms upon dissociation are obtained by

$$\Omega = \left| M_{J_{a1}} + M_{J_{a2}} \right|. \qquad\qquad 4.2$$

States with $\Omega \neq 0$, differing only in sign of both $M_{J_{a1}}$ and $M_{J_{a2}}$ form a degenerate pair. States with $\Omega = 0$ are labelled (+) or (-) according to the character of a reflection in a plane including the molecular axis; (+) refers to a symmetric total wavefunction and (-) to an asymmetric one. For ICl, there are always an even number of valence states 0 correlating to one dissociation limit; consequently, there are an equal number of 0^+ and 0^- states.

For example, the first dissociation limit gives $I(^2P_{3/2})$ and $Cl(^2P_{3/2})$; $J_{a1} = J_{a2} = 3/2$ lead to the values of $\Omega = 3, 2, 1, 0, 1, 2, 3, 2, 1, 0, 1, 2, 1, 0, 1, 0$. The manifold is then composed of ten different electronic states labelled 3, 2(2), 1(3), $0^+(2)$, $0^-(2)$ where $\Omega \neq 0$ states each encompass two substates named e and f.

With the same manipulation, five electronic states lead to the second dissociation limit: $\Omega = 2, 1(2), 0^+, 0^-$.

Table 4.1. Summary of the known electronic states of $I^{35}Cl$. (in units of cm^{-1} and 10^{-1}nm)

State Signature (c) (a)	T_e	ω_e	$10^2 B_e$	r_e	Dissociation Limit	Reference
$X(0^+)(^1\Sigma^+)$	0	384.324	11.41546	2.32	$I(^2P_{3/2}) + Cl(^2P_{3/2})$ (17557.57)	10
$A'(2)(^3\pi_2)$	12682.05	224.57	8.653	2.666		5
$A(1)(^3\pi_1)$	13742.9	211.0	8.529	2.685		this work
$a(1)(^3\pi_1)$	17338.0	72.85	3.820	4.01		26
$B(0^+)(^3\pi_0)$	17375.58	204.271	8.6523	2.666		27
$B'(0^+)(^3\pi_0)$	18155	~30	~4.5	~3.7	$I(^2P_{3/2}) + Cl(^2P_{1/2})$ (18439.9)	29
$b(1)$	18273.9	25.06	3.586	4.14		29
$b'(2)(^3\Delta_2)$	18275.7	31.20	3.497	4.19		9
	18029.1	~0.7	~5.6	~3.7		9
----	---	---	---	---	$I(^2P_{1/2}) + Cl(^2P_{3/2})$ (~25166)	1

Table 4.1 (suite)

State Signature (c) (a)	T_e	ω_e	$10^2 B_e$	r_e (Å)	Dissociation Limit	References
----	----	----	---	---	$I(^2P_{1/2}) + Cl(^2P_{1/2})$ (~ 26043)	
E (0⁺)	39059.485	165.676	5.8029	3.255	$I^+(^3P_2) + Cl^-(^1S_0)$ (~ 72554)	8 6
D'(2)	39061.830	173.627	5.4782	3.350		8
β (1)	39103.666	170.310	5.6707	3.292	$I^+(^3P_1) + Cl^-(^1S_0)$ (~ 79651)	8
(1)	45552.805	184.854	5.8931	3.231		30 32
f (0⁺)	44923.79	184.40	5.777	3.26	$I^+(^3P_0) + Cl^-(^1S_0)$ (~ 79006)	31 32

The third dissociation limit is associated with a manifold composed of exactly the same labels. The fourth dissociation leads to $I(^2P_{1/2})$ and $Cl(^2P_{1/2})$. Only three electronic states compose this manifold, $\Omega = 1$, 0^+ and 0^-.

The electronic states giving ions upon dissociation are called ion-pair states. The first family or cluster of ion-pair states is correlated upon dissociation to $I^+(^3P_2)$ + $Cl^-(^1S_0)$; they are electronic states with $\Omega = 2$, 1, and 0^+ sometimes called a family of states with the same J_a complex. It is assumed that J_a (molecular or total) is defined and that one M_{J_a} (atomic) in equation 4.2 stays the same while the other takes different values. The symmetry of the 0 state is deduced from the value of Ω for the top member (largest Ω) of the family : if even, the symmetry of the 0 state is positive, if odd, the symmetry is negative. (The rule is similar for the valence states above; but J_a would probably not be a defined quantity for them).

The next two ion-pair states, $\Omega = 1$ and 0^-, correlate upon dissociation to $I^+(^3P_1)$ and $Cl^-(^1S_0)$. The dissociation leading to $I^+(^3P_0)$ and $Cl^-(^1S_0)$ is correlated with only one 0^+ state.

4.2 Valence states of ICl

Of the states correlated with neutral atoms upon dissociation, the best-known are the $X(0^+)$ and $A(1)$ states.

The X state is characterized by a large vibrational frequency, $384.293 cm^{-1}$, and a small equilibrium bond distance of 0.232nm (2.32Å) [3] (see Table 4.1). The first dissociation energy has been determined to be at $17557.57 cm^{-1}$ [5]. The A state dissociates at the same energy, but its minimum is at $13742.9 cm^{-1}$ [26]. It has a smaller vibrational frequency, $209.1 cm^{-1}$, and a bond distance at equilibrium of 0.269nm (2.69Å).

The next state characterized is the B (0^+) state which dissociates adiabatically into two neutral atoms in their ground state (1st dissociation) due to a crossing with an $\Omega = 0^+$ dissociative state [5] (in iodine, the B state is correlated to the 2nd dissociation limit). This crossing gives two minima to the B state in ICl and generates another state (adiabatic) labelled B' correlating to the second dissociation.

A weakly-bound state with $\Omega = 1$ leading to the first dissociation has been identified by Brand and others [7,27]. It has a characteristic electronic energy of $17338.0 cm^{-1}$, a vibrational frequency of $32.85 cm^{-1}$ and a potential depth of only $219.6 cm^{-1}$. Out of ten electronic states correlated to the first dissociation, only four had been observed and more or less characterized before this work. Only recently, Spivey and others [1] have published a partial fit for A' $(\Omega = 2)$ state, which is dealt with in more detail in this thesis.

The second dissociation limit relates to a manifold of five electronic states. The diabatic B state would correlate with this limit [28] but, as mentioned earlier, is restructured into adiabatic B and B' states by an avoided crossing. The adiabatic B' state has been characterized with a T_e of 18155 cm^{-1}, an ω_e of ~ 30cm^{-1} and r_e of ~ 0.37nm [29]. Two other states, $\Omega = 1$ and 2, have been observed in our laboratory with a large internuclear distance at equilibrium, 0.42nm and a small well depth, $D_e \sim 160$cm^{-1} [9].

None of the electronic states correlated with the third and fourth dissociation have yet been observed. Figure 4.1 represents the Rydberg-Klein-Rees (RKR) potential curve of the known electronic states for I^{35}Cl.

4.3 Ion-pair states

The previously known ion-pair states of the first family, lying lowest, were E (0^+) and β (1) whose potential minimum lie within the remarkable narrow range of 39059 to 39104cm^{-1} [6]. These states are strongly bound, have similar internuclear distances at equilibrium, 0.326 to 0.329nm, and only slightly different vibrational frequencies, 165.7 and 170.3cm^{-1} [8]. Even if the first 6000cm^{-1} are characterized in both states, much more data are needed to cover the entire potential depth of ~ 35000 cm^{-1}. With so many similarities, it is not surprising to find that these states perturb one another. The third
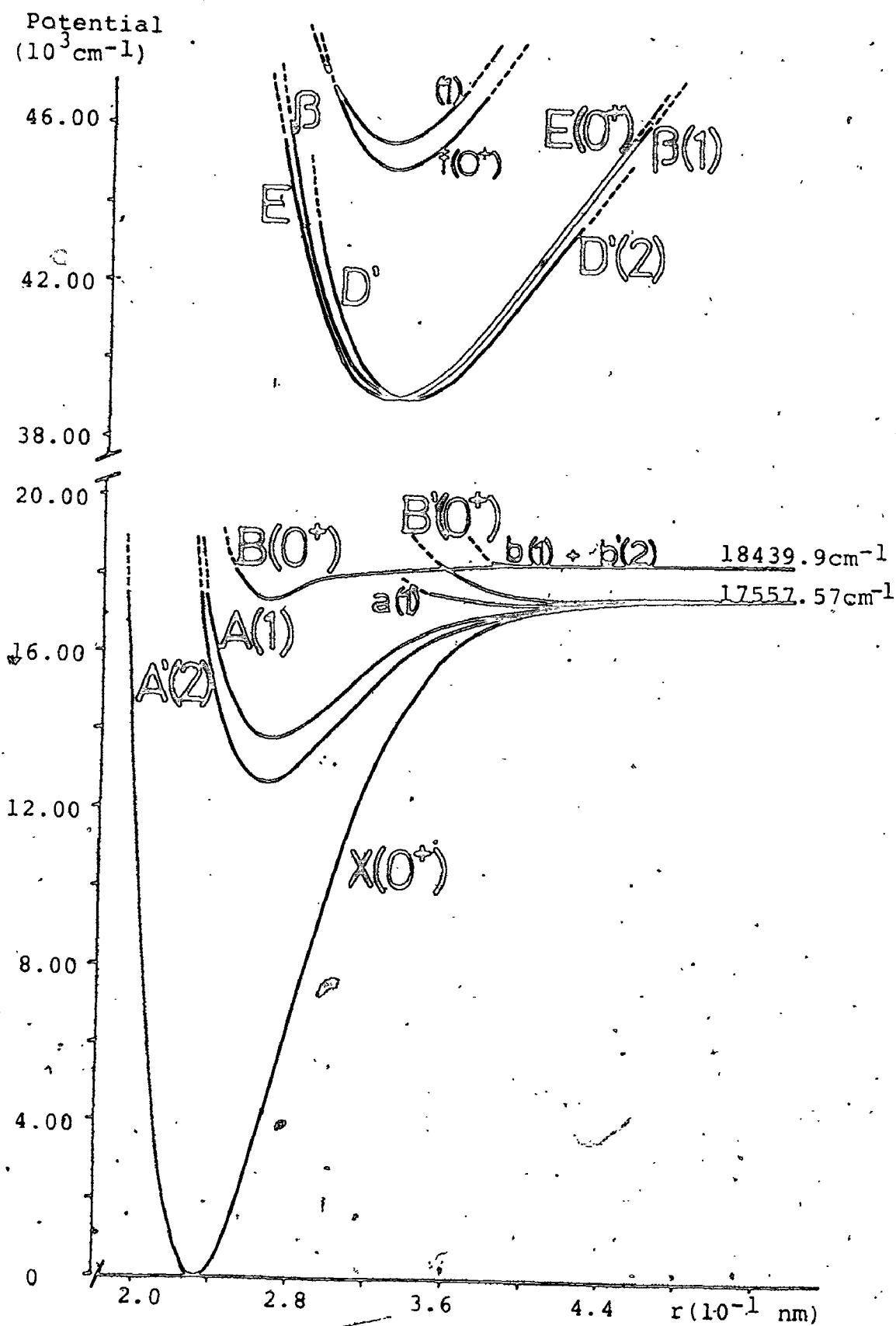
Figure 4.1 RKR potential curves of known states for $I^{35}Cl$.

member, D' ($\Omega=2$), by comparison with I_2, is believed to lie very close to the other two and perhaps be perturbed by them too. The ion-pair state D' makes the other subject of this thesis.

The second family of ion-pair states has revealed only the $\Omega=1$ state, the 0⁻ state being inaccessible with our technique. It has a T_e of 45552.8cm⁻¹, a vibrational frequency of 184.9cm⁻¹ and an equilibrium distance of 0.32nm (3.2Å) [30].

The only member of the third family, the f (0^+) state, shows a T_e of 44923.8cm⁻¹, a vibrational frequency of 184.4cm⁻¹ and internuclear bond of 0.326nm (3.26Å) at equilibrium. In spite of the relatively small energy gap between the f state and the $\Omega=1$ state, Ω doubling has not been detected in the latter (in the portion observed) [31].

In summary, of the six lowest ion-pair states of ICl, four were rather well known in the region near their minimum. Characterization of the third member of the first cluster of ion-pair states, namely the D' ($\Omega=2$) state, is described in chapter 5. The allowed transition from this ion-pair state to the lowest excited state A' ($\Omega=2$) enables us to characterize that state, extending the technique of polarization-labelling from two to three steps.

CHAPTER FIVE

Ion-pair state D' ($\Omega=2$)

The third member of the first cluster of ion-pair states is called D' ($\Omega=2$) by analogy with the physically similar D'(2g) state of molecular iodine (I_2). This state is very strongly bound as to be expected by its diabatic dissociation channel into ions. The three members of that cluster lie within a very narrow range of $50cm^{-1}$ (see Figure 4.1) [8]. This situation prepares the ground for the only way currently available to access the D' state from X by Optical-Optical-Double-Resonance : by heterogeneous perturbation with the neighboring β ($\omega=1$) state.

The fact that these three states all lie in such a narrow range is very interesting and is a beautiful subject of study by itself. Before this work was undertaken, D' state was not characterized and one of the other two states showed difficulties to fit a Dunham expansion. A better knowledge of the third member of the family was sought to help clarify the situation. As D' is the

lowest ion-pair state in other halogen molecules, it has a prominent role as upper level in fluorescence experiments [32]. The same phenomenon is expected in ICl. A good characterization of D' potential may then be of great help in fluorescence studies.

The experimental conditions used to access D' are first stated, followed by a description of the results and a discussion of the two avoided crossings observed. A comparison of the constants for rotational-electronic coupling within the cluster of three ion-pair states is made with the Van Vleck pure precession case.

5.1 Experimental

All spectra were recorded by Optical-Optical-Double-Resonance (OODR) using the polarization-labelling technique. The apparatus and procedure involved were described in chapter 3. The different dyes used in the pump were Rhodamine 590 (R6G) and Rhodamine 610 (RhB) and in the probe were BBQ, QUI, DPS, Coumarin 440 and Coumarin 480 (see Table 3.1).

The access through β made use of a heterogeneous perturbation which is the result of fine electronic-rotation interactions. Theoretical calculations by Dr A.R. Hoy[11] showed that there is a good mixing of wavefunctions between β and D' at the bottom of the potential with a fast exponential decrease as v increases. In this

region, the signal intensity is proportional to the r^{-2} matrix element between β and D' (see equation 2.43) and dependent on the value of the rotational quantum number J which rendered low J data difficult to get. When $v_{D'}$ is in the range $v=15-30$, the r^{-2} matrix element is unfavorable but this is more than compensated for by the fact that the energy difference between vibrational levels of β and D', with $v_{\beta} \equiv v_{D'}$, is getting gradually smaller. The signal strength in this higher region is mainly inversely proportional to ΔE between the same v's of β and D'.

5.2 Results

With restrictions mentioned above, data were recorded for $v=0-2$, where two avoided crossings between D' and E states at $v=0$ and 1 are well characterized. As predicted, signals with small intensity were photographed for $v_{D'}=15-18$ and stronger ones for $v_{D'}=20-28$. We were unable to distinguish D' signals from collision satellites of the strong $\beta - A$ signals when $v_{D'} > 28$.

a) Low vibrational levels

The bottom of the D' potential shows a very interesting phenomenon : two avoided crossings occur at different J for $v=0$ and 1 between $D'(\lambda=2)$ and $E(\lambda=0)$. But direct interactions between states with $\Delta\lambda>1$ are strictly forbidden by the selection rules for perturbations (see section 2.4.a). Consequently, there should be a crossing of the

two potential curves in a first approximation. Examination of the experimental procedure facilitates the understanding of the situation. Whenever a strong signal results from probing the β-A-X sequence, satellite signals representing D'←A and E←A appear to the red of the β←A transition signals. This means that both D' and E states have their wavefunctions mixed with that of β by heterogeneous perturbation resulting from an electronic-rotational interaction. From that, D' and E wavefunctions are no longer considered pure but are hybrid or mixed wavefunctions and can interact together, through their "acquired β properties".

The fact that the probe gives P and R signals means that the transitions recorded by this technique are of $\Delta\Omega=0$ nature. Then from the intermediate level $A(\Omega=1)$, the second transition leads to a state of $\Omega=1$ character. This is also supported by the fact that the intensity ratio between D' and β stays the same for the same J and same v regardless of which vibrational level is pumped in A state [7]. Therefore, the perturbation must happen in the final state, D'.

When two states have equal energy, the same J and same parity, there is an avoided crossing (see Figure 5.1) [12]. This means that, if these conditions were not met, there would be a crossing of the potential curve of the two states without interactions between them. As in this
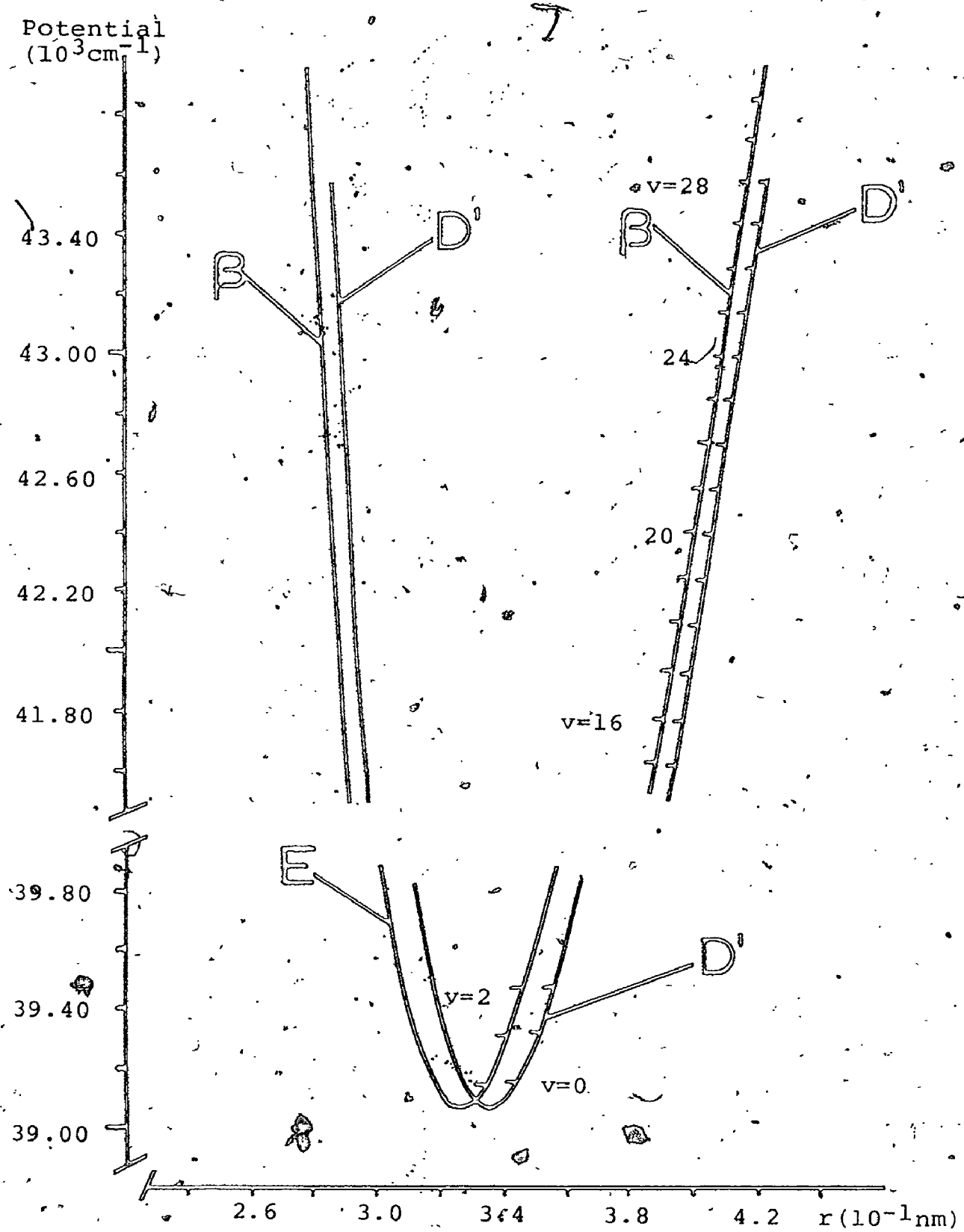
Figure 5.1 The D' potential curve is shown beside the E
one at the bottom and the β one at higher v, for $I^{35}Cl$
(energy relative to the ground state minimum).

case the conditions are fulfilled, the crossing is avoided (adiabatic situation) and the rotational-vibrational energy levels are not readily fit by a simple Dunham expansion. This is probably the main cause of trouble in trying to fit the bottom part of E state with its higher vibrational levels.

Enough data were cumulated at v=0 and 1 to clearly show the two avoided crossings between the e sublevel of D' and the E state. The f sublevel of D' is left unaffected by the heterogeneous perturbation as shown by the straight line which goes without deflection through the avoided crossing region (see Figure 5.2). The $E(0^+)$ state has only an e sublevel and therefore does not show an unperturbed level. For v=0, the point of closest approach is $J=46$ where the coupled levels are ~1.5cm^{-1} apart (see Figure 5.2). The total intensity stolen by E and D' signals from β increases with J instead of with J(J+1) as predicted by simple perturbation theory (see section 2.4). The distribution of intensity between the two signals follows a pattern of its own where, for a particular J value, the upper root (higher energy term) of E,D' pair is not mixed with β and therefore has no intensity (see Figure 5.3). This is explained by looking at a 3X3 matrix where E,D' terms are degenerate. It factorizes into a 2X2 and a 1X1 matrix, the latter being unmixed with β.
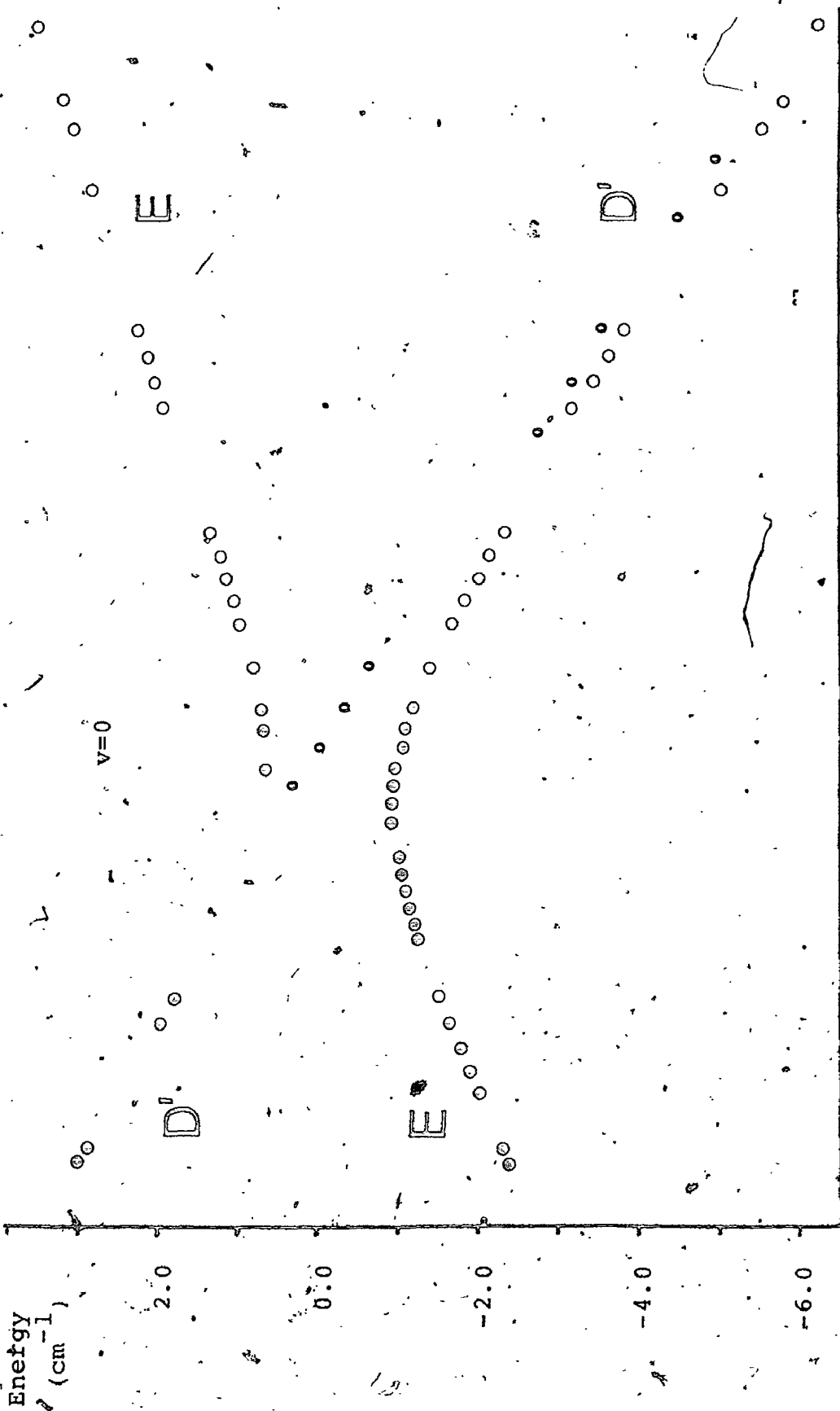
Figure 5.2 Differential energy $(G_{vJ} -39145 -0.056J(J+1))$ as a function of $J(J+1)$, at vibrational level 0 for D' and E states of $I^{35}Cl$; o for e sublevel and o for f sublevel.
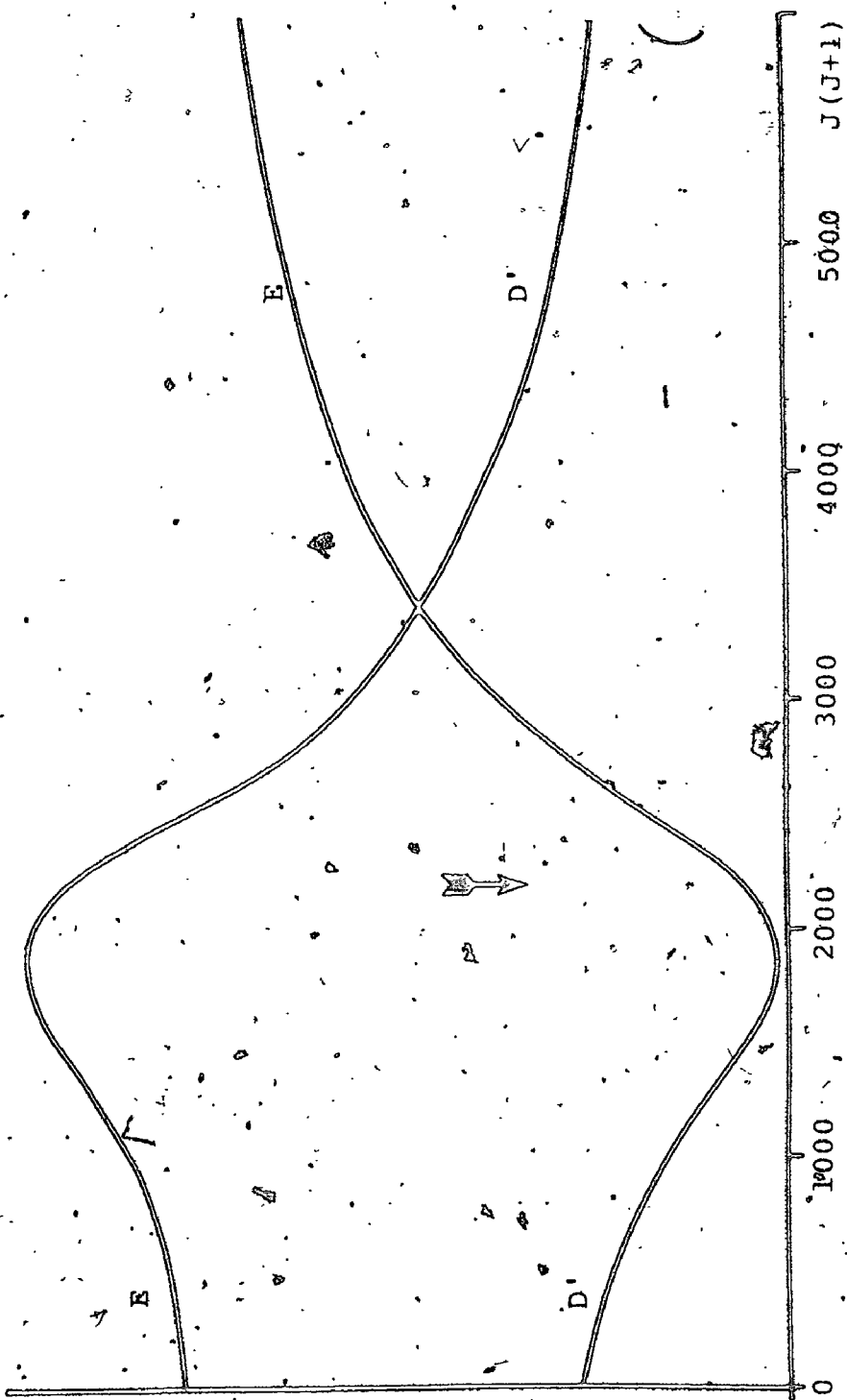
Figure 5.3. Calculated intensity divided by $J(J+1)$ for vibrational level 0 of D' and E states of $I^{35}Cl$. The arrow marks the point of closest approach.

Table 5.1. Dunham parameters for D' ($\Omega=2$) ion-pair state of $I^{35}Cl$ from simultaneous fit with β and E states up to v=30, including the interaction parameter $W_{1,2}$ (all in units of cm^{-1}).[a]

$Y_{0,0}(\approx T_e)$	39061.830[b]	(0.080)[c]
$Y_{1,0}(\approx \omega_e)$	173.6275	(0.035)
$Y_{2,0}(\approx -\omega_e x_e)$	-0.55722	(0.0027)
$10^4 Y_{3,0}(\approx \omega_e y_e)$	9.169	(0.56)

e sublevel

$10^2 Y_{0,1}(\approx B_e)$	5.4782	(0.0041)
$10^4 Y_{1,1}(\approx -\alpha_e)$	-2.019	(0.010)
$10^8 Y_{0,2}(\approx -D_e)$	-2.03	(0.56)

f sublevel

$10^2 Y_{0,1}(\approx B_e)$	5.4786	(0.0065)
$10^4 Y_{1,1}(\approx -\alpha_e)$	-2.054	(0.028)
$10^8 Y_{0,2}(\approx -D_e)$	-2.21	(0.12)

$W_{1,2}$	1.860	(0.077)
r_e $(10^{-1} nm)$	3.350	

a) Stated to reproduce the fit within its standard deviation [33].
b) Relative to the ground state minimum.
c) Errors stated are 3σ.

$$\begin{vmatrix} a & d & 0 \\ d & b & e \\ 0 & e & c \end{vmatrix} \rightarrow \begin{vmatrix} a & d & 0 \\ d & b^* & 0 \\ 0 & 0 & c^* \end{vmatrix} \equiv \begin{vmatrix} a & d \\ d & b^* \end{vmatrix} + \begin{vmatrix} c^* \end{vmatrix}$$

This occurs for a J just below the J of closest approach. Exactly the same thing is observed for v=1, with a J of closest approach around 70 (see Figure 5.4).

With D' state now characterized, that region of the potential is better known and it is possible to do a simultaneous non-linear least-squares fit of the three states to three Dunham expansions including an off-diagonal rotational constant of the form of equation 2.43 [8]. Table 5.1 shows the Dunham parameters for D' from the simultaneous fit (up to v=30 for E and β). The parameters $W_{\Omega, \Omega \pm 1}$ are quite well determined and can be compared to Van Vleck pure precession values for Hund's case c (equation 2.45 and 2.46) which assumes that $J_a = L + S$ is defined (see Table 5.2).

Table 5.2 · Theoretical and experimental values of the electronic-rotational coupling element for Ω=2, 1 and 0.

	Theory	This work
$W_{1,2}$	2.0	1.860
$W_{1,0}$	2.45	2.384
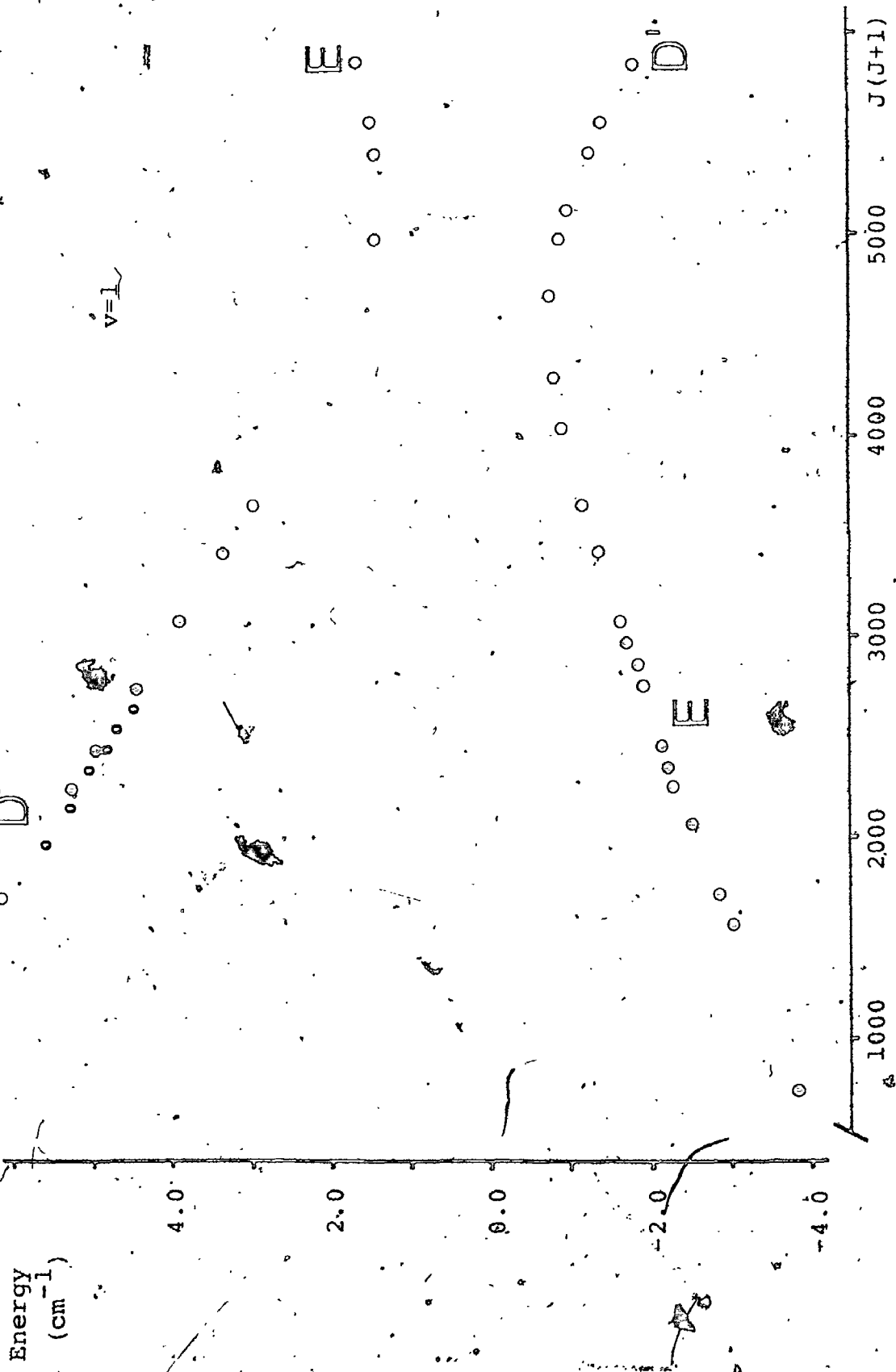
Figure 5.4 Differential energy as a function of $J(J+1)$ for $v=1$ of D' and E states of $I^{35}Cl$.

$W_{1,2}$ and $W_{1,0}$ obtained from the fit of our data are respectively 93% and 97% of Van Vleck pure precession values. This shows that the three states of the first cluster of ion-pair states of ICl are very similar to the pure precession case determined by Van Vleck and are close to the ideal situation of Hund's coupling case c.

As a strongly bound electronic state, D' is expected to be strongly harmonic at the bottom of its potential. By comparing the α_e determined by the simultatneous fit, $2.019(0.010) \times 10^{-4} cm^{-1}$ and $2.054(0.028) \times 10^{-4} cm^{-1}$ (see Table 5.1) to the α_e^M of a Morse potential, $2.27 \times 10^{-4} cm^{-1}$ (equation 2.28), we see that they are very close to one another. The first centrifugal distortion constant, $D_e = 2.18 \times 10^{-8} cm^{-1}$ (equation 2.29) falls within the error margin of the two D_e's of the fit, $2.03(0.56) \times 10^{-8} cm^{-1}$ and $2.21(0.12) \times 10^{-8} cm^{-1}$, confirming the harmonic character of the lower portion of D' state of ICl.

Table 5.3 lists the off-diagonal rotational constant $B_{1,2}$, the term values and the RKR potential up to v=28 for D' state of $I^{35}Cl$. It was necessary to include another rotational constant off-diagonal in state (as above) and in v (not listed in this table) to have a satisfactory convergence of the fit [8]. Their estimation by perturbation theory were accurate enough in this situation.

Table 5.3 Vibrational term values and RKR potential for D' state of $I^{35}Cl$ from simultaneous fit of the three ion-pair states and from a simple fit of v=15 to 28 of D' state (in units of cm^{-1} relative to the ground state minimum, and 10^{-1} nm).

v	$10^2 B_v$	G_v	r_{min}	r_{max}	G_v'	$10^2 B_v$	r_{min}	r_{max}
		0 – 30				.15 – 28		
0	494	39148.5	3.269	3.438				
1	375	39321.0	3.213	3.506				
2	271	39492.4	3.177	3.556				
3	179	39662.8	3.148	3.597				
4	100	39832.0	3.123	3.634				
5	31	40000.1	3.102	3.669				
6	−25	40167.1	3.083	3.701				
7	−73	40333.1	3.066	3.731				
8	−112	40498.0	3.050	3.760				
9	−143	40661.8	3.035	3.788				
10	−167	40824.4	3.021	3.815				
11	−184	40986.3	3.008	3.841				
12	−196	41146.9	2.996	3.867				
13	−203	41306.5	2.984	3.892				
14	−205	41465.1	2.973	3.916				
15	−204	41622.6	2.963	3.940	41622.5	5.156	2.966	3.943
16	−199	41779.1	2.953	3.964	41779.1	5.136	2.956	3.967
17	−192	41934.6	2.943	3.987	41934.6	5.116	2.946	3.990
18	−183	42089.0	2.934	4.010	42089.0	5.096	2.937	4.013
19	−172	42242.5	2.925	4.033	42242.5	5.077	2.928	4.036
20	−160	42394.9	2.916	4.056	42394.9	5.057	2.919	4.058
21	−147	42546.4	2.908	4.078	42546.3	5.037	2.911	4.080
22	−133	42696.8	2.900	4.100	42696.7	5.017	2.902	4.103
23	−119	42846.3	2.892	4.122	42846.2	4.998	2.895	4.124
24	−105	42994.7	2.885	4.144	42994.7	4.978	2.887	4.146
25	−91	43142.2	2.877	4.166	43142.2	4.958	2.879	4.168
26	−77	43288.7	2.870	4.187	43288.7	4.938	2.872	4.189
27	−63	43434.3	2.863	4.209	43434.3	4.918	2.865	4.210
28	−50	43578.8	2.857	4.230	43579.0	4.899	2.858	4.231

b). Higher vibrational levels

We signals were photographed for $v_{D'}$ =15-18 and progressively stronger signals for $v_{D'}$ >20, with a peak intensity around $v_{D'}$ =25 as predicted by Dr. Hoy's calculations. The gap from v=3 to 14 is not serious as it is situated in the lower portion of D' state which is not very anharmonic. At the present time, it is not possible to obtain signals in this gap, due the restrictive hetero- geneous perturbation with β; the difference in energy between these two states keeps increasing as $v_{D'}$ decreases lower than 15 and permits no more observable signals. Even if signals extend to $v_{D'}$ =28, only the lower part (~12%) of that strongly bound state is covered in this work.

For convenience, we made a Dunham fit from $v_{D'}$=15 to 28 which is essentially equivalent to the simultaneous fit in that region (see Table 5.3 and Table 5.4). While the e and f sublevels were treated separately in the procedure and the fit, the two sets of rotational constants were averaged together to make the RKR potential curve.

In the low 20's, the R branch of D'←A signal lies practically beneath the P branch of the β←A pair. This makes the data quite sparse and hard to get precisely. The P and R branches of both states get closer and closer as v increases in the range of $v_{D'}$ =22-28 (see Plate 5.1). This

*NOTE Weak D' signals at v=27 may not be visible on Plate 5.1.

Table 5.4 Effective Dunham parameters for D'
($\Omega=2$) state of $I^{35}Cl$ for v=15 to 28 (in units of cm^{-1})[a]

$Y_{0,0}$	39056.614^{b}	$(3.1)^{c}$
$Y_{1,0}$	174.3908	(0.44)
$Y_{2,0}$	-0.594116	(0.020)
$10^3 Y_{3,0}$	1.50167	(0.30)
e sublevel		
$10^2 Y_{0,1}$	5.4625	(0.011)
$10^4 Y_{1,1}$	-1.979	(0.043)
$10^8 Y_{0,2}$	-1.350	(0.61)
f sublevel		
$10^2 Y_{0,1}$	5.4420	(0.012)
$10^4 Y_{1,1}$	-1.922	(0.047)
$10^8 Y_{0,2}$	0.813	(0.82)

a) Stated to reproduce the fit within its standard
   deviation [33].
b) Relative to ground state minimum.
c) Errors stated are 3σ.
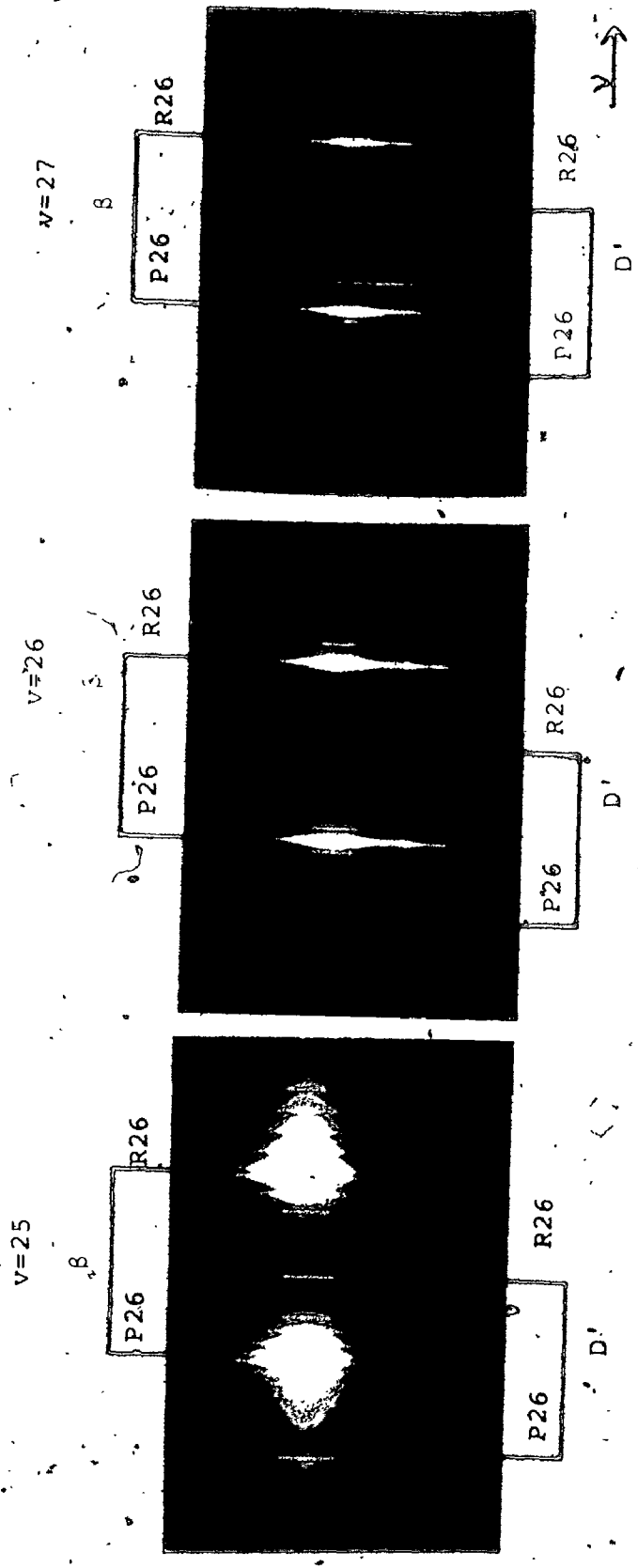
Plate 5.1 Vibrational progression of a two-photon experiment to $v=25,26,27$ of D' and β state, P26 and R26 pairs. As v increases, the D' pair gets weaker and closer to the β pair.

provides an experimental confirmation that the energy gap
between D' and β is getting narrower (see Figure 5.1). A
short extrapolation indicates that an avoided crossing is
expected near $v_{D'}=31$ between D' and β states. The isotope
shift holds everywhere confirming a good v numbering.

At $v_{D'}$ larger than 28, it is no longer possible to
discern D' signals in the face of interference from the
collision satellites of the strong β+A pairs. The Ω-
doubling, which distinguishes the e and f sublevels, is of
the order of or smaller than the standard deviation of the
fit throughout the range of observation (see Table 5.1).
However, we have kept the distinction between them for a
matter of consistency.

The centrifugal constant, D, $1.35(0.61)\times10^{-8}cm^{-1}$, used
in the fit from $v_{D'}=15$ to 28, e sublevel, is only slightly
smaller than its value at equilibrium, $2.03(0.56)\times10^{-8}cm^{-1}$.
A range of more than ten vibrational levels is covered by
that D and there seemed to have no need for a vibrational
dependence. These two points provide further evidence for
the harmonicity of D' state of ICl.

In summary, the lower portion of the D' (Ω=2) state of
ICl is now well characterized bringing to five the number
of known ion-pair states out of the six lowest ones. The
D'(2) state is very similar to $E(0^+)$ and β(1) states which
are members of the same cluster of ion-pair states; they

all have similar values for electronic energy, vibrational energy and equilibrium internuclear distance. (see Table 4.1). We have gathered extensive data to map two avoided crossing between the D' and E states, and helped resolve fitting problems associated with the first cluster of ion-pair states of ICl. The characterization of D' ($\Omega = 2$) state can be of great help in fluorescence experiments [1] because it is one of the lowest ion-pair state where an excited ICl molecule will most likely start to fluoresce (if enough energy is given to it). The transition D'$\rightarrow$A' is believed to be more intense than E$\rightarrow$B, E$\rightarrow$X or $\beta \rightarrow$A in ICl, as it is the case in I_2 and Br_2 [34]. The three lowest ion-pair states are very good examples of the Van Vleck pure precession case with Hund's coupling case (c).

CHAPTER SIX

Valence state A' ($\Omega=2$)

With the ion-pair state D' ($\Omega=2$) well characterized, it becomes possible to look for valence states of $\Omega=2$ signature (case c). The only one believed to be moderately bound [2] is the A' ($\Omega=2$) state which is the first excited state above the ground state. By analogy with the iodine molecule, A' is expected just below the A ($\Omega=1$) state. The D'-A' transition is considered as a parallel transition ($\Delta\Omega=0$) and therefore fully allowed. A lasing action has been observed particularly for that same transition in I_2.

This chapter first gives the experimental conditions for gathering A' signals, then presents the results and their treatment by different fitting methods, the Dunham expansion and a near-dissociation expansion. A long-range theory by LeRoy [35] is also used to evaluate the behavior of the centrifugal distortion constants near dissociation.

1.0

2.8   2.5

3.2   2.2

3.6

4.0   2.0

1.1   1.8

1.25   1.4   1.6
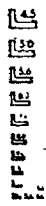
with the help of the C_5 constant.

6.1 Experimental

All spectra were recorded by Optical-Optical-Triple-Resonance (OOTR), in an ↑↑↓ sequence, using the polarization-labelling technique described in chapter 3. In pump1, Rhodamine 590 (R6G), Rhodamine 610 (RhB) or Rhodamine 640 were used; in pump 2, BBQ, QUI and Coumarin440 served as dyes; in the probe, we used p-Terphenyl (PTP); TMQ, PBD, BBQ, QUI, DPS, Stilbene 420 and Coumarin 440. The three lasers were adjusted to be resonant with chosen rovibrational levels in the sequence $X \rightarrow A \rightarrow D' \rightarrow A'$ (see Figure 6.1). The three-photon signals were generally as strong or stronger than their two-photon counterpart. It is probable that the conditions were sometimes fulfilled for the sample to amplify the probe at signal frequencies.

The A' term values were obtained by subtracting the measured signal frequencies from the D' term value of the specific v,J level populated by the two pumps. In so doing, we have to keep in mind that the term values of D' come from a fit with a standard deviation of $0.04 cm^{-1}$.

By using the vibrational levels 21 to 27 of D', we have recorded signals terminating on the levels $v=2-14$ of A' by vertical transitions from the inner wall of D', and signals in $v=20-38$ by vertical transitions from the outer wall of D' (see Figure 6.2). Via $v=0 \rightarrow 1$ of the ion-pair
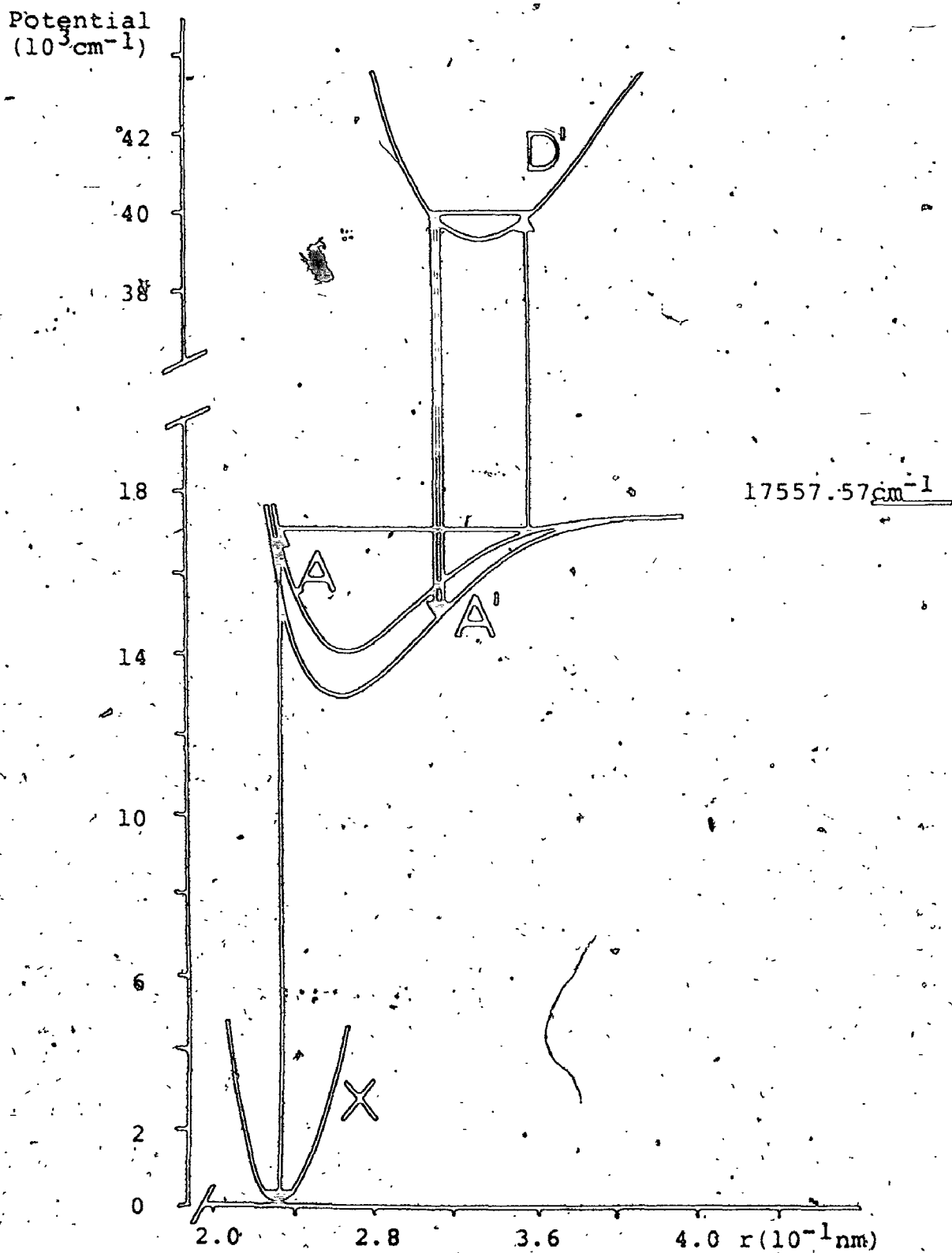
Figure 6.1 Experimental scheme of the sequence X→A→D'→A' in ICl.
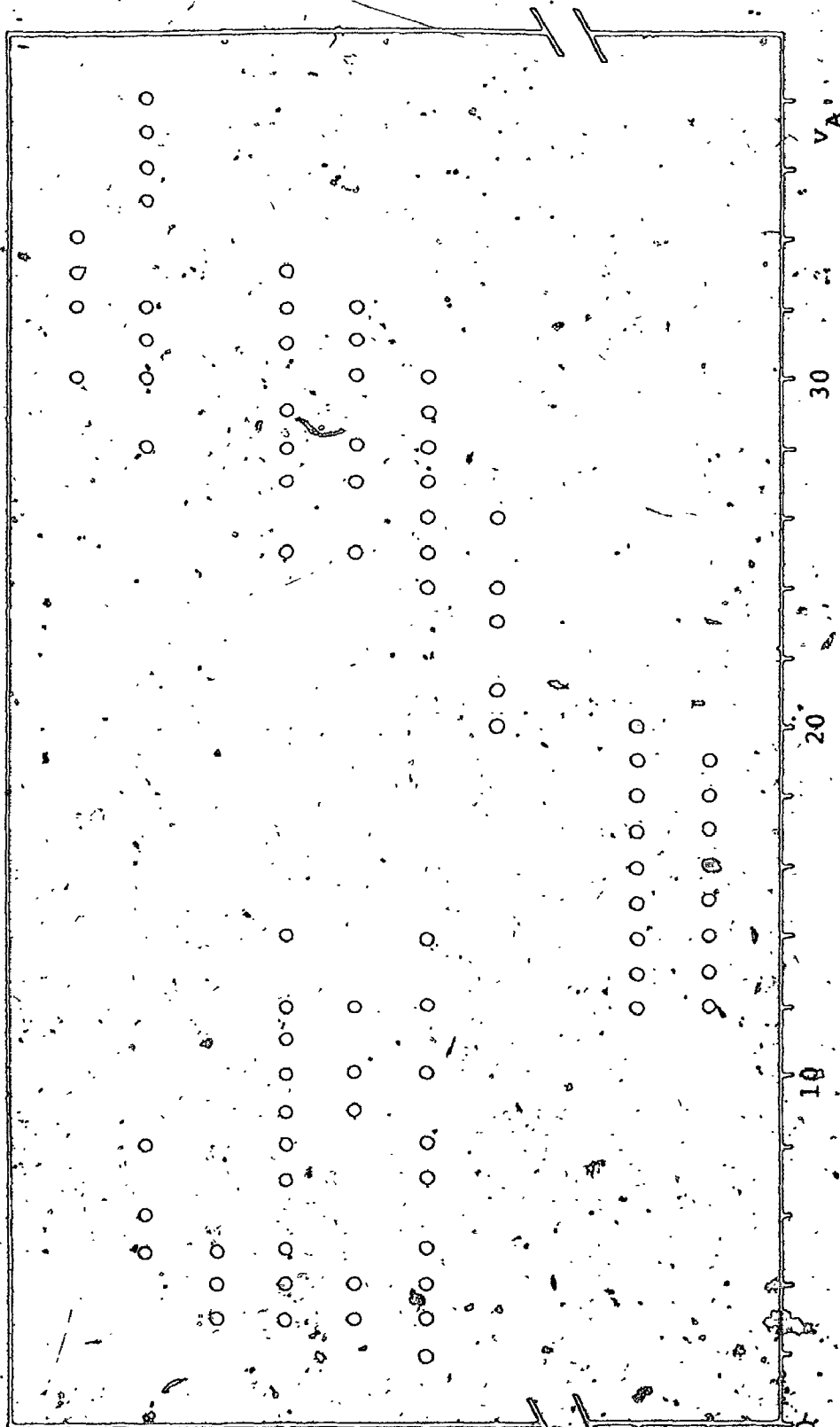
Figure 6.2 Tabulation of the vibrational levels accessed in A' state by probing the vibrational levels of B' state in $I^{35}Cl$.

state, we photographed signals to v=12-20 of A'. Unfortunately, we were not able to record any v=0 and 1 signals in A' due to inherent technical limitations. Figure. 6.3 shows the range of J covered in each vibrational level of A' state of ICl. The lack of low J values was compensated for by a deliberate search for high J values, even though this put some stress on the determination of the centrifugal distortion constants.

6.2 Results

The A' (Ω=2 or $^3\pi_2$) state of ICl is very anharmonic. This makes it difficult to fit all levels to the usual Dunham expansion, and at the same time requires the use of centrifugal distortion constants D_v, H_v and L_v. We have determined the centrifugal constants via a partial RKR potential, v=0-36, using it as input to a set of Schrödinger equations solved for five different J values. This led to stable results for centrifugal distortion constants up to v=32, but results were judged to be unreliable at higher vibrational levels.

It is possible to estimate the value of the centrifugal constants near dissociation with the LeRoy long-range theory [35]. This theory assumes that the two atoms lie sufficiently far apart that their electronic clouds overlap negligibly. Therefore, their interaction energy can be expressed as a sum of inverse-power terms
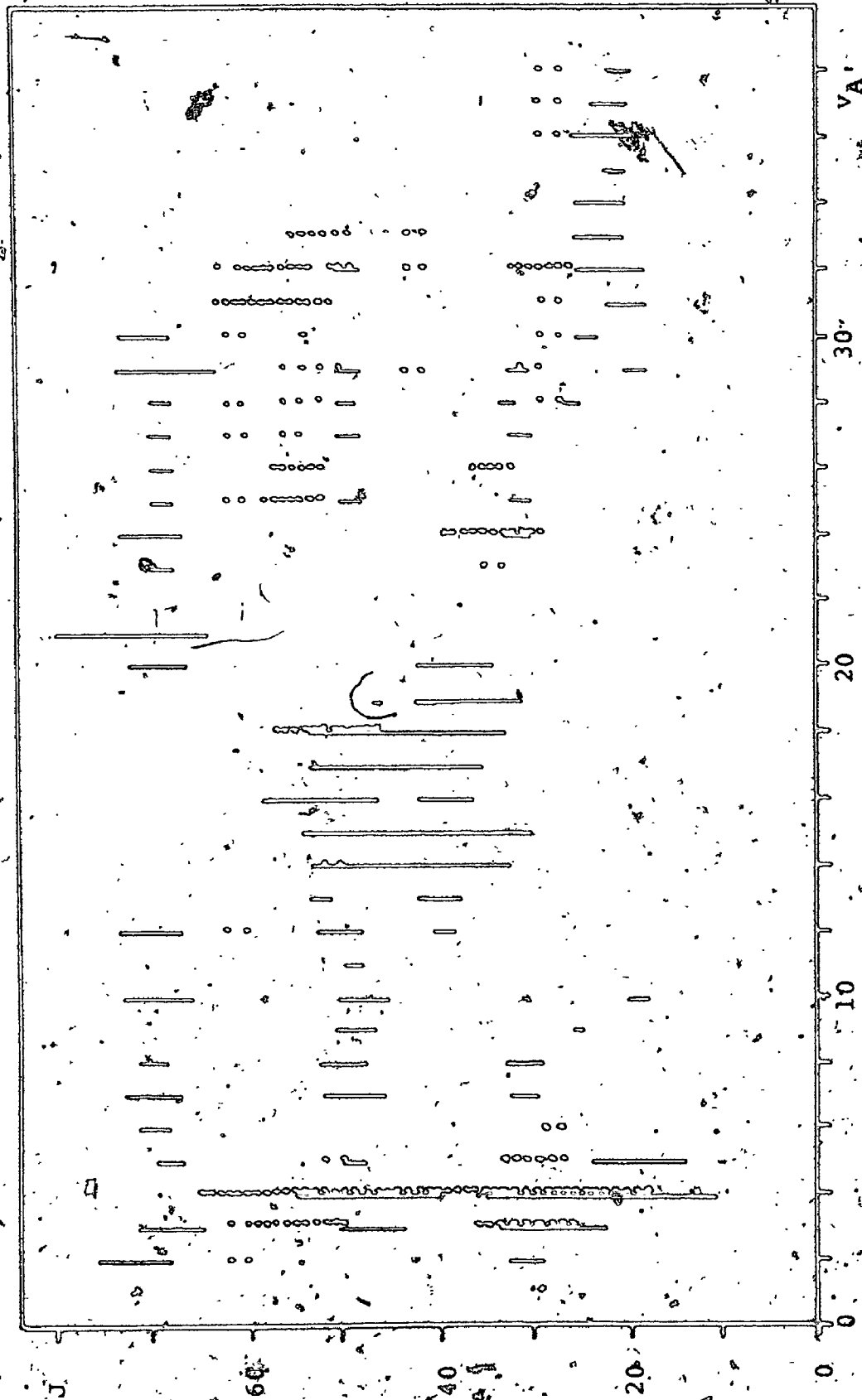
Figure 6.3 Tabulation of the rotational levels probed in the different vibrational levels of A' state in I^{35}Cl. The solid lines represent e sublevel data and the dots, f sublevel. A complete compilation of data is available in Appendix 3.

$$V(r) = D_e - \sum_m C_m/r^m \qquad 6.1$$

where D_e is the dissociation energy. The nature of the atoms produced by dissociation determines the values of m appearing in equation 6.1. For the A' state of ICl, giving the two atoms in their ground states, the coefficients m participating in the potential are m=5 for quadrupole-quadrupole interactions (first order), and m=6, 8, and 10 for the always present dispersion terms (second order interaction). The leading term, m=5, of this expansion is used to determine constants $X_5(i)$

$$X_5(i) = \frac{\overline{X_5(i)}}{[\mu^5 (C_5)^2]^{1/3}} \qquad 6.2$$

where μ is the reduced mass, C_5 the leading term in the expansion and $\overline{X_5(i)}$ is a constant which can be evaluated for all m (see Table 6.1).

Table 6.1 List of $\overline{X_5(i)}$ constants for the long-range LeRoy theory [35].

	i=0	1	2	3	4
$\overline{X_5(i)}$	9170.9	1178.3	-15.377	-0.17742	-5.3435×10^{-3}

The near-dissociation behavior of the vibrational term values and the rotational constants can be expressed as follows, for m=5 as the leading term

$$D_e - E_v = X_5(0) (v_D - v)^{10/3} \qquad 6.3$$

$$B_v = X_5(1) (v_D - v)^{4/3} \qquad 6.4$$

$$D_v = -X_5(2) (v_D - v)^{-2/3} \qquad 6.5$$

$$H_v = X_5(3) (v_D - v)^{-8/3} \qquad 6.6$$

$$L_v = X_5(4) (v_D - v)^{-14/3} \qquad 6.7$$

The vibrational index at dissociation, v_D, is determined by a plot of vibrational spacing to the power 3/7 versus the vibrational number

$$\Delta G_v^{3/7} = \frac{X_5(0)^{3/7}}{0.3} (v_D - v) \qquad 6.8$$

where $\Delta G_v = E_{(v+1)} - E_v$. By using the data for $v = 35-38$, $J = 20$ (e sublevel), we get v_D equal to 51.1. We must consider this as a preliminary estimate of the vibrational index at dissociation to be used hereafter only as a guide.

We need another parameter, C_5, in order to calculate the behavior of the centrifugal constants near dissociation. The use of a simple combination rule [36] can provide a fairly good estimate

$$C_{ab} = \frac{2 C_{aa} C_{bb}}{[(\alpha_a/\alpha_b) C_{bb} + (\alpha_b/\alpha_a) C_{aa}]} \qquad 6.9$$

where α_a and α_b are the atomic static dipole polarizability for Cl and I [37]. C_{aa} and C_{bb} are respectively the C_5

constant of A' ($^3\pi_{2u}$) state for Cl$_2$ and I$_2$ (positive values in respect of equation 6.1) [38,39]. The estimated C_5 for A' state of ICl is then 1.18×10^5 Å^{5}cm^{-1}.

Table 6.2   Value of atomic static dipole polarizability for I and Cl, and C_5 parameter of A' ($^3\pi_{2u}$) state of Cl$_2$ and I$_2$.

	I or I$_2$	Cl or Cl$_2$	ICl
α (Å^3)	3.54	2.61	----
C_5 (10^5Å^{5}cm^{-1})	2.09	0.704	1.18

According to the LeRoy theory, each centrifugal distortion constant should be linearly related to the appropriate power of $(y_D - v)$. With the data available, it was not possible to determine D, H and L at these high vibrational levels and so check their behavior. Instead, we used the predicted value of these constants near dissociation to guide our extrapolation to vibrational levels larger than 32 (see Figure 6.4).

We must keep in mind that we have assumed that C_5 is the leading term in the long-range expansion (equation 6.1) of the A' potential and that this condition still holds where we use the long-range theory. Should this not be true, possibly because the C_6 contribution is larger at medium-long-range, the relations 6.2 to 6.8 are no longer
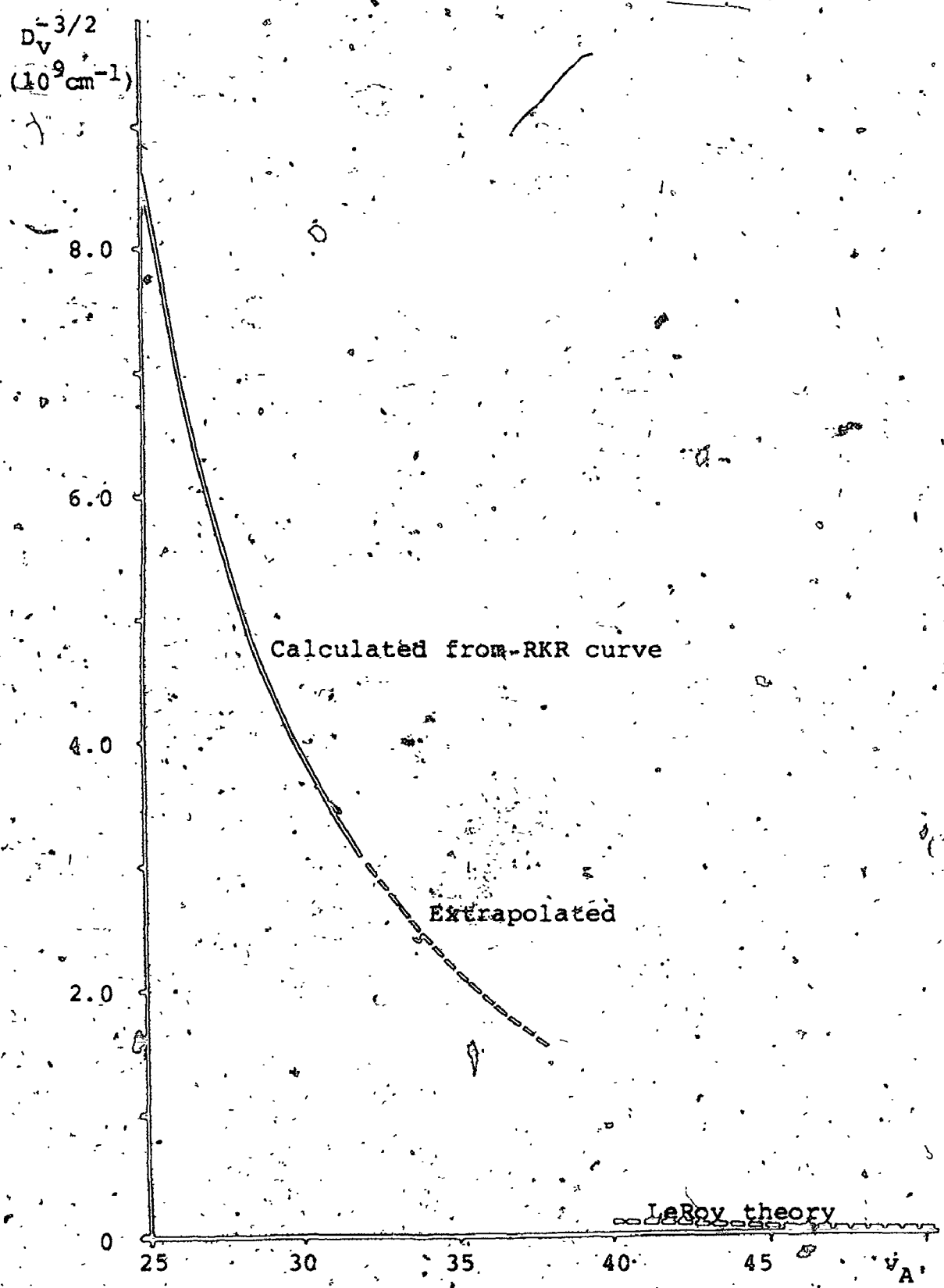
Figure 6.4 Plot of $D_v^{-3/2}$ (from equation 6.5) in function of the vibrational level, up to v=32 and the predicted values of $D_v^{-3/2}$ by LeRoy theory for v=40-51.

completely satisfactory. We must be careful about the confidence of our extrapolated values of D_v, H_v and L_v because our extrapolation is in a region where the $D_v^{-3/2}$ curve changes greatly; at medium and small internuclear distance ($v < 32$) the curve shows a pronounced slope and in the long-range region ($v > 40$), the curve has a small slope (predicted by theory).

In order to have the best estimation of the Dunham parameters near equilibrium, we made a partial fit of levels from $v=2$ to 14, encompassing both e and f sublevels (see Table 6.3). In so doing, the range covered was approximately 46% of the potential depth, and the standard deviation was kept to a very acceptable level ($\sigma = 0.04 \text{cm}^{-1}$) These equilibrium values were used to anchor T_e and B_e in further fits. Next, we made a fit of the data, including e and f sublevels, up to $v=28$ with a reasonable standard deviation of 0.05cm^{-1} (see Table 6.4). New trials to extend the Dunham expansion further dramatically endangered the value of the fit. We then opted to attack the problem from the other side, by using a top-down near-dissociation expansion (NDE) [40]

$$D_e - G_{(v,J)} = (v_D-v)^{10/3} \exp(a_0 + a_1(v_D-v) + a_2(v_D-v)^2 + \ldots)$$
$$-(v_D-v)^{4/3} J(J+1) \exp(b_0 + b_1(v_D-v) + \ldots) \qquad 6.10$$

With the help of the extrapolated D_v, H_v and L_v, the data from $v=23$ to 38 were fitted to this near-dissociation

Table 6.3   Dunham parameters for the A' (2) state of I ^{35}Cl from a fit of v=2-14 with 388 lines and a σ=0.04cm^{-1} (all in units of cm^{-1})[a]

$Y_{0,0}(\approx T_e)$	12682.05[b] (0.27)[c]
$Y_{1,0}(\approx \omega_e)$	224.5705 (0.15)
$Y_{2,0}(\approx -\omega_e x_e)$	-1.88153 (0.029)
$10^2 Y_{3,0}(\approx \omega_e y_e)$	-1.0684 (0.24)
$10^4 Y_{4,0}$	-3.228 (0.70)
e sublevel	
$10^2 Y_{0,1}(\approx B_e)$	8.6475 (0.048)
$10^4 Y_{1,1}(\approx -\alpha_e)$	-6.483 (0.23)
$10^6 Y_{2,1}(\approx \gamma_e)$	-6.914 (3.2)
$10^8 Y_{3,1}$	-3.161 (1.3)
f sublevel	
$10^2 Y_{0,1}(\approx B_e)$	8.6594 (0.038)
$10^4 Y_{1,1}(\approx -\alpha_e)$	-7.011 (0.10)
$10^6 Y_{2,1}(\approx \gamma_e)$	-----
$10^7 Y_{3,1}$	-5.842 (0.41)

a) Stated to reproduce the fit within the standard deviation [33].
b) Relative to the ground state minimum.
c) Errors stated are 3σ.

Table 6.4   Effective Dunham parameters for a fit of A'
(2) state, v=2-28 including 710 lines, for $I^{35}Cl$ (σ = 0.05 cm^{-1}, all parameters in units of cm^{-1})[a]

$Y_{0,0}(\approx T_e)$[b]	12682.05[c]	(0.27)[d]
$Y_{1,0}(\approx \omega_e)$	224.6526	(0.013)
$Y_{2,0}(\approx -\omega_e x_e)$	-1.92809	(0.0030)
$10^3 Y_{4,0}$	-1.52127	(0.041)
$10^5 Y_{5,0}$	6.62881	(0.33)
$10^6 Y_{6,0}$	-1.52420	(0.085)
$10^{10} Y_{8,0}$	3.6767	(0.20)
e sublevel		
$10^2 Y_{0,1}(\approx B_e)$[b]	8.6075	(0.048)
$10^4 Y_{1,1}(\approx -\alpha_e)$	-6.4877	(0.032)
$10^6 Y_{2,1}(\approx \gamma_e)$	-8.519	(0.42)
$10^8 Y_{4,1}$	-1.4034	(0.14)
$10^{11} Y_{5,1}$	4.55	(3.6)
f sublevel		
$10^2 Y_{0,1}(\approx B_e)$[b]	8.6594	(0.038)
$10^4 Y_{1,1}(\approx -\alpha_e)$	-6.9724	(0.057)
$10^6 Y_{2,1}(\approx \gamma_e)$	-2.281	(1.4)
$10^7 Y_{3,1}$	-3.2597	(0.96)
$10^9 Y_{4,1}$	-7.067	(1.9)

a) Stated to reproduce the fit within the standard
   deviation [33].
b) Fixed to values in Table 6.3.
c) Relative to the ground state minimum.
d) Errors stated are 3σ.

expansion (see Table 6.5). As the NDE fit overlapped quite well with the Dunham fit, we did not attempt further adjustments on D_v, H_v and L_v.

We merged the two fits by averaging the rotationless term values and rotational constants for v=25 and 26, dropping the extreme two vibrational levels of each fit to avoid the stress on the fit produced by the end-levels. Then we had an explicit list of G_v and B_v from v=2 to 38 of A'(2) state. As the Ω doubling was of the order of (or smaller than) the standard deviation of the fits, we averaged the rotational constant of the two sublevels in each vibrational level. It must be remembered that the A' term values were determined from a fit of D' state which carried its own standard deviation (0.04cm^{-1}). The RKR potential covering the entire range of our data of A' for I^{35}Cl was calculated (see Figure 6.5 and Table 6.6).

We said earlier in this chapter that the A'(2) state is anharmonic: in other words, the outer wall of the RKR potential is much less steep than the inner wall, as also reflected by the magnitude of $\omega_e x_e$. Thus for A', $\omega_e x_e$ =1.8815(290)cm^{-1} is more than three times larger than $\omega_e x_e$ for D', 0.5572(27)cm^{-1}. The "anharmonic factor" [13] x_e = $\omega_e x_e /\omega_e$ is 3.2x10^{-3} for D' and 8.4x10-3 for A', the latter being more than two and a half times larger than the former.

From equations 2.28 to 2.31, we can estimate the equi-

Table 6.5   Long-range expansion parameters (LeRoy) for a fit of A' (2) state of $I^{35}Cl$, from v=23 to 38 including 250 lines ($\sigma=0.04cm^{-1}$ and parameters in units of cm^{-I})[a]

$v_{D'}$	51.1	
D_e	17557.57^b	
a_0	-1.501312	$(0.76)^c$
$10\, a_1$	-8.8062304	(2.2)
$10\, a_2$	1.14651304	(0.27)
$10^3 a_3$	-7.81725662	(1.7)
$10^4 a_4$	2.91272582	(0.60)
$10^6 a_5$	-5.61003682	(1.1)
$10^8 a_6$	4.3674797	(0.87)
e sublevel		
b_0	-6.006643	(0.11)
$10\, b_1$	-1.165460	(0.14)
$10^3 b_2$	4.43974	(0.61)
$10^5 b_3$	-6.51045	(0.85)
f sublevel		
b_0	-6.04077	(0.086)
$10\, b_1$	-1.124376	(0.12)
$10^3 b_2$	4.281719	(0.52)
$10^5 b_3$	-6.31658	(0.77)

a) Stated to reproduce the fit within the standard deviation [33].
b) Relative to ground state minimum.
c) Errors stated are 3σ.
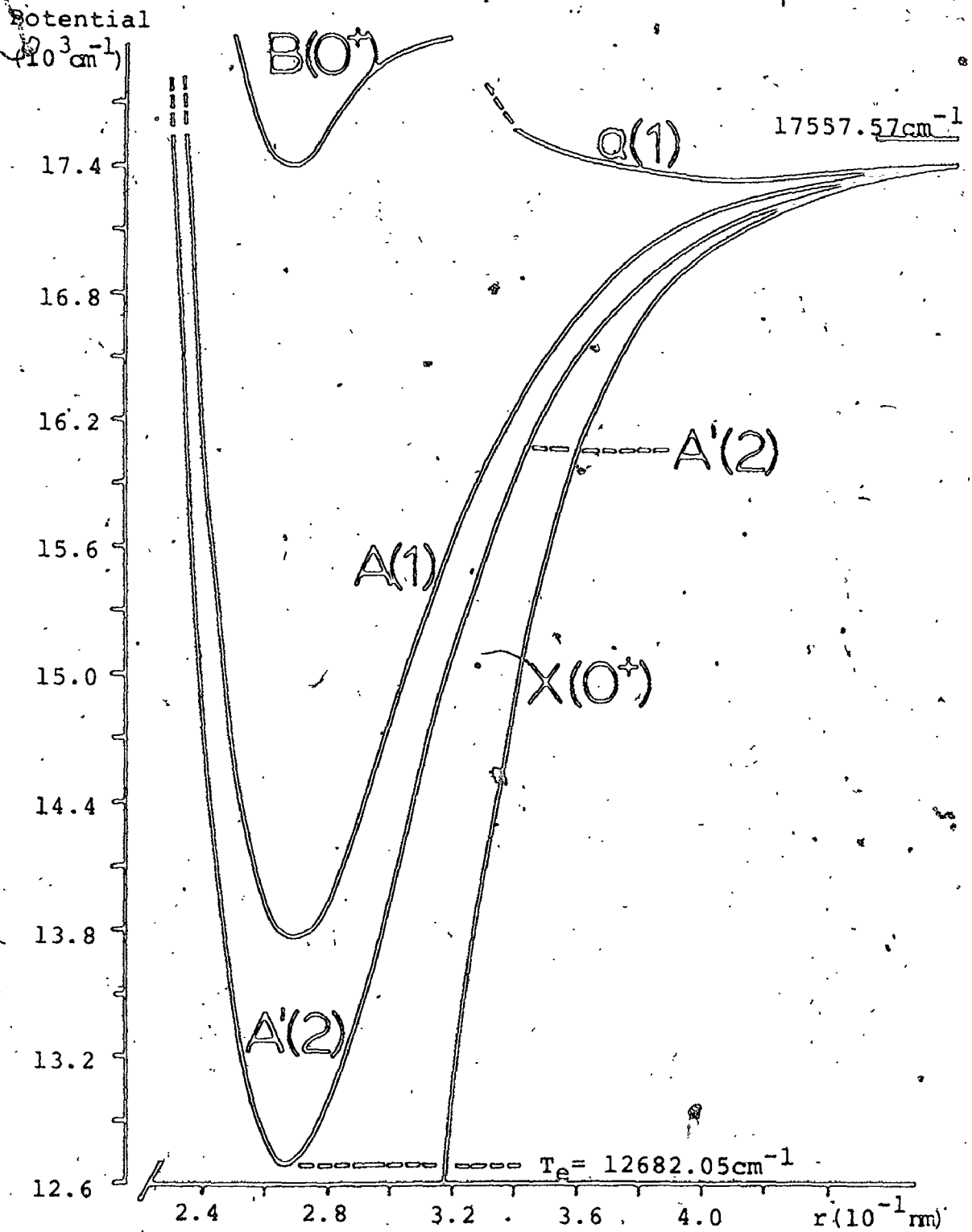
Figure 6.5 RKR potential curve of A" state and other states in·the area for I³⁶Cl.

Table ⬡ Effective term value, rotational constant, centrifugal distortion constants and turning points for the RKR potential up to v=38 for the A' (2) state of $I^{35}Cl$. The equilibrium bond distance is 2.665×10^{-1}nm. (in units of cm^{-1} or 10^{-1}nm)[a]

v	G_v [b]	$10^2 B_v$	$10^8 D_v$	$-10^{14} H_v$	$-10^{18} L_v$	r_{min}	r_{max}
0	12793.90	8.6196	5.27			2.596	2.744
1	13014.68	8.5512	5.31			2.550	2.809
2	13231.58	8.4815	5.44	6.0		2.520	2.857
3	13444.51	8.4105	5.61	7.0		2.497	2.899
4	13653.42	8.3377	5.80	7.6		2.479	2.938
5	13858.20	8.2633	6.99	9.0		2.462	2.974
6	14058.75	8.1868	6.18	10.0		2.448	3.010
7	14254.96	8.1081	6.39	10.8		2.436	3.044
8	14446.70	8.0269	6.64	12.2		2.424	3.078
9	14633.85	7.9430	6.91	13.8		2.414	3.112
10	14816.27	7.8558	7.22	15.8		2.404	3.145
11	14993.83	7.7653	7.57	18.2		2.395	3.180
12	15166.38	7.6709	7.97	21.5		2.387	3.214
13	15333.77	7.5723	8.42	25.5		2.379	3.249
14	15495.85	7.4692	9.93	30.6		2.372	3.285
15	15652.43	7.3610	9.49	36.8		2.366	3.322
16	15803.36	7.2473	10.12	44.2		2.360	3.361
17	15948.45	7.1278	10.85	52.9		2.354	3.401
18	16087.49	7.0019	11.70	63.1		2.349	3.442
19	16220.29	6.8688	12.68	75.0		2.344	3.486
20	16346.65	6.7283	13.85	88.8		2.339	3.532
21	16466.35	6.5799	15.23	105.4	18	2.335	3.582
22	16579.19	6.4225	16.85	125.0	25	2.331	3.634
23	16685.00	6.2567	18.75	147.8	34	2.328	3.690
24	16783.59	6.0807	20.95	176.9	48	2.324	3.751
25	16874.90	5.8912	23.55	219.0	69	2.322	3.817

Table 6.6 (suite)

v	G_v b	$10^2 B_v$	$10^8 D_v$	$-10^{14} H_v$	$-10^{18} L_v$	r_{min}	r_{max}
26	16958.76	5.6919	26.56	261.9	96	2.319	3.889
27	17035.24	5.4760	29.82	304.8	123	2.317	3.968
28	17104.30	5.2579	33.27	355.4	169	2.315	4.056
29	17166.29	5.0350	36.78	403.6	218	2.313	4.151
30	17221.67	4.8094	40.30	467.4	289	2.311	4.256
31	17270.94	4.5829	43.73	559.9	506	2.310	4.370
32	17314.67	4.3571	47.2	679.3	777	2.308	4.493
33	17353.37	4.133	51.4	874	1120	2.307	4.627
34	17387.52	3.911	55.8	1170		2.306	4.771
35	17417.52	3.692	61.5	1540		2.306	4.929
36	17443.70	3.476		2000		2.305	5.101
37	17466.35	3.26		2400		2.303	5.292
38	17485.70	3.053		2800		2.301	5.506

a) Stated to reproduce the fit within the standard
   deviation [33].
b) Relative to the ground state minimum.

librium value of some Dunham parameters given the value of ω_e, $\omega_e x_e$, B_e and α_e. First, α_e from the fit of the lower part of A' state can be compared to its predicted value in a Morse potential

$$\alpha_e^M = 6(\sqrt{\omega_e x_e B_e^3} - B_e^2)/\omega_e = 7.3 \times 10^{-4} cm^{-1} \qquad 6.11$$

This value of α_e^M is beyond 9σ from the observed α_e for both sublevels, $6.48(23) \times 10^{-4} cm^{-1}$ and $7.01(10) \times 10^{-4} cm^{-1}$, but is nevertheless quite close to their values. Concurrently with the size of $\omega_e x_e$ and x_e, this confirms the anharmonicity of the A' state.

The evaluation of the centrifugal constants at equilibrium is more interesting in the sense that it should tell us if their computed values are in the correct range and show the right trend at the bottom of the potential well

$$D_e = 4B_e^3/\omega_e^2 = 5.13 \times 10^{-8} cm^{-1} \qquad 6.12$$

$$H_e = 2D_e(12B_e^2 - \alpha_e\omega_e)/3\omega_e^2$$
$$= -4.2 \times 10^{-14} cm^{-1} \qquad 6.13$$

$$L_e = \frac{1}{B_e^2 D_e}\left[3B_e H_e D_e^2 - 5D_e^4 + B_e^2 H_e^2 - \frac{8D_e^3 B_e^2 \omega_e x_e}{3\omega_e^2}\right]$$
$$= -3.9 \times 10^{-19} cm^{-1} \qquad 6.14$$

Clearly, the expectations are confirmed. The trend of D_v and H_v as listed in Table 6.6 is parallel to their

equilibrium values estimated by equations 6.12 and 6.13. The same point is confirmed for L_v, even though the effect of L_v is insignificant for the low vibrational levels, where it has not been determined.

A correction is given in equation 2.32 for T_e

$$Y'_{00} = \frac{B_e}{4} + \frac{\alpha_e \omega_e}{12B_e} + \frac{\alpha_e^2 \omega_e^2}{144B_e^2} - \frac{\omega_e x_e}{4} = -0.109 \text{ cm}^{-1} \qquad 6.15$$

This correction has not been applied to the values given in tables throughout this thesis because it is smaller than the quoted uncertainty (equivalent to 3σ) for T_e.

An estimation of T_e at $12680(20)\text{cm}^{-1}$ and ω_e at $226(4)\text{cm}^{-1}$ by Spivey and others [1] must be considered as an inspired guess. In our calculation of the equilibrium Dunham parameters, it would naturally be better to have access to data down to $v=0$, but limitations imposed by Franck-Condon factors put these levels out of reach. It would be necessary to pump vibrational levels of D' in the range $v=30-40$, and to use probe energies of about 35000cm^{-1} ($\sim 285\text{nm}$) in order to access the v-0 level of A'. These requirements are beyond the capabilities of our equipment.

In an attempt to discern perturbations in the higher part of the A' potential, we purposely sought ^{37}Cl data at high vibrational levels. As nine other valence states converge to the first dissociation limit, it is more than likely that perturbations will occur. From our data of A'

however, we did not discern any sign of such effects. This may be due to the fact that, using state-selective spectroscopy, large regions of v and J are not observed. The isotope relationship (equation 2.23 and 2.24) holds at the bottom and the top (up to v=34) of the potential, confirming the vibrational numbering and giving no evidence of perturbation phenomena.

The lower electronic states of I_2, Cl_2, Br_2 and ICl are organized in qualitatively the same manner [2,41]. In the ICl case, A' ($\Omega=2$) is the first excited state, lying .1061cm^{-1} below the well known A ($\Omega=1$) state. It is characterized by an electronic energy of 12682.05(27)cm^{-1}, a vibrational frequency of 224.57(15)cm^{-1} and shows a pronounced anharmonic character. Its vibrational energy and equilibrium internuclear distance show some similarity with the other relatively bound states having ($^3\pi$) case (a) signature, namely the A(1) and B(0^+) (see Table 4.1). With data covering 89% of the potential depth, the RKR curve has been determined, along with the centrifugal constants, D, H and L. The bond distance at equilibrium was evaluated at 0.2665 nm (2.665 Å). No evidence of perturbation was observed other than the expected small Ω doubling.

CHAPTER 7

GENERAL CONCLUSION

We successfully characterized the lower part of the ion-pair state D' ($\Omega = 2$) of ICl, using a two-step, polarization-labelling technique in an Optical-Optical-Double-Resonance (OODR) experiment. Transitions to D' state were allowed by heterogeneous perturbation with the neighboring ß ($\Omega = 1$) state. The main spectroscopic constants and the Rydberg-Klein-Rees (RKR) potential up to the vibrational level v=28 for the D'($\Omega = 2$) state of I^{35}Cl were determined. At the same time, extensive data were cumulated to map two avoided crossings between D'(2) and E(0^+) state at v=0 and 1. We have evaluated the electronic interaction term $W_{\Omega, \Omega \pm 1}$ between these states. By comparing them to the pure precession values, we conclude that the three lowest ion-pair states of ICl, D', ß and E, are good examples of Van Vleck pure precession case with case (c) signature.

Extension of the technique to three steps, ↑↑↑ (OOR), enabled us to probe the downward transition D' → A'. The main spectroscopic constants and the centrifugal distortion constants were determined for the A' (Ω=2) state of $I^{35}Cl$, with data up to ~70cm^{-1} from the first dissociation limit, I. ($^2P_{3/2}$) + Cl ($^2P_{3/2}$). The anharmonicity of the A' state necessitated the use of two expansions to fit the data: the usual Dunham expansion and a "top-down" near-dissociation expansion (NDE). The merge of these two fits provided us with the terms needed for the RKR potential up to v=38 for the A'(2) state of $I^{35}Cl$.

This thesis brought a significant addition to the knowledge of the electronic states of ICl, initiated the characterization of three previously unobserved states, a(1), b(1) and b'(2), and the acquisition of data on high vibrational levels of the ground state X(0^+). The data for A' state may be useful in studying the long-range potential and in determining the C_m constants in the equation

$$V(r) = D_e - \sum_{m=5} C_m/r^m \qquad\qquad 7.1$$

concurrently with the other states characterized in the medium to long-range region.

REFERENCES

1 - J.David Spivey, J.Gail Ashmore and Joel Tellinghuisen, Chem.Phys.Lett., 109, 5, pp.456-461 (1984).

2 - R.S. Mulliken, J. Chem. Phys., 55, pp.288-309 (1971).

3 - E. Hulthen, Nils Johansson and Ulla Pilsäter, Ark. Fys., 14, 3, pp.31-48 (1958).

4 - E. Hulthén, N. Järlsäter and L. Koffman, Ark. Fys., 18, 35, pp.479-512 (1960).

5 - G.W. King, and R.G. McFadden, Chem. Phys. Lett., 58, pp.119-121 (1978). G.W. King, I.M. Littlewood, R.G. McFadden and J.R. Robins, Chem. Phys., 41, pp.379-386 (1979).

6 - J.C.D. Brand, U.D. Desphande, A.R. Hoy and S.M. Jaywant, J. Mol. Spectrosc., 100, 2, pp.416-428 (1983).

7 - J.C.D. Brand, D. Bussieres, A.R. Hoy, S.M. Jaywant and D.B. Miller, Opt. Comm., 48,3, pp.185-199 (1983).

8 - D. Bussières and A.R. Hoy, Can. J. Phys., 62, 2, pp.1941-1946 (1984).

9 - J.C.D. Brand and A.R.Hoy, private communication.

10- J.C.D. Brand, D. Bussières and A.R. Hoy, Molec. Phys. (preliminary communication), 53, 2, pp.525-529 (1984).

11- A.R. Hoy, private communication.

12- Gerhard Herzberg, <u>Molecular Spectra and Molecular structure</u>, Vol I, Spectra of Diatomic Molecules, Second edition, D. Van Nostrand Co. Inc., 658 pages, 1950.

13- Jeffrey I. Steinfeld, <u>Molecules and Radiation : An introduction to modern molecular spectroscopy</u>, second edition, M.I.T. Press, 348 pages, 1974.

14- W.C Stwalley, J. Chem. Phys., 63 7, pp.3062-3080 (1973)

15- R.T. Birge, E.C. Kemble, W.F. Colby, F.W. Loomis and L. Page, Nat. Res. Counc. Bull. 57, (1930).

16- Jon T. Hougen, NBS Monograph 115, 52 pages, (1970).

17- J.W. Cooley, Math. Comp., 15, pp.363-374 (1961).

18- J.H. Van Vleck, Phys. Rev., 33, pp.467-468 (1929).

19- ibid ref. 12, p285.

20- I. Kovacs, <u>Rotational structure in the spectra of diatomic molecules</u>, New York, American Elsevier, 320 pages, 1969.

21- Richard Earl Teets, <u>Polarization labelling spectroscopy of molecules</u>, Ph. D. Thesis, Stanford University, 130 pages, 1978.

22- Keith John Cross, <u>Visible laser spectroscopy of Nitrogen dioxide and Iodine</u>, Ph. D. Thesis, University of Western Ontario, 197 pages, 1980.

23- Wolfgang Demtröder, <u>Laser spectroscopy : Basic concepts and Instrumentation</u>, Springer Series in Chemical Physics, Vol.5, Springer-Verlag, 964 pages, 1981.

24- Akira Brian Yamashita, Theoretical and experimental studies in visible laser spectroscopy, Ph. D. Thesis, University of Western Ontario, 260 pages, 1983.

25- J.C.D. Brand, K.J. Cross, N.P. Ernsting and A.B. Yamashita, Opt. Comm., 37, 3, pp.178-182 (1981).

26- J.A. Coxon, R.M. Gordon and M.A. Wickramaaratchi, J. Mol. Spectrosc., 79, 2, pp.363-379 (1980). J.A. Coxon and M.A. Wickramaaratchi, J. Mol. Spectrosc., 79, 2, pp.380-395 (1980).

27- J.C.D. Brand, D. Bussières, A.R. Hoy and S.M. Jaywant, Can. J. Phys., 62, 12, pp.1947-1953 (1984).

28- Weldon G. Brown and G.E. Gibson, Phys. Rev., 40, pp.529-543 (1932).

29- Robert D. Gordon and K.K. Innes, J. Mol. Spectrosc., 78, 2, pp.350-352 (1979). and J. Chem. Phys., 71, 7, pp.2824-2839 (1979). Steven G. Hansen, J.D. Thompson, Richard Akumedy and Brian J. Howard, Chem. Soc., Farad. Trans. 2, 78, pp.1293-1310 (1982).

30- J.C.D. Brand, U.D. Desphande, A.R. Hoy and E.J. Woods, Can. J. Chem., 61, 5, pp-846-849 (1983).

31- J.C.D. Brand, A.R. Hoy and S.M. Jaywant, J. Mol. Spectrosc., 106, 2, pp.388-394 (1984).

32- M.S. DeVries, N.J.A. VanVeen, T. Baller and A.E. DeVries, Chem. Phys., 56, 2, pp.157-165 (1981)

33- James K.G. Watson, J. Mol. Spectrosc., 66, 3, pp.500-502 (1977).

34- A. Sur and J. Tellinghuisen, J. Mol. Spectrosc., 88, 2, pp.323-346 (1981). Joel Tellinghuisen, J. Mol. Spectrosc., 94, 2, pp.231-252 (1982).

35- Robert J. LeRoy, <u>Semiclassical Methods in Molecular Scattering and Spectroscopy,</u> Chapter 3, pp109-126, M.S. Child editor, D. Reidel Pub. Co., Boston, 1980.

36- H.L. Kramer and D.R. Herschbach, J. Chem. Phys., 53, 7, pp.2792-2800 (1970).

37- R.R. Teachout and R.T. Pack, Atomic Data, 3, pp.195-214 (1971).

38- M. Sauté, B. Bussery and M. Aubert-Frécon,Molec. Phys., 51, 6, pp.1459-1474 (1984).

39- M. Sauté and M. Aubert-Frécon, J. Chem. Phys., 77, 11, pp.5639-5646 (1982).

40- J.W. Tromp and Robert J. LeRoy, Can. J. Phys., 60, 1, pp.26-34 (1982).

41- K.P. Huber and G. Herzberg, <u>Molecular spectra and Molecular structure,</u> Vol.4, Van Nostrand, Princeton, 1979.

APPENDIX 1

D' ($\Omega=2$) data for $I^{35}Cl$ at low vibrational levels

for v=0 and 1, e sublevel (lower root)

f sublevel

e sublevel (upper root)

v=2, e and f sublevels

VD	JD	JX	PUMP	PROBE	G(V,J)
0	17	19	15406.651	23136.959	39159.742
0	19	19	15406.651	23141.112	39163.895
0	25	27	15242.821	23277.825	39179.382
0	27	27	15242.821	23283.882	39185.439
0	27	27	17556.930	20969.806	39185.472
0	29	27	17556.930	20976.324	391^1.990
0	31	33	15374.922	23123.790	39198.909
0	33	33	15374.922	23131.219	39206.338
0	37	39	15496.592	22976.060	39222.451
0	39	39	15496.592	22984.786	39231.177
0	38	38	16024.761	22841.526	39226.756
0	40	38	16024.761	22850.510	39235.740
0	38	40	15353.143	23114.772	39226.772
0	40	40	15353.143	23123.738	39235.738
0	39	39	16021.532	22840.309	39231.184
0	41	39	16021.532	22849.539	39240.414
0	39	39	15368.050	23113.401	39231.250
0	41	39	15368.050	23122.551	39240.400
0	40	40	16018.199	22839.067	39235.710
0	42	40	16018.199	22848.467	39245.110
0	46	46	15996.365	22830.964	39265.144
0	48	46	15996.365	22841.534	39275.714
0	45	47	15466.596	22964.798	39259.981
0	47	47	15466.596	22975.183	39270.366
0	47	45	15348.460	23114.429	39270.425
0	45	45	15348.460	23104.035	39260.031
0	47	49	15970.360	22829.471	39270.393
0	49	49	15970.360	22840.210	39281.132
0	47	49	15458.250	22961.678	39270.470
0	49	49	15458.250	22972.431	39281.223
0	50	52	15445.107	22956.367	39286.638
0	52	52	15445.107	22967.677	39297.948
0	52	52	15971.359	22821.242	39297.950
0	54	52	15971.359	22832.947	39309.655
0	53	53	15455.856	22950.861	39303.873
0	55	57	15367.753	23380.061	39315.668
0	57	57	15367.753	23392.380	39327.987
0	56	56	15442.529	22944.762	39321.774
0	58	56	15442.529	22957.345	39334.357
0	64	64	15353.290	23356.389	39374.539
0	66	64	15353.290	23370.660	39388.810
0	63	65	15242.757	23066.226	39367.599
0	65	65	15242.757	23080.248	39381.621
0	71	73	15459.469	22782.556	39426.258
0	73	73	15459.469	22798.294	39441.996
0	74	74	15473.553	22775.492	39449.989
0	76	74	15473.553	22791.977	39466.474
1	27	27	17556.930	21134.877	39350.543

VD	JD	JX	PUMP	PROBE	G(V,J)
1	39	39	16021.532	23005.462	39396.337
1	41	39	16021.532	23014.697	39405.572
1	45	47	17485.157	21111.651	39425.395
1	47	47	17485.157	21122.321	39436.065
1	48	46	15996.365	23007.321	39441.501
1	47	49	15970.359	22995.109	39436.030
1	49	49	15970.359	23006.152	39447.073
1	52	52	15971.359	22987.736	39464.444
1	54	52	15971.359	22999.920	39476.628
1	53	53	16090.961	22862.101	39470.459
1	55	53	16090.961	22874.502	39482.860
1	58	58	16066.336	22854.018	39502.288
1	60	58	16066.336	22868.416	39515.786
1	63	65	16010.082	22847.178	39536.882
1	65	65	16010.082	22861.737	39551.441
1	68	68	16010.044	22838.690	39573.995
1	70	68	16010.044	22854.163	39589.468
1	71	73	15459.469	22953.588	39597.290
1	73	73	15459.469	22969.561	39613.263
1	74	74	15473.553	22946.908	39621.405
1	76	74	15473.553	22963.416	39637.913
0	46	47	15473.288	22964.411	39266.286
0	48	47	15473.288	22974.739	39276.614
0	50	51	15456.825	22957.155	39287.378
0	52	51	15456.825	22968.368	39298.591
0	62	63	15348.411	23362.303	39361.039
0	64	63	15348.411	23376.085	39374.821
0	64	65	15388.455	22927.771	39374.842
0	66	65	15388.455	22942.034	39389.105
0	70	71	15353.989	22913.368	39418.840
0	72	71	15353.989	22928.916	39434.388
1	30	31	16287.401	22779.332	39371.444
1	32	31	16287.401	22786.193	39378.305
1	44	45	16119.177	22881.962	39428.492
1	46	45	16119.177	22891.855	39438.385
1	48	49	16102.076	22836.120	39448.758
1	50	49	16102.076	22836.054	39459.502
1	49	50	16097.571	22836.039	39454.061
1	51	50	16097.571	22885.512	39465.014
0	17	19	15406.651	23142.422	39165.205
0	19	19	15406.651	23146.442	39169.225
0	31	33	15374.922	23127.466	39202.585
0	33	33	15374.922	23134.561	39209.680
0	47	47	15466.595	22976.832	39272.014
0	49	49	15458.250	22974.127	39282.919
0	49	49	15970.360	22841.960	39282.882
0	50	52	15445.107	22958.242	39288.513
0	52	52	15445.107	22969.874	39300.145

VD	JD	JX	PUMP	PROBE	G(V,J)
0	53	53	15455.856	22953.250	39306.262
0	52	52	15971.359	22823.425	39300.133
0	54	52	15971.359	22835.570	39312.278
0	55	57	15367.753	23382.919	39318.526
0	57	57	15367.753	23395.762	39331.369
0	56	56	15442.529	22947.881	39324.893
0	58	56	15442.529	22960.993	39338.005
0	63	65	15242.757	23071.349	39372.722
0	65	65	15242.757	23086.012	39387.385
0	64	64	15353.290	23361.862	39380.012
0	66	64	15353.290	23376.761	39394.911
0	71	73	15459.469	22790.394	39434.096
0	73	73	15459.469	22806.886	39450.588
0	74	74	15473.553	22784.488	39458.985
0	76	74	15473.553	22801.712	39476.209
1	39	39	16021.532	23014.882	39405.757
1	41	39	16021.532	23023.735	39414.610
1	47	49	15970.360	23002.729	39443.651
1	49	49	15970.360	23013.272	39454.194
1	52	52	15971.345	22994.086	39470.780
1	54	52	15971.345	23005.729	39482.423
1	53	53	16090.961	22868.157	39476.515
1	55	53	16090.961	22880.015	39488.373
1	58	58	16066.316	22859.613	39506.963
1	60	58	16066.316	22872.586	39519.936
1	70	68	16010.044	22856.575	39591.880
1	73	73	15459.469	22972.263	39615.965
1	74	74	15473.553	22949.804	39624.301
1	76	74	15473.553	22966.840	39641.337
2	53	53	16090.961	23039.095	39647.453
2	55	53	16090.961	23050.917	39659.275
2	58	58	16066.336	23030.417	39677.787
2	60	58	16066.336	23043.313	39690.683
2	63	65	16010.076	23021.145	39710.843
2	65	65	16010.076	23035.076	39724.774
2	68	68	16010.051	23011.254	39746.566
2	70	68	16010.051	23026.259	39761.571
2	30	31	16287.401	22950.651	39542.763
2	32	31	16287.401	22957.489	39549.601
2	37	38	16264.674	22943.404	39568.547
2	39	38	16264.674	22951.771	39576.914
2	47	48	16224.189	22930.932	39614.541
2	49	48	16224.189	22941.448	39625.057
2	48	49	16102.076	23047.237	39619.875
2	50	49	16102.076	23057.956	39630.594

APPENDIX 2

$\underline{D}'$ ($\Omega=2$) data of ICl for higher vibrational levels

from v=15 to 28, e sublevel

f sublevel

NOTE   An asterisk (*) in the last column marks data
for isotopic molecule $I^{37}Cl$.

VD	JD	JX	PUMP	PROBE	G(V,J)	3.7CL
15	30	32	16901.132	24457.261	41670.388	
15	32	32	16901.132	24463.804	41676.931	
15	47	47	16836.054	24454.222	41738.780	
16	19	19	17006.028	24557.518	41798.590	
16	21	19	17006.028	24561.730	41802.802	
16	23	23	16995.578	24557.176	41807.381	
16	25	23	16995.578	24562.227	41812.432	
16	30	32	16901.132	24613.597	41826.724	
16	32	32	16901.132	24620.109	41833.236	
16	34	34	16836.141	24676.765	41840.150	
16	43	43	16903.703	24565.398	41876.210	
16	47	47	16836.054	24610.374	41894.932	
16	49	47	16836.054	24620.378	41904.936	
17	23	23	16995.578	24712.552	41962.757	
17	32	32	16901.132	24775.431	41988.558	
17	47	47	16836.054	24765.322	42049.880	
18	19	19	17006.028	24867.304	42108.376	
18	21	19	17006.028	24871.501	42112.573	
18	23	23	16995.578	24866.946	42117.151	
18	41	43	16903.703	24865.881	42176.693	
18	41	41	16903.723	24833.000	42112.111	*
20	26	26	16522.553	25636.097	42430.353	
21	21	21	16631.682	25693.567	42569.629	
21	27	29	16604.284	25689.356	42584.466	
21	28	28	16580.564	25659.248	42516.029	*
21	29	29	16611.619	25687.756	42590.201	
21	29	31	16597.733	25687.734	42590.178	
21	32	34	16587.114	25685.180	42599.538	
21	41	41	16568.937	25676.366	42633.075	
21	71	69	16622.939	25439.542	42803.406	
22	27	29	16604.284	25839.615	42734.725	
22	28	28	16580.564	25806.773	42663.554	*
22	29	31	16597.733	25837.984	42740.428	
22	29	29	16611.619	25838.039	42740.484	
22	31	29	16611.619	25844.154	42746.599	
22	30	30	16575.058	25805.142	42669.280	*
22	31	31	17018.130	25423.634	42746.475	
22	33	31	17018.130	25430.137	42752.978	
22	34	34	16587.122	25842.062	42756.428	
22	36	36	16676.596	25743.444	42763.443	
22	38	38	16668.738	25741.803	42771.010	
22	40	38	16668.738	25749.696	42778.903	
22	67	69	16663.083	25520.986	42924.994	
22	69	69	16663.083	25534.758	42938.766	
22	69	69	16622.939	25574.874	42938.738	
22	71	69	16622.939	25588.958	42952.822	
22	72	70	16668.134	25535.094	42960.042	
23	30	32	16683.190	25897.397	42892.582	

VD	JD	JX	PUMP	PROBE	G(V,J)	3.7CL
23	36	36	16676.596	25892.637	42912.636	
23	67	69	16663.083	25669.629	43073.637	
23	69	69	16663.083	25683.274	43087.282	
23	70	70	16668.134	25669.284	43094.232	
23	72	70	16668.134	25683.540	43108.488	
24	15	15	16684.875	25721.440	43006.580	
24	18	20	17050.734	25721.374	43011.706	
24	19	19	17057.236	25721.262	43013.542	
24	21	19	17057.236	25725.310	43017.590	
24	19	19	17057.236	25721.287	43013.567	
24	21	19	17057.236	25725.324	43017.604	
24	21	21	17052.050	25721.227	43017.657	
24	30	30	16629.592	25669.930	42961.328	☆
24	31	31	17018.130	25721.184	43044.025	
24	33	31	17018.130	25727.654	43050.495	
24	31	33	16622.652	25721.220	43044.069	
24	33	33	16622.652	25727.686	43050.535	
24	33	33	16767.891	25963.094	43050.491	
24	35	33	16767.891	25969.956	43057.353	
24	34	34	16836.141	25890.466	43053.851	
24	36	34	16836.141	25897.526	43060.911	
24	35	37	16966.441	25669.623	42977.022	☆
24	37	37	16966.441	25676.582	42983.981	☆
24	39	39	16933.209	25769.713	43072.265	
24	41	43	16848.937	25824.183	43080.229	
24	43	43	16848.937	25832.649	43088.695	
24	44	46	16933.011	25722.348	43093.174	
24	46	46	16933.011	25731.394	43102.220	
25	18	20	17050.734	25868.787	43159.119	
25	19	19	17057.236	25868.757	43161.037	
25	21	19	17057.236	25872.818	43165.098	
25	19	19	17057.236	25868.749	43161.029	
25	21	19	17057.236	25872.761	43165.041	
25	19	19	17057.236	25868.682	43160.962	
25	21	19	17057.236	25872.746	43165.026	
25	21	21	17052.050	25868.642	43165.072	
25	22	24	16863.980	26043.188	43167.259	
25	24	24	16863.980	26047.831	43171.902	
25	23	23	17090.579	25824.340	43169.546	
25	25	23	17090.579	25829.178	43174.384	
25	23	23	17129.127	25785.830	43169.584	
25	25	23	17129.127	25790.685	43174.439	
25	24	26	17057.696	25768.417	43090.338	☆
25	26	26	17057.696	25773.238	43095.159	☆
25	28	30	16966.229	25918.573	43182.457	
25	30	30	16966.229	25924.374	43188.258	
25	28	28	17111.064	25787.104	43182.392	
25	30	28	17111.064	25792.940	43188.228	

VD	JD	JX	PUMP	PROBE	G(V,J) 37CL
25	30	32	17051.022	25825.244	43188.261
25	34	34	16836.141	26037.733	43201.118
25	36	34	16836.141	26044.753	43208.138
25	36	38	17057.519	25790.158	43208.146
25	38	38	17057.519	25797.589	43215.577
25	36	38	17057.519	25790.192	43208.180
25	38	38	17057.519	25797.613	43215.601
25	39	39	16933.211	25916.930	43219.484
25	41	39	16933.211	25924.951	43227.505
25	44	46	16932.977	25869.447	43240.239
25	46	46	16932.977	25878.456	43249.248
25	45	45	16847.307	25970.096	43244.756
25	47	45	16847.307	25979.315	43253.975
25	47	47	16836.048	25969.401	43253.953
25	49	47	16836.048	25978.999	43263.551
25	48	48	16830.224	25969.091	43258.735
25	50	48	16830.224	25978.887	43268.531
25	55	57	16854.903	25872.019	43294.776
25	57	57	16854.903	25883.200	43305.957
25	56	58	16846.926	25872.371	43300.331
25	58	58	16846.926	25883.735	43311.695
26	15	15	17184.652	25896.872	43300.627
26	17	19	17201.117	25867.572	43303.733
26	18	20	17050.734	26015.284	43305.616
26	19	19	17057.236	26015.164	43307.444
26	21	19	17057.236	26019.195	43311.475
26	19	19	17057.236	26015.243	43307.523
26	21	19	17057.236	26019.250	43311.530
26	19	19	17057.236	26015.206	43307.486
26	21	19	17057.236	26019.230	43311.510
26	22	24	17184.032	25869.591	43313.714
26	23	23	17090.579	25970.726	43315.932
26	25	23	17090.579	25975.543	43320.749
26	29	31	17153.512	25873.337	43331.560
26	30	32	17051.022	25971.599	43334.616
26	32	32	17051.022	25977.823	43340.840
26	31	31	17181.751	25851.226	43337.688
26	33	31	17181.751	25857.633	43344.095
26	36	38	17057.519	25936.491	43354.479
26	38	38	17057.519	25943.875	43361.863
26	36	38	17057.519	25936.468	43354.456
26	38	38	17057.519	25943.846	43361.834
26	39	39	16933.209	26063.128	43365.680
26	41	39	16933.209	26071.110	43373.662
26	50	52	16847.280	26061.922	43414.551
26	52	52	16847.280	26072.063	43424.692
26	53	53	16836.166	26005.599	43341.303
26	56	56	16829.603	26061.689	43446.193
26	58	56	16829.603	26073.050	43457.554

VD	JD	JX	PUMP	PROBE	G(V,J)	37CL
27	15	15	17184.652	26042.348	43446.103	
27	16	16	17259.661	25965.227	43447.635	
27	18	16	17259.661	25968.662	43451.070	
27	18	20	17050.734	26160.752	43451.084	
27	20	20	17050.734	26164.581	43454.913	
27	19	19	17057.236	26160.634	43452.914	
27	21	19	17057.236	26164.671	43456.951	
27	19	19	17057.236	26160.669	43452.949	
27	21	19	17057.236	26164.687	43456.967	
27	21	21	17052.050	26160.553	43456.983	
27	23	21	17052.050	26164.956	43461.386	
27	22	24	17184.011	26015.083	43459.185	
27	22	24	17184.011	26015.083	43459.185	
27	24	26	17057.696	26055.108	43377.029	☆
27	26	26	17057.696	26059.912	43381.833	☆
27	29	31	17153.521	26018.727	43476.959	
28	15	15	17184.652	26186.885	43590.640	
28	17	15	17184.652	26190.052	43593.807	
15	31	32	16904.482	24457.061	41673.538	
16	31	32	16904.482	24613.431	41829.908	
16	33	32	16904.482	24620.078	41836.555	
16	43	42	16913.376	24565.398	41876.101	
16	49	50	16911.072	24511.793	41904.796	
17	31	32	16904.482	24768.694	41985.171	
18	41	42	16913.376	24865.881	42176.584	
18	49	50	16911.072	24820.715	42213.718	
21	28	29	16607.863	25688.514	42587.203	
21	33	34	16591.295	25684.222	42602.761	
21	38	39	16659.812	25591.767	42620.922	
22	28	29	16607.863	25838.770	42737.459	
22	33	34	16591.295	25834.463	42753.002	
22	53	54	16838.313	25472.132	42840.117	
23	39	40	16904.411	25574.965	42845.831	☆
23	41	40	16904.411	25582.760	42853.626	☆
23	46	47	16867.428	25573.658	42874.641	☆
23	48	47	16867.428	25582.805	42883.788	☆
23	48	49	16871.987	25620.988	42963.537	
23	50	49	16871.987	25630.905	42973.454	
23	48	49	16871.987	25621.008	42963.557	
23	50	49	16871.987	25630.909	42973.458	
23	50	51	16858.931	25620.975	42973.433	
23	52	51	16858.931	25631.306	42983.764	
23	53	54	16838.313	25621.044	42989.029	
23	55	54	16838.313	25631.971	42999.956	
23	56	57	16816.430	25621.183	43005.467	
23	58	57	16816.430	25632.676	43016.960	
23	61	60	16743.649	25683.377	43035.098	
23	62	63	16768.826	25622.107	43041.258	
23	64	63	16768.826	25634.825	43053.976	

VD	JD	JX	PUMP	PROBE	G(V,J)	37CL
23	63	64	16760.383	25622.299	43047.542	
24	18	19	17055.266	25721.363	43011.673	
24	21	22	16911.102	25784.966	42938.924	☆
24	23	22	16911.102	25789.258	42943.216	☆
24	25	26	16653.210	25721.073	43026.901	
24	27	26	16653.210	25726.324	43032.152	
24	28	29	16973.008	25771.121	43034.955	
24	30	29	16973.008	25777.024	43040.858	
24	28	29	17023.058	25721.057	43034.951	
24	30	29	17023.058	25726.958	43040.842	
24	37	38	17117.924	25586.092	43064.485	
24	43	42	17002.018	25689.439	43088.784	
24	43	44	16949.345	25722.269	43088.731	
24	45	44	16949.345	25791.129	43097.591	
24	45	46	16922.631	25669.757	43015.705	☆
24	47	46	16922.631	25678.649	43024.597	☆
24	48	49	16871.987	25769.050	43111.599	
24	50	49	16871.987	25778.919	43121.468	
24	48	49	16904.538	25669.933	43029.152	☆
24	50	49	16904.538	25679.418	43038.637	☆
24	49	50	16911.072	25723.458	43116.461	
24	51	50	16911.072	25733.528	43126.531	
24	49	50	16865.519	25769.002	43116.452	
24	51	50	16865.519	25779.072	43126.522	
24	53	54	16838.313	25769.022	43137.007	
24	55	54	16838.313	25779.894	43147.879	
24	56	57	16816.430	25769.115	43153.399	
24	62	63	16768.826	25769.825	43188.976	
24	64	63	16768.826	25782.512	43201.663	
24	63	64	16760.383	25769.979	43195.222	
24	65	64	16760.383	25782.848	43208.091	
25	18	19	17055.266	25868.785	43159.095	
25	19	20	17078.035	25768.321	43079.834	☆
25	21	22	17046.987	25868.665	43165.042	
25	23	22	17046.987	25873.160	43169.537	
25	25	26	17078.107	25824.542	43174.352	
25	27	26	17078.107	25829.805	43179.615	
25	25	26	17116.350	25786.346	43174.399	
25	27	26	17116.350	25791.622	43179.675	
25	25	26	17116.350	25786.325	43174.378	
25	27	26	17116.350	25791.621	43179.674	
25	28	29	16973.008	25918.458	43182.292	
25	30	29	16973.008	25924.336	43188.170	
25	28	29	17023.058	25868.426	43182.310	
25	30	29	17023.058	25874.291	43188.175	
25	38	39	17004.729	25769.797	43132.264	☆
25	40	39	17004.729	25777.307	43139.774	☆
25	38	39	17054.945	25791.325	43215.613	
25	40	39	17054.945	25799.162	43223.450	

VD	JD	JX	PUMP	PROBE	G(V,J)	37CL
25	39	40	16924.002	25917.038	43219.484	
25	41	40	16924.002	25925.042	43227.488	
25	46	47	17004.610	25796.157	43249.271	
25	48	47	17004.610	25805.593	43258.707	
25	47	48	16910.705	25814.275	43168.989	☆
25	49	50	16911.072	25870.452	43263.455	
25	51	50	16911.072	25880.494	43273.497	
25	49	50	16865.519	25916.065	43263.515	
25	51	50	16865.519	25926.080	43273.530	
25	50	51	16858.931	25916.030	43268.488	
25	52	51	16858.931	25926.217	43278.675	
25	53	54	16838.313	25915.978	43283.963	
25	55	54	16838.313	25926.762	43294.747	
26	13	14	17111.670	25970.382	43297.739	
26	15	14	17111.670	25973.272	43300.629	
26	18	19	17055.266	26015.297	43305.607	
26	21	22	17046.987	26015.119	43311.496	
26	23	22	17046.987	26019.579	43315.956	
26	25	26	17116.350	25932.763	43320.816	
26	27	26	17116.350	25937.997	43326.050	
26	27	28	17052.926	25912.389	43241.532	☆
26	28	29	17023.058	26014.824	43328.708	
26	30	29	17023.058	26020.669	43334.553	
26	28	29	16973.008	26064.885	43328.719	
26	30	29	16973.008	26070.744	43334.578	
26	30	31	17115.625	25838.299	43249.762	☆
26	32	31	17115.625	25844.266	43255.729	☆
26	38	39	17054.945	25937.585	43361.873	
26	40	39	17054.945	25945.395	43369.683	
26	38	39	17111.877	25880.622	43361.842	
26	40	39	17111.877	25888.444	43369.664	
26	39	40	16924.002	26063.292	43365.738	
26	41	40	16924.002	26071.291	43373.737	
26	50	51	16858.931	26062.052	43414.510	
26	52	51	16858.931	26072.255	43424.713	
27	13	14	17111.670	26115.901	43443.258	
27	15	14	17111.670	26118.766	43446.123	
27	25	26	17116.350	26078.208	43466.261	
27	27	26	17116.350	26083.422	43471.475	
27	27	28	17052.926	26055.263	43384.406	☆
27	29	28	17052.926	26060.654	43389.797	☆
27	31	30	17019.125	26166.320	43483.100	
27	38	39	17111.877	26025.906	43507.126	

APPENDIX 3

A' ($\omega=2$) data for ICl

from v=2 to 38, e sublevel

f sublevel

NOTE An asterisk (*) in the last column marks data
for isotopic molecule $I^{37}Cl$.

VA	JA	JX	UPPER TERM	PROBE	G(V,J)	37CL
2	30	31	42746.492	29436.074	13310.418	
2	32	31	42746.492	29425.410	13321.082	
2	31	32	42749.700	29434.100	13315.600	
2	68	69	42938.738	29310.481	13628.257	
2	70	69	42938.738	29287.036	13651.702	
2	71	70	42945.742	29282.086	13663.656	
2	68	67	42925.029	29296.771	13628.258	
2	69	68	42931.834	29291.961	13639.873	
2	72	71	42952.846	29277.088	13675.758	
2	73	72	42960.048	29271.994	13688.054	
2	74	73	42967.350	29266.848	13700.502	
2	75	74	42974.751	29261.577	13713.174	
3	22	23	42873.787	29386.770	13487.017	
3	23	24	42876.183	29385.305	13490.878	
3	24	25	42878.679	29383.769	13494.910	
3	26	25	42878.679	29375.202	13503.477	
3	26	27	42883.971	29380.479	13503.492	
3	28	27	42883.971	29371.211	13512.760	
3	27	28	42886.767	29378.718	13508.049	
3	29	28	42886.767	29369.134	13517.633	
3	28	29	42889.663	29376.901	13512.762	
3	30	29	42889.663	29386.956	13522.707	
3	25	28	42881.275	29382.110	13499.165	
3	27	28	42881.275	29373.204	13508.071	
3	23	26	43090.311	29617.164	13473.147	*
3	25	26	43090.311	29609.282	13481.029	*
3	30	31	42746.492	29223.792	13522.700	
3	32	31	42746.492	29213.192	13533.300	
3	31	30	42898.951	29370.977	13527.974	
3	33	30	42898.951	29360.076	13538.875	
3	27	28	42737.471	29229.436	13508.035	
3	28	29	42740.378	29227.611	13512.767	
3	32	33	42753.009	29219.785	13533.224	
3	29	30	42743.385	29225.760	13517.625	
3	31	30	42743.385	29215.437	13527.948	
3	31	32	42749.700	29221.808	13527.892	
3	33	32	42749.700	29210.816	13538.884	
3	48	49	43116.548	29474.518	13642.030	
3	50	49	43116.548	29457.918	13658.630	
3	43	44	43093.177	29489.735	13603.442	
3	44	45	43097.653	29486.818	13610.835	
3	45	46	43102.226	29483.859	13618.367	
3	46	47	43106.902	29480.817	13626.085	
3	47	48	43111.675	29477.721	13633.954	
3	49	48	43111.675	29461.447	13650.228	
3	49	50	43121.520	29471.267	13650.253	
3	51	50	43121.520	29454.363	13667.157	
3	50	51	43126.590	29467.945	13658.645	

VA	JA	JX	UPPER TERM	PROBE	G(V,J)	37CL
3	68	69	42938.738	29100.881	13837.857	
3	70	69	42938.738	29077.676	13861.062	
3	65	66	42918.323	29114.111	13804.212	
3	66	67	42925.029	29109.774	13815.255	
3	68	67	42925.029	29087.189	13837.840	
3	67	68	42931.834	29105.357	13826.477	
3	69	68	42931.834	29082.457	13849.377	
3	69	70	42945.742	29096.393	13849.349	
3	71	70	42945.742	29072.791	13872.951	
3	70	71	42952.846	29091.819	13861.027	
4	18	19	43013.596	29331.642	13681.954	
4	20	19	43013.596	29325.157	13688.439	
4	11	12	43002.462	29338.057	13664.405	
4	12	13	43003.754	29337.288	13666.466	
4	13	14	43005.146	29336.556	13668.590	
4	14	15	43006.636	29335.719	13670.917	
4	15	16	43008.227	29334.801	13673.426	
4	16	17	43009.917	29333.825	13676.092	
4	17	18	43011.706	29332.795	13678.911	
4	19	18	43011.706	29326.674	13685.032	
4	19	20	43015.584	29330.438	13685.146	
4	21	20	43015.584	29323.658	13691.926	
4	22	21	43017.673	29322.057	13695.616	
4	23	22	43019.861	29320.377	13699.484	
4	24	23	43022.148	29318.653	13703.495	
4	25	24	43024.535	29316.882	13707.653	
4	27	26	43029.609	29313.116	13716.493	
4	29	28	43035.080	29309.077	13726.003	
4	30	29	43037.965	29306.972	13730.993	
4	31	30	43040.950	29304.800	13736.150	
4	32	31	43044.034	29302.552	13741.482	
4	33	32	43047.217	29300.239	13746.978	
4	23	26	43090.311	29412.731	13677.580	*
4	25	26	43090.311	29404.920	13685.391	*
4	19	22	43081.749	29417.926	13663.823	*
4	20	23	43083.747	29416.749	13666.998	*
4	21	24	43085.840	29415.448	13670.392	*
4	23	24	43085.840	29408.195	13677.645	*
4	22	25	43088.028	29414.131	13673.897	*
4	24	25	43088.028	29406.632	13681.396	*
4	24	27	43092.690	29411.284	13681.406	* 0
4	26	27	43092.690	29403.153	13689.537	*
4	25	28	43095.163	29409.796	13685.367	*
4	27	28	43095.163	29401.335	13693.828	*
4	28	29	43097.732	29399.401	13698.331	*
4	29	30	43100.395	29397.442	13702.953	*
4	30	31	43103.154	29395.414	13707.740	*
4	31	32	43106.008	29393.281	13712.727	*

VA	JA	JX	UPPER TERM	PROBE	G(V,J)	37CL
4	32	33	43108.956	29291.135	13817.821	*
4	33	34	43112.000	29388.934	13723.066	*
4	35	36	43118.372	29384.268	13734.104	*
4	25	28	42881.275	29173.637	13707.638	
4	27	28	42881.275	29164.806	13716.469	
4	31	30	42898.951	29162.788	13736.163	
4	33	30	42898.951	29152.002	13746.949	
4	48	49	43116.548	29267.332	13849.216	
4	50	49	43116.548	29250.888	13865.660	
4	40	41	43080.346	29290.326	13790.020	
4	41	42	43084.524	29287.686	13796.838	
4	42	43	43088.801	29285.001	13803.800	
4	43	44	43093.177	29282.195	13810.982	
4	44	45	43097.653	29279.382	13818.271	
4	45	46	43102.228	29276.462	13825.766	
4	46	47	43106.902	29273.481	13833.421	
4	48	47	43106.902	29257.631	13849.271	
4	47	48	43111.675	29270.449	13841.226	
4	49	50	43121.520	29264.141	13857.379	
4	51	50	43121.520	29247.377	13874.143	
4	50	51	43126.590	29260.896	13865.694	
4	52	51	43126.590	29243.790	13882.800	
4	53	52	43131.760	29240.112	13891.648	
4	54	53	43137.029	29236.416	13900.613	
5	18	19	43013.596	29127.125	13886.471	
5	20	19	43013.596	29120.691	13892.905	
5	14	15	43006.636	29131.079	13875.557	
5	15	16	43008.227	29130.213	13878.014	
5	16	17	43009.917	29129.244	13880.673	
5	17	18	43011.706	29128.223	13883.483	
5	19	18	43011.706	29122.162	13889.544	
5	19	20	43015.584	29125.954	13889.630	
5	21	20	43015.584	29119.182	13896.402	
5	20	21	43017.673	29124.732	13892.941	
5	23	26	43090.311	29212.248	13878.063	*
5	24	27	43092.690	29210.860	13881.830	*
5	22	25	43088.028	29213.635	13874.393	*
5	48	49	43116.548	29064.351	14052.197	
5	50	49	43116.548	29048.046	14068.502	
5	68	69	42938.738	28694.062	14244.676	
5	70	69	42938.738	28671.246	14267.492	
5	67	68	42931.834	28698.333	14233.501	
7	30	31	42746.492	28416.149	14330.343	
7	32	31	42746.492	28405.953	14340.539	
7	48	49	43116.548	28671.220	14445.328	
7	50	49	43116.548	28655.191	14461.357	
7	45	46	43102.228	28679.665	14422.563	
7	46	47	43106.902	28676.941	14429.961	

VA	JA	JX	UPPER TERM	PROBE	G(V,J) 37CL
7	47	48	43111.675	28674.096	14437.579
7	49	48	43111.675	28658.379	14453.296
7	49	50	43121.520	28668.264	14453.256
7	51	50	43121.520	28651.898	14469.622
7	52	51	43126.590	28648.544	14478.046
7	68	69	42938.738	28304.728	14634.010
7	70	69	42938.738	28282.360	14656.378
7	67	66	42918.323	28295.269	14623.054
7	68	67	42925.029	28291.026	14634.003
7	69	68	42931.834	28286.734	14645.100
7	69	70	42945.742	28300.631	14645.111
7	71	70	42945.742	28277.949	14667.793
7	72	71	42952.846	28273.473	14679.373
7	73	72	42960.048	28268.940	14691.108
8	30	31	42746.492	28225.185	14521.307
8	32	31	42746.492	28215.105	14531.387
8	29	30	42743.385	28226.916	14516.469
8	31	32	42749.700	28223.412	14526.288
8	48	49	43116.548	28481.407	14635.1
8	50	49	43116.548	28465.556	14650.992
8	47	48	43111.675	28484.228	14627.447
8	49	50	43121.520	28478.529	14642.991
8	51	50	43121.520	28462.395	14659.125
8	52	51	43126.590	28459.091	14667.499
8	68	69	42938.738	28116.897	14821.841
8	70	69	42938.738	28094.746	14843.992
8	71	70	42945.742	28090.481	14855.261
9	25	28	42881.275	28195.723	14685.552
9	48	49	43116.548	28296.263	14820.285
9	50	49	43116.548	28280.610	14835.938
9	47	46	43102.228	28289.501	14812.727
9	46	47	43106.902	28301.705	14805.197
9	48	47	43106.902	28286.569	14820.333
9	47	48	43111.675	28299.022	14812.653
9	49	48	43111.675	28283.581	14828.094
9	51	50	43121.520	28277.485	14844.035
9	50	51	43126.590	28290.689	14835.901
10	18	19	43013.596	28170.469	14843.127
10	20	19	43013.596	28164.337	14849.259
10	48	49	43116.548	28115.927	15000.621
10	50	49	43116.548	28100.449	15016.099
10	45	46	43102.228	28123.757	14978.471
10	46	47	43106.902	28121.240	14985.662
10	48	47	43106.902	28106.264	15000.638
10	49	48	43111.675	28103.383	15008.292
10	49	50	43121.520	28113.295	15008.225
10	51	50	43121.520	28097.444	15024.076
10	50	51	43126.590	28110.544	15016.046

VA	JA	JX	UPPER TERM	PROBE	G(V,J) 37CL
10	68	69	42938.738	27755.492	15183.246
10	70	69	42938.738	27733.870	15204.868
10	67	66	42918.323	27745.663	15172.660
10	66	67	42925.029	27762.821	15162.208
10	68	67	42925.029	27741.803	15183.226
10	67	68	42931.834	27759.159	15172.675
10	69	68	42931.834	27737.858	15193.976
10	69	70	42945.742	27751.763	15193.979
10	71	70	42945.742	27729.834	15215.908
10	70	71	42952.846	27747.991	15204.855
10	72	71	42952.846	27725.736	15227.110
10	73	72	42960.048	27721.589	15238.459
11	48	49	43116.548	27940.588	15175.960
11	50	49	43116.548	27925.270	15191.278
12	38	39	39405.794	24125.805	15279.989
12	40	39	39405.794	24113.758	15292.036
12	48	49	43116.548	27770.183	15346.365
12	50	49	43116.548	27755.085	15361.463
12	51	52	39297.963	23928.689	15369.274
12	53	52	39297.963	23912.709	15385.254
12	68	69	42938.738	27414.336	15524.402
12	70	69	42938.738	27393.194	15545.544
12	67	68	42931.834	27417.762	15514.072
12	69	68	42931.834	27396.973	15534.861
12	69	70	42945.742	27410.861	15534.881
12	71	70	42945.742	27389.462	15556.280
12	70	71	42952.846	27407.336	15545.510
12	72	71	42952.846	27385.655	15567.191
12	73	72	42960.048	27381.787	15578.261
13	38	39	39405.794	23960.000	15445.794
13	40	39	39405.794	23948.083	15457.711
13	38	37	39397.426	23951.607	15445.819
13	37	38	39401.556	23961.465	15440.091
13	39	38	39401.556	23949.843	15451.713
13	39	40	39410.141	23958.429	15451.712
13	41	40	39410.141	23946.209	15463.932
13	40	41	39414.597	23956.853	15457.744
13	42	41	39414.597	23944.338	15470.259
13	51	52	39297.963	23763.994	15533.969
13	53	52	39297.963	23748.186	15549.777
14	38	39	39405.794	23799.504	15606.290
14	40	39	39405.794	23787.758	15618.036
14	32	33	39381.994	23807.355	15574.639
14	33	34	39385.689	23806.149	15579.540
14	34	35	39389.493	23804.925	15584.568
14	36	35	39389.493	23794.343	15595.150
14	35	36	39393.405	23803.584	15589.821
14	37	36	39393.405	23792.734	15600.671

VA	JA	JX	UPPER TERM	PROBE	G(V,J) 37CL
14	36	37	39397.426	23802.252	15595.174
14	38	37	39397.426	23791.078	15606.348
14	37	38	39401.556	23800.854	15600.702
14	39	38	39401.556	23789.425	15612.131
14	39	40	39410.141	23797.998	15612.143
14	41	40	39410.141	23785.946	15624.195
14	40	41	39414.597	23796.508	15618.089
14	42	41	39414.597	23784.155	15630.442
14	41	42	39419.161	23794.950	15624.211
14	43	42	39419.161	23782.327	15636.834
14	42	43	39423.834	23793.380	15630.454
14	44	43	39423.834	23780.467	15643.367
14	45	44	39428.616	23778.554	15650.062
14	46	45	39433.507	23776.642	15656.865
14	47	46	39438.506	23774.652	15663.854
14	46	49	39270.388	23613.431	15656.957
14	48	49	39270.388	23599.338	15671.050
14	48	49	43116.548	27445.555	15670.993
14	50	49	43116.548	27430.898	15685.650
14	43	44	43093.177	27456.377	15636.800
14	45	46	43102.228	27452.197	15650.031
14	46	47	43106.902	27450.023	15656.879
14	48	47	43106.902	27435.980	15670.922
14	47	48	43111.675	27447.830	15663.845
14	49	48	43111.675	27433.471	15678.204
14	49	50	43121.520	27443.258	15678.262
14	50	51	43126.590	27440.918	15685.672
14	51	52	39297.963	23604.715	15693.248
14	53	52	39297.963	23589.156	15708.807
15	38	39	39405.794	23644.570	15761.224
15	40	39	39405.794	23632.979	15772.815
15	30	31	39374.930	23654.107	15720.823
15	31	32	39378.408	23653.057	15725.351
15	32	33	39381.994	23651.962	15730.032
15	33	34	39385.689	23650.786	15734.903
15	34	35	39389.493	23649.628	15739.865
15	36	35	39389.493	23639.219	15750.274
15	35	36	39393.405	23648.411	15744.994
15	37	36	39393.405	23637.693	15755.712
15	36	37	39397.426	23647.141	15750.285
15	38	37	39397.426	23636.129	15761.297
15	37	38	39401.556	23645.860	15755.696
15	39	38	39401.556	23634.563	15766.993
15	39	40	39410.141	23643.129	15767.012
15	41	40	39410.141	23631.247	15778.894
15	40	41	39414.597	23641.750	15772.847
15	42	41	39414.597	23629.573	15785.024
15	41	42	39419.161	23640.268	15778.893
15	43	42	39419.161	23627.831	15791.330

VA	JA	JX	UPPER TERM	PROBE	G(V,J)	37CL
15	42	43	39423.834	23638.793	15785.041	
15	44	43	39423.834	23626.065	15797.769	
15	46	49	39270.388	23459.147	15811.241	
15	48	49	39270.388	23445.264	15825.124	
15	46	49	39270.388	23459.168	15811.220	
15	45	48	39265.151	23460.688	15804.463	
15	47	48	39265.151	23447.079	15818.072	
15	50	51	39281.137	23441.535	15839.602	
15	51	52	39286.649	23439.585	15847.064	
15	52	53	39292.257	23437.635	15854.622	
15	53	54	39297.963	23435.568	15862.395	
15	54	55	39303.768	23433.510	15870.258	
15	46	49	39270.388	23459.251	15811.137	
15	48	49	39270.388	23445.324	15825.064	
15	48	49	43116.548	27291.566	15824.982	
15	51	52	39297.963	23450.935	15847.028	
15	53	52	39297.963	23435.629	15862.334	
15	51	52	39297.963	23450.985	15846.978	
15	53	52	39297.963	23435.590	15862.373	
15	51	52	39297.963	23451.021	15846.942	
15	53	52	39297.963	23435.677	15862.286	
16	38	39	39405.794	23495.313	15910.481	
16	40	39	39405.794	23483.936	15921.858	
16	36	37	39397.426	23497.769	15899.657	
16	38	37	39397.426	23486.952	15910.474	
16	39	38	39401.556	23485.456	15916.100	
16	39	40	39410.141	23493.997	15916.144	
16	41	40	39410.141	23482.346	15927.795	
16	40	41	39414.597	23492.674	15921.923	
16	42	41	39414.597	23480.738	15933.859	
16	46	49	39270.388	23310.757	15959.631	
16	48	49	39270.388	23297.073	15973.315	
16	47	44	39265.151	23298.734	15966.417	
16	47	46	39275.717	23309.268	15966.449	
16	49	46	39275.717	23295.347	15980.370	
16	48	47	39281.137	23307.813	15973.324	
16	50	47	39281.137	23293.576	15987.561	
16	49	48	39286.649	23306.246	15980.403	
16	51	48	39286.649	23291.748	15994.901	
16	50	49	39292.257	23304.671	15987.586	
16	52	49	39292.257	23289.884	16002.373	
16	51	50	39297.963	23303.034	15994.929	
16	53	50	39297.963	23287.973	16009.990	
16	54	51	39303.768	23286.025	16017.743	
16	55	52	39309.674	23284.030	16025.644	
16	56	53	39315.683	23282.039	16033.644	
16	57	54	39321.797	23279.943	16041.854	
16	58	55	39328.015	23277.814	16050.201	

VA	JA	JX	UPPER TERM	PROBE	G(V,J)	37CL
16	46	49	39270.388	23310.730	15959.658	
16	48	49	39270.388	23297.055	15973.333	
16	46	47	39260.006	23300.451	15959.555	
16	45	48	39265.151	23312.118	15953.033	
16	47	48	39265.151	23298.795	15966.356	
16	49	50	39275.717	23295.334	15980.383	
16	50	51	39281.137	23293.574	15987.563	
16	52	53	39292.257	23289.896	16002.361	
16	53	54	39297.963	23287.943	16010.020	
16	46	49	39270.388	23310.733	15959.655	
16	48	49	39270.388	23297.069	15973.319	
16	51	52	39297.963	23303.116	15994.847	
16	53	52	39297.963	23288.011	16009.952	
16	51	52	39297.963	23303.122	15994.841	
16	53	52	39297.963	23288.019	16009.944	
16	49	50	39286.649	23306.338	15980.311	
16	50	51	39292.257	23304.737	15987.520	
16	52	51	39292.257	23289.917	16002.340	
16	52	53	39303.768	23301.398	16002.370	
16	54	53	39303.768	23286.012	16017.756	
16	53	54	39309.674	23299.704	16009.970	
16	55	54	39309.674	23284.018	16025.656	
16	56	55	39315.683	23281.980	16033.703	
16	51	52	39297.963	23303.182	15994.781	
16	53	52	39297.963	23288.093	16009.870	
17	38	39	39405.794	23351.924	16053.870	
17	40	39	39405.794	23340.708	16065.086	
17	38	39	39405.794	23352.060	16053.734	
17	40	39	39405.794	23340.854	16064.940	
17	35	36	39393.405	23355.429	16037.976	
17	37	36	39393.405	23345.057	16048.348	
17	36	37	39397.426	23354.350	16043.076	
17	38	37	39397.426	23343.685	16053.741	
17	37	38	39401.556	23353.199	16048.357	
17	39	38	39401.556	23342.300	16059.256	
17	39	40	39410.141	23350.865	16059.276	
17	41	40	39410.141	23339.371	16070.770	
17	40	41	39414.597	23349.611	16064.986	
17	42	41	39414.597	23337.871	16076.726	
17	43	42	39419.161	23336.348	16082.813	
17	44	43	39423.834	23334.768	16089.066	
17	46	49	39270.388	23168.334	16102.054	
17	48	49	39270.388	23154.863	16115.525	
17	46	49	39270.388	23168.272	16102.116	
17	48	49	39270.388	23154.862	16115.526	
17	48	49	39281.137	23165.570	16115.567	
17	50	49	39281.137	23151.609	16129.528	
17	51	52	39297.963	23161.222	16136.741	
17	53	52	39297.963	23146.364	16151.599	

VA	JA	JX	UPPER TERM	PROBE	G(V,J) 37CL
17	51	52	39297.963	23161.303	16136.660
17	53	52	39297.963	23146.456	16151.507
18	38	39	39405.794	23214.806	16190.988
18	40	39	39405.794	23203.788	16202.006
18	33	34	39385.689	23219.847	16165.842
18	34	35	39389.493	23218.931	16170.562
18	35	36	39393.405	23217.950	16175.455
18	36	37	39397.426	23216.944	16180.482
18	37	38	39401.556	23215.924	16185.632
18	39	38	39401.556	23205.204	16196.352
18	39	40	39410.141	23213.752	16196.389
18	41	40	39410.141	23202.443	16207.698
18	40	41	39414.597	23212.603	16201.994
18	42	41	39414.597	23201.077	16213.520
18	41	42	39419.161	23211.465	16207.696
18	42	43	39423.834	23210.277	16213.557
18	43	44	39428.616	23209.052	16219.564
18	45	44	39428.616	23196.685	16231.931
18	46	45	39433.507	23195.197	16238.310
18	46	49	39270.388	23032.053	16238.335
18	48	49	39270.388	23018.853	16251.535
18	48	49	39281.137	23029.615	16251.522
18	50	49	39281.137	23015.896	16265.241
18	51	52	39297.963	23025.614	16272.349
18	51	52	39297.963	23025.654	16272.309
18	53	52	39297.963	23011.084	16286.879
19	38	39	39405.794	23083.972	16321.822
19	40	39	39405.794	23073.197	16332.597
19	31	32	39378.408	23090.158	16288.250
19	32	33	39381.994	23089.390	16292.604
19	33	34	39385.689	23088.591	16297.098
19	34	35	39389.493	23087.695	16301.798
19	35	36	39393.405	23086.827	16306.578
19	36	37	39397.426	23085.930	16311.496
19	38	37	39397.426	23075.692	16321.734
19	37	38	39401.556	23085.008	16316.548
19	39	38	39401.556	23074.477	16327.079
19	39	40	39410.141	23083.055	16327.086
19	41	40	39410.141	23071.992	16338.149
19	40	41	39414.597	23082.006	16332.591
19	42	41	39414.597	23070.699	16343.898
19	41	42	39419.161	23080.955	16338.206
19	46	49	39270.388	22902.104	16368.284
20	38	39	39405.794	22959.725	16446.069
20	40	39	39405.794	22949.179	16456.615
20	34	35	39389.493	22963.055	16426.438
20	35	36	39393.405	22962.301	16431.104
20	37	36	39393.405	22952.509	16440.896

VA	JA	JX	UPPER TERM	PROBE	G(V,J)	37CL
20	36	37	39397.426	22961.476	16435.950	
20	37	38	39401.556	22960.648	16440.908	
20	39	38	39401.556	22950.366	16451.190	
20	39	40	39410.141	22958.880	16451.261	
20	41	40	39410.141	22948.051	16462.090	
20	40	41	39414.597	22957.995	16456.602	
20	42	41	39414.597	22946.902	16467.695	
20	41	42	39419.161	22957.091	16462.070	
20	42	43	39423.834	22956.127	16467.707	
20	68	69	42789.236	26130.106	16659.130	
20	70	69	42789.236	26111.784	16677.452	
20	67	66	42768.740	26118.554	16650.186	
20	66	67	42775.472	26134.193	16641.279	
20	68	67	42775.472	26116.310	16659.162	
20	67	68	42782.304	26132.159	16650.145	
20	69	68	42782.304	26114.064	16668.240	
20	69	70	42796.268	26128.052	16668.216	
20	71	70	42796.268	26109.452	16686.816	
20	72	71	42803.399	26107.093	16696.306	
21	68	69	42789.236	26017.634	16771.602	
21	70	69	42789.236	25999.742	16789.494	
21	64	63	42749.142	26011.843	16737.299	
21	65	64	42755.575	26009.885	16745.690	
21	66	65	42762.107	26007.893	16754.214	
21	65	66	42768.740	26023.080	16745.660	
21	67	66	42768.740	26005.902	16762.838	
21	66	67	42775.472	26021.284	16754.188	
21	68	67	42775.472	26003.890	16771.582	
21	67	68	42782.304	26019.494	16762.810	
21	69	68	42782.304	26001.855	16780.449	
21	69	70	42796.268	26015.825	16780.443	
21	71	70	42796.268	25997.705	16798.563	
21	70	71	42803.399	26013.965	16789.434	
21	72	71	42803.399	25995.588	16807.811	
21	71	72	42810.630	26012.071	16798.559	
21	73	72	42810.630	25993.461	16817.169	
21	72	73	42817.961	26010.130	16807.831	
21	74	73	42817.961	25991.309	16826.652	
21	73	74	42825.391	26008.224	16817.167	
21	75	74	42825.391	25989.133	16836.258	
21	74	75	42832.921	26006.273	16826.648	
21	76	75	42832.921	25986.943	16845.978	
21	77	76	42840.551	25984.731	16855.820	
21	78	77	42848.280	25982.490	16865.790	
21	79	78	42856.108	25980.239	16875.869	
21	80	79	42864.036	25977.982	16886.054	
23	68	69	42789.236	25814.950	16974.286	
23	70	69	42789.236	25798.071	16991.165	

VA	JA	JX	UPPER TERM	PROBE	G(V,J)	37CL
24	30	31	42746.492	25906.489	16840.003	
24	32	31	42746.492	25898.896	16847.596	
24	68	69	42938.738	25874.600	17064.138	
24	70	69	42938.738	25858.302	17080.436	
24	67	66	42918.323	25862.183	17056.140	
24	68	67	42925.029	25860.910	17064.119	
24	69	68	42931.834	25859.644	17072.190	
24	71	70	42945.742	25857.024	17088.718	
24	72	71	42952.846	25855.706	17097.140	
24	73	72	42960.048	25854.354	17105.694	
24	68	69	42789.236	25725.150	17064.086	
24	70	69	42789.236	25708.833	17080.403	
25	30	31	42746.492	25816.957	16929.535	
25	32	31	42746.492	25809.627	16936.865	
25	48	49	43116.548	26104.364	17012.184	
25	50	49	43116.548	26092.942	17023.606	
25	68	69	42938.738	25792.791	17145.947	
25	70	69	42938.738	25777.093	17161.645	
26	68	69	42938.738	25718.992	17219.746	
26	70	69	42938.738	25703.908	17234.830	
27	30	31	42746.492	25660.645	17085.847	
27	32	31	42746.492	25653.807	17092.685	
27	48	49	43116.548	25954.099	17162.449	
27	50	49	43116.548	25943.529	17173.019	
27	68	69	42938.738	25653.232	17285.506	
27	70	69	42938.738	25638.758	17299.980	
28	25	28	42881.272	25743.036	17138.236	
28	27	28	42881.272	25737.500	17143.772	
28	31	30	42898.951	25742.751	17156.200	
28	33	30	42898.951	25735.975	17162.976	
28	48	49	43116.548	25890.326	17226.222	
28	50	49	43116.548	25880.273	17236.275	
28	68	69	42938.738	25595.119	17343.619	
28	70	69	42938.738	25581.418	17357.320	
29	18	19	43013.596	25830.068	17183.528	
29	20	19	43013.596	25826.156	17187.440	
29	30	31	42746.492	25533.754	17212.738	
29	32	31	42746.492	25527.488	17219.004	
29	48	49	43116.548	25833.812	17282.736	
29	50	49	43116.548	25824.168	17292.380	
29	68	69	42938.738	25544.433	17394.305	
29	70	69	42938.738	25531.470	17407.268	
29	71	72	42960.048	25546.217	17413.831	
29	73	72	42960.048	25532.797	17427.251	
29	70	71	42952.846	25545.599	17407.247	
29	72	71	42952.846	25532.355	17420.491	
29	69	70	42945.742	25545.016	17400.726	
29	71	70	42945.742	25531.941	17413.801	

VA	JA	JX	UPPER TERM	PROBE	G(V,J) 37CL
29	67	68	42931.834	25543.845	17387.989
29	69	68	42931.834	25531.088	17400.746
29	66	67	42925.029	25543.343	17381.686
29	68	67	42925.029	25530.736	17394.293
29	65	66	42918.323	25542.841	17375.482
29	67	66	42918.323	25530.389	17387.934
29	64	65	42911.717	25542.367	17369.350
29	66	65	42911.717	25530.069	17381.648
29	63	64	42905.210	25541.935	17363.275
29	65	64	42905.210	25529.773	17375.437
30	23	26	43377.023	26164.647	17212.376 *
30	25	26	43377.023	26160.035	17216.988 *
30	68	69	42938.738	25500.510	17438.228
30	70	69	42938.738	25488.263	17450.475
30	73	72	42960.048	25490.760	17469.288
30	72	71	42952.846	25489.916	17462.930
30	71	70	42945.742	25489.077	17456.665
30	69	68	42931.834	25487.526	17444.308
30	68	67	42925.029	25486.775	17438.254
31	18	19	43013.596	25726.983	17286.613
31	20	19	43013.596	25723.432	17290.164
31	20	21	42112.580	24822.411	17290.169
31	22	21	42112.580	24818.497	17294.083
31	27	28	42881.272	25575.987	17305.285
32	18	19	43013.596	25684.047	17329.549
32	20	19	43013.596	25680.679	17332.917
32	20	21	42112.580	24779.683	17332.897
32	22	21	42112.580	24775.987	17336.593
32	23	26	43377.023	26068.468	17308.555 *
32	25	26	43377.023	26064.277	17312.746 *
32	48	49	43116.548	25702.031	17414.517
32	50	49	43116.548	25693.888	17422.660
33	20	21	42112.580	24741.909	17370.671
33	22	21	42112.580	24738.412	17374.168
33	23	26	43377.023	26028.361	17348.662 *
33	25	26	43377.023	26024.385	17352.638 *
34	20	21	42112.580	24708.646	17403.934
34	22	21	42112.580	24705.343	17407.237
34	23	26	43377.023	25992.916	17384.107 *
34	25	26	43377.023	25989.205	17387.818 *
35	20	21	42112.580	24679.637	17432.943
35	22	21	42112.580	24676.462	17436.118
36	20	21	42112.580	24654.353	17458.227
36	22	21	42112.580	24651.431	17461.149
36	20	19	42108.405	24650.198	17458.207
36	19	20	42110.442	24653.602	17456.840
36	21	20	42110.442	24650.796	17459.646
36	21	22	42114.820	24655.192	17459.628
36	23	22	42114.820	24652.125	17462.695

VA	JA	JX	UPPER TERM	PROBE	G(V,J) '37CL
36	22	23	42117.162	24656.041	17461.121
36	23	24	42119.606	24656.932	17462.674
36	24	25	42122.152	24657.873	17464.279
36	25	26	42124.799	24658.861	17465.938
37	20	21	42112.580	24632.597	17479.983
37	22	21	42112.580	24629.854	17482.726
37	20	19	42108.405	24628.415	17479.990
37	21	20	42110.442	24629.116	17481.326
37	23	22	42114.820	24630.687	17484.133
38	20	21	42112.580	24614.044	17498.536
38	22	21	42112.580	24611.519	17501.061
2	60	60	43035.038	29493.750	13541.288
2	62	60	43035.038	29472.997	13562.041
3	26	28	43032.228	29528.705	13503.523
3	28	28	43032.228	29519.498	13512.730
3	27	29	43035.012	29527.003	13508.009
3	29	29	43035.012	29517.422	13517.590
3	28	30	43037.895	29525.161	13512.734
3	30	30	43037.895	29515.265	13522.630
3	29	31	43040.878	29523.272	13517.606
3	31	31	43040.878	29513.034	13527.844
3	30	32	43043.960	29521.321	13522.639
3	32	32	43043.960	29510.740	13533.220
3	31	33	43047.142	29519.298	13527.844
3	33	33	43047.142	29508.376	13538.766
3	32	34	43050.424	29517.213	13533.211
3	34	34	43050.424	29505.968	13544.456
3	35	35	43053.805	29503.481	13550.324
3	36	36	43057.285	29500.920	13556.365
3	50	50	43126.532	29467.945	13658.587
3	52	50	43126.532	29450.703	13675.829
3	50	50	43116.480	29457.893	13658.587
3	51	51	43121.456	29454.315	13667.141
3	51	53	43131.708	29464.558	13667.150
3	53	53	43131.708	29446.965	13684.743
3	54	54	43136.984	29443.192	13693.792
3	55	55	43142.360	29439.342	13703.018
3	60	60	43035.038	29283.399	13751.639
3	62	60	43035.038	29262.826	13772.212
3	54	54	42999.950	29306.164	13693.786
3	55	55	43005.547	29302.526	13703.021
3	56	56	43011.244	29298.854	13712.390
3	57	57	43017.042	29295.083	13721.959
3	59	57	43017.042	29275.494	13741.548
3	58	58	43022.940	29291.247	13731.693
3	60	58	43022.940	29271.338	13751.602
3	59	59	43028.939	29287.352	13741.587
3	61	59	43028.939	29267.121	13761.818

VA	JA	JX	UPPER TERM	PROBE	G(V,J) 37CL
3	61	61	43041.237	29279.384	13761.853
3	63	61	43041.237	29258.475	13782.762
3	62	62	43047.537	29275.293	13772.244
3	64	62	43047.537	29254.048	13793.489
3	63	63	43053.938	29271.135	13782.803
3	65	63	43053.938	29249.559	13804.379
4	29	31	43040.878	29314.948	13725.930
4	31	31	43040.878	29304.798	13736.080
4	18	20	43013.540	29331.669	13681.871
4	19	21	43015.528	29330.437	13685.091
4	20	22	43017.615	29329.241	13688.374
4	21	23	43019.802	29327.907	13691.895
4	22	24	43022.088	29326.529	13695.559
4	23	25	43024.474	29325.085	13699.389
4	24	26	43026.959	29323.577	13703.382
4	25	27	43029.544	29321.990	13707.554
4	26	28	43032.228	29320.342	13711.886
4	27	29	43035.012	29318.636	13716.376
4	29	29	43035.012	29309.106	13725.906
4	28	30	43037.895	29316.848	13721.047
4	30	30	43037.895	29307.018	13730.877
4	30	32	43043.960	29313.085	13730.875
4	32	32	43043.960	29302.590	13741.370
4	31	33	43047.142	29311.126	13736.016
4	33	33	43047.142	29300.271	13746.871
4	34	34	43050.424	29297.901	13752.523
4	35	35	43053.805	29295.439	13758.366
4	36	36	43057.285	29292.923	13764.362
4	37	37	43060.866	29290.352	13770.514
4	38	38	43064.545	29287.701	13776.844
4	39	39	43068.325	29285.002	13783.323
4	40	40	43072.204	29282.231	13789.973
4	41	41	43076.183	29279.393	13796.790
4	42	42	43080.261	29276.468	13803.793
4	43	43	43084.440	29273.505	13810.935
4	44	44	43088.718	29270.453	13818.265
4	45	45	43093.095	29267.348	13825.747
4	46	46	43097.573	29264.185	13833.388
4	47	47	43102.150	29260.949	13841.201
4	48	48	43106.827	29257.640	13849.187
4	52	50	43126.532	29243.797	13882.735
4	41	41	43084.440	29287.679	13796.761
4	42	42	43088.718	29284.979	13803.739
4	43	43	43093.095	29282.197	13810.898
4	44	44	43097.573	29279.379	13818.194
4	45	45	43102.150	29276.442	13825.708
4	46	46	43106.827	29273.469	13833.358
4	47	47	43111.603	29270.432	13841.171

VA	JA	JX	UPPER TERM	PROBE	G(V,J)	37CL
4	48	48	43116.480	29267.335	13849.145	
4	49	49	43121.456	29264.169	13857.287	
4	53	53	43131.708	29240.165	13891.543	
4	54	54	43136.984	29236.464	13900.520	
4	56	56	43147.836	29228.846	13918.990	
4	58	58	43159.088	29220.984	13938.104	
4	59	59	43164.863	29216.953	13947.910	
4	60	60	43170.739	29212.875	13957.864	
4	61	61	43176.715	29208.702	13968.013	
4	62	62	43182.791	29204.476	13978.315	
4	64	64	43195.242	29195.850	13999.392	
4	65	65	43201.619	29191.409	14010.210	
4	60	60	43035.038	29077.156	13957.882	
4	62	60	43035.038	29056.761	13978.277	
5	27	29	43328.780	29408.048	13920.732	
5	29	29	43328.780	29398.687	13930.093	
5	29	31	43040.878	29110.857	13930.021	
5	31	31	43040.878	29100.774	13940.104	
5	27	29	43035.012	29114.385	13920.627	
5	29	29	43035.012	29105.003	13930.009	
5	28	30	43037.895	29112.663	13925.232	
5	30	30	43037.895	29102.925	13934.970	
5	30	32	43043.960	29108.967	13934.993	
5	32	32	43043.960	29098.592	13945.368	
5	31	33	43047.142	29107.007	13940.135	
5	33	33	43047.142	29096.317	13950.825	
5	50	50	43126.532	29058.017	14068.515	
5	52	50	43126.532	29041.061	14085.471	
6	27	29	43328.780	29208.049	14120.731	
6	29	29	43328.780	29198.745	14130.035	
12	60	60	43035.038	27588.988	15446.050	
12	62	60	43035.038	27570.265	15464.773	
14	50	50	43126.532	27440.880	15685.652	
14	52	50	43126.532	27425.614	15700.918	
18	53	51	39470.675	23183.774	16286.901	
18	52	52	39476.436	23196.839	16279.597	
18	54	52	39476.436	23182.033	16294.403	
18	53	53	39482.305	23195.358	16286.947	
18	55	53	39482.305	23180.295	16302.010	
18	54	54	39488.284	23193.832	16294.452	
18	56	54	39488.284	23178.512	16309.772	
18	55	55	39494.371	23192.227	16302.144	
18	57	55	39494.371	23176.621	16317.750	
18	56	56	39500.566	23190.722	16309.844	
18	50	50	39465.023	23199.783	16265.240	
18	52	50	39465.023	23185.350	16279.673	
18	49	49	39459.479	23201.161	16258.318	
18	51	49	39459.479	23187.160	16272.319	

VA	TA	JX	UPPER TERM	PROBE	G(V,J) 37CL
18	48	48	39454.044	23202.568	16251.476
18	50	48	39454.044	23188.825	16265.219
18	47	47	39448.718	23203.873	16244.845
18	49	47	39448.718	23190.468	16258.250
18	46	46	39443.501	23205.137	16238.364
23	33	35	42606.202	25851.221	16754.981
23	35	35	42606.202	25842.643	16763.559
24	33	35	42606.202	25754.619	16851.583
24	35	35	42606.202	25746.286	16859.916
24	29	29	42587.193	25750.720	16836.473
24	30	30	42590.110	25750.088	16840.022
24	31	31	42593.127	25749.379	16843.748
24	30	32	42596.244	25756.263	16839.981
24	32	32	42596.244	25748.614	16847.630
24	31	33	42599.463	25755.728	16843.735
24	33	33	42599.463	25747.857	16851.606
24	32	34	42602.782	25755.179	16847.603
24	34	34	42602.782	25747.086	16855.696
24	34	36	42609.722	25754.030	16855.692
24	36	36	42609.722	25745.470	16864.252
24	35	37	42613.344	25753.425	16859.919
24	37	37	42613.344	25744.622	16868.722
24	38	38	42617.066	25743.742	16873.324
24	39	39	42620.889	25742.873	16878.016
25	54	54	42999.950	25952.248	17047.702
25	56	54	42999.950	25939.475	17060.475
25	52	52	42989.057	25953.689	17035.368
25	54	52	42989.057	25941.353	17047.704
25	53	53	42994.453	25952.980	17041.473
25	55	53	42994.453	25940.421	17054.032
25	55	55	43005.547	25951.506	17054.041
25	57	55	43005.547	25938.516	17067.031
25	56	56	43011.244	25950.783	17060.461
25	58	56	43011.244	25937.554	17073.690
25	60	60	43035.038	25947.677	17087.361
25	62	60	43035.038	25933.631	17101.407
26	33	35	42606.202	25583.908	17022.294
26	35	35	42606.202	25576.138	17030.064
26	32	34	42602.782	25584.218	17018.564
26	34	34	42602.782	25576.646	17026.136
26	34	36	42609.722	25583.541	17026.181
26	36	36	42609.722	25575.600	17034.122
26	54	54	42999.950	25874.555	17125.395
26	56	54	42999.950	25862.283	17137.667
26	52	52	42989.057	25875.554	17113.503
26	54	52	42989.057	25863.673	17125.384
26	55	53	42994.453	25862.982	17131.471
26	57	55	43005.547	25861.568	17143.979

VA	JA	JX	UPPER TERM	PROBE	G(V,J) 37CL
26	56	56	43011.244	25873.561	17137.683
27	54	54	42999.950	25804.651	17195.299
27	56	54	42999.950	25792.915	17207.035
27	60	60	43035.038	25803.226	17231.812
27	62	60	43035.038	25790.335	17244.703
28	27	29	43328.780	26184.948	17143.832
28	29	29	43328.780	26179.019	17149.761
28	50	50	43126.532	25890.270	17236.262
28	52	50	43126.532	25879.803	17246.729
28	54	54	42999.950	25742.343	17257.607
28	56	54	42999.950	25731.153	17268.797
28	60	60	43035.038	25742.627	17292.411
28	62	60	43035.038	25730.309	17304.729
29	29	31	43040.878	25831.024	17209.854
29	31	31	43040.878	25824.966	17215.912
29	41	41	43084.440	25832.465	17251.975
29	43	41	43084.440	25824.130	17260.310
29	50	50	43126.532	25834.196	17292.336
29	52	50	43126.532	25824.139	17302.393
29	54	54	42999.950	25687.271	17312.679
29	56	54	42999.950	25676.600	17323.350
30	27	29	43328.780	26070.947	17257.833
30	29	29	43328.780	26065.547	17263.233
30	54	54	42999.950	25638.936	17361.014
30	60	60	43035.038	25642.657	17392.381
30	62	60	43035.038	25631.605	17403.433
31	27	29	43328.780	26023.436	17305.344
31	29	29	43328.780	26018.295	17310.485
31	54	54	42999.950	25596.714	17403.236
31	56	54	42999.950	25587.159	17412.791
31	51	51	42983.761	25594.359	17389.402
31	52	50	42978.565	25584.615	17393.950
31	52	52	42989.057	25595.113	17393.944
31	54	52	42989.057	25585.853	17403.204
31	53	53	42994.453	25595.901	17398.552
31	55	53	42994.453	25586.485	17407.968
31	55	55	43005.547	25597.599	17407.948
31	57	55	43005.547	25587.863	17417.684
31	56	56	43011.244	25598.461	17412.783
31	58	56	43011.244	25588.596	17422.648
31	57	57	43017.042	25599.376	17417.666
31	59	57	43017.042	25589.351	17427.691
31	58	58	43022.940	25600.270	17422.670
31	60	58	43022.940	25590.120	17432.820
31	59	59	43028.939	25601.249	17427.690
31	60	60	43035.038	25602.177	17432.861
31	62	60	43035.038	25591.743	17443.295
31	61	61	43041.237	25603.186	17438.051
31	63	61	43041.237	25592.632	17448.605

VA	JA	JX	UPPER TERM	PROBE	G(V,J) /37CL
31	59	59	43028.939	25601.204	17427.735
31	61	59	43028.939	25590.922	17438.017
32	27	29	43328.780	25981.456	17347.324
32	29	29	43328.780	25976.576	17352.204
32	26	28	43326.018	25980.989	17345.029
32	28	28	43326.018	25976.270	17349.748
32	28	30	43331.642	25981.911	17349.731
32	30	30	43331.642	25976.837	17354.805
32	29	31	43334.602	25982.377	17352.225
32	31	31	43334.602	25977.144	17357.458
32	32	32	43337.660	25977.515	17360.145
32	29	31	43040.878	25688.639	17352.239
32	31	31	43040.878	25683.437	17357.441
32	41	41	43084.440	25696.043	17388.397
32	43	41	43084.440	25688.969	17395.471
32	50	50	43126.532	25703.792	17422.740
32	52	50	43126.532	25695.343	17431.189
32	49	49	43121.456	25702.831	17418.625
32	51	49	43121.456	25694.548	17426.908
32	51	51	43131.708	25704.785	17426.923
32	53	51	43131.708	25696.185	17435.523
32	54	54	42999.950	25560.062	17439.888
32	56	54	42999.950	25551.027	17448.923
32	57	55	43005.547	25552.006	17453.541
32	58	56	43011.244	25553.021	17458.223
32	59	57	43017.042	25554.074	17462.968
32	60	58	43022.940	25555.152	17467.788
32	60	60	43035.038	25567.232	17467.806
32	62	60	43035.038	25557.448	17477.590
33	41	41	43084.440	25661.384	17423.056
33	43	41	43084.440	25654.641	17429.799
33	50	50	43126.532	25671.035	17455.497
33	52	50	43126.532	25663.091	17463.441
33	48	48	43116.480	25668.665	17447.815
33	50	48	43116.480	25661.024	17455.456
33	49	49	43121.456	25669.836	17451.620
33	51	49	43121.456	25662.039	17459.417
33	51	51	43131.708	25672.262	17459.446
33	53	51	43131.708	25664.204	17467.504
33	52	52	43136.984	25673.536	17463.448
33	54	52	43136.984	25665.354	17471.630
33	53	53	43142.360	25674.830	17467.530
36	27	29	43328.780	25859.171	17469.609
36	29	29	43328.780	25855.358	17473.422
37	27	29	43328.780	25838.151	17490.629
37	29	29	43328.780	25834.610	17494.170
38	27	29	43328.780	25820.427	17508.353
38	29	29	43328.780	25817.141	17511.639

nal levels of the ground state, Preliminary communica-
tion, Molec. Phys., 53, 2, pp.525-529 (1984)

8- Brand J.C.D., Bussières D. and Hoy A.R., The A' ($^3\pi_2$)
state of ICl, submitted to J. Mol. Spectrosc.

END

10·03·86

FIN